Chem Soc Rev

REVIEW ARTICLE

View Article Online
View Journal | View Issue

Cite this: *Chem. Soc. Rev.*, 2023, **52**, 4672

Modulation of engineered nanomaterial interactions with organ barriers for enhanced drug transport

Vincent Lenders, †[a] Xanthippi Koutsoumpou, †[a] Philana Phan,†[b] Stefaan J. Soenen, [ac] Karel Allegaert,[defg] Steven de Vleeschouwer,[hij] Jaan Toelen,[fgk] Zongmin Zhao[b] and Bella B. Manshian *[a]

The biomedical use of nanoparticles (NPs) has been the focus of intense research for over a decade. As most NPs are explored as carriers to alter the biodistribution, pharmacokinetics and bioavailability of associated drugs, the delivery of these NPs to the tissues of interest remains an important topic. To date, the majority of NP delivery studies have used tumor models as their tool of interest, and the limitations concerning tumor targeting of systemically administered NPs have been well studied. In recent years, the focus has also shifted to other organs, each presenting their own unique delivery challenges to overcome. In this review, we discuss the recent advances in leveraging NPs to overcome four major biological barriers including the lung mucus, the gastrointestinal mucus, the placental barrier, and the blood–brain barrier. We define the specific properties of these biological barriers, discuss the challenges related to NP transport across them, and provide an overview of recent advances in the field. We discuss the strengths and shortcomings of different strategies to facilitate NP transport across the barriers and highlight some key findings that can stimulate further advances in this field.

Received 26th January 2023

DOI: 10.1039/d1cs00574j

rsc.li/chem-soc-rev

1. Introduction

Since its first introduction, nanomedicine has aimed to manifest itself as a major solution to problems in the drug delivery field. Indeed, nanomaterials have been able to mitigate major therapeutic limitations, including protection from rapid degradation, improved drug absorption, improved targeted delivery and – related to this – reduced off-target side effects. These improved therapeutic traits have led to promising preclinical and clinical therapeutic applications.[3] Application areas include nanovaccines,[4] hemostasis,[5] targeted cancer therapy,[6–8] with well-known commercial examples Abraxane® and Doxil®, and inflammation.[9] Recently, the clinical translation of nanomaterials has been boosted by the introduction of the COVID-19 lipid nanoparticle mRNA vaccines, illustrated by the start of over 55 clinical trials using new nanoparticle technologies since 2019.[10]

However, despite these achievements, major challenges remain in the field of nanomedicine. For example, industrial manufacturing of nanomaterials on a large scale remains, although evolving, a grey area, with limited knowledge of key parameters and process conditions during synthesis.[11] However, also regarding the selective delivery of therapeutic agents to specific targeted tissues, nanomedicine has not been able to live up to its original hype. Ever since the sobering meta-analysis by Wilhelm and colleagues, revealing that only a

[a] *Translational Cell and Tissue Research Unit, Department of Imaging and Pathology, KU Leuven, Herestraat 49, B3000 Leuven, Belgium. E-mail: bella.manshian@kuleuven.be*
[b] *Department of Pharmaceutical Sciences, College of Pharmacy, University of Illinois at Chicago, Chicago, IL 60612, USA*
[c] *NanoHealth and Optical Imaging Group, Department of Imaging and Pathology, KU Leuven, Herestraat 49, B3000 Leuven, Belgium*
[d] *Department of Hospital Pharmacy, Erasmus MC University Medical Center, CN Rotterdam, 3015, The Netherlands*
[e] *Clinical Pharmacology and Pharmacotherapy, Department of Pharmaceutical and Pharmacological Sciences, KU Leuven, B3000 Leuven, Belgium*
[f] *Leuven Child and Youth Institute, KU Leuven, 3000 Leuven, Belgium*
[g] *Woman and Child, Department of Development and Regeneration, KU Leuven, 3000 Leuven, Belgium*
[h] *Department of Neurosurgery, University Hospitals Leuven, Leuven, Belgium*
[i] *Laboratory of Experimental Neurosurgery and Neuroanatomy, Department of Neurosciences, KU Leuven, Leuven, Belgium*
[j] *Leuven Brain Institute (LBI), KU Leuven, Leuven, Belgium*
[k] *Department of Pediatrics, University Hospitals Leuven, 3000 Leuven, Belgium*
† These authors contributed equally.

median nanomaterial delivery efficiency of 0.7% to solid tumors has been achieved, increased attention has been focused on investigating the reasons behind this low target efficiency.[12] After intravenous injection of nanoparticles (NPs), adsorption of opsonin results in the formation of a protein layer around the NPs, referred to as the protein corona. Subsequently, NPs are recognized by the mononuclear phagocyte system (MPS). Uptake of the NPs by macrophages then clears the NPs from the bloodstream, usually within minutes.[13] In a similar fashion, inhalation and subsequent alveolar deposition of NPs is subjected to clearance by alveolar macrophages, significantly reducing the lung residence time of these NPs.[14] Rapid opsonization and subsequent clearance of nanoparticles are therefore major contributors to low targeting efficiencies and underwhelming therapeutic effects of NP-based strategies. A well-accepted solution to avoid interaction of nanomaterials with immune cells is stealth coating, for example surface PEGylation, which prevents adsorption of proteins.[15] Also, circulatory cell mimicking or hitchhiking particles have been shown to decrease the clearance rates, by leveraging the biological features of, for example, red blood cells or circulatory immune cells, and thereby avoiding MPS phagocytosis.[16–18] Alternatively, partial blocking of the MPS may enhance the performance of NPs, for example through pretreatment with liposomes or by inducing a partial depletion of erythrocytes by injection of allogeneic anti-erythrocyte antibodies.[19,20]

The second reason for the only modest nanomedicine success has been the failure of several active and passive targeting strategies to, effectively, increase NP accumulation in target organs. For example, many NP delivery strategies have

Karel Allegaert

*Karel Allegaert (MD, PhD) is a pediatrician (1999)-neonatologist (2000) and clinical pharmacologist (2003). He is full professor at KU Leuven, departments of Development and Regeneration, and Pharmaceutical and Pharmacological Sciences, and senior consultant (part-time) at Erasmus University, Rotterdam, Department of Clinical Pharmacy (**https://www.researchgate.net**/profile/Karel-Allegaert; ORCID: 0000-0001-9921-5105). His research is mainly focused on perinatal and pediatric clinical pharmacology and its co-variates (maturational, non-maturational, pharmacogenetics, disease-related), with the subsequent use of in vivo datasets to develop prediction models and translation to support drug development in these special populations (neonates, children and pregnant women, or during lactation).*

Jaan Toelen

Jaan Toelen (MD, PhD) is a staff member in Pediatrics at the University Hospitals Leuven and an associate-professor at KU Leuven, Department of Development and Regeneration (ORCID: 0000-0001-9339-5408). His research is mainly focused on pre- and postnatal lung development and neonatal lung disorders such as bronchopulmonary dysplasia and congenital diaphragmatic hernia with both a basic science and a translational-clinical perspective. His research group uses several animal models to study these conditions and to test experimental strategies before further clinical translation.

Zongmin Zhao (left) and Philana Phan (right)

Zongmin Zhao is an Assistant Professor in the College of Pharmacy at the University of Illinois Chicago. He received a PhD degree from Virginia Tech and was a postdoctoral fellow at Harvard University. The research interests of his group are focused on developing bioinspired and biomimetic strategies to improve the diagnosis and treatment of diseases including cancer, autoimmune diseases, acute injuries, and drug addictions. Dr Zhao has published >50 articles in journals including Cell, Nature Biomedical Engineering, PNAS, Science Advances, Advanced Materials, etc. He is currently an Associate Editor of Bioengineering & Translational Medicine.
Philana Phan is currently a second-year PhD student in the laboratory of Dr Zongmin Zhao. She completed her BA in biochemistry from New College of Florida in 2020. Her research interests at UIC are focused on the development of cell-based immunotherapies and understanding the immunomodulatory mechanisms behind these therapeutics in the treatment of cancer.

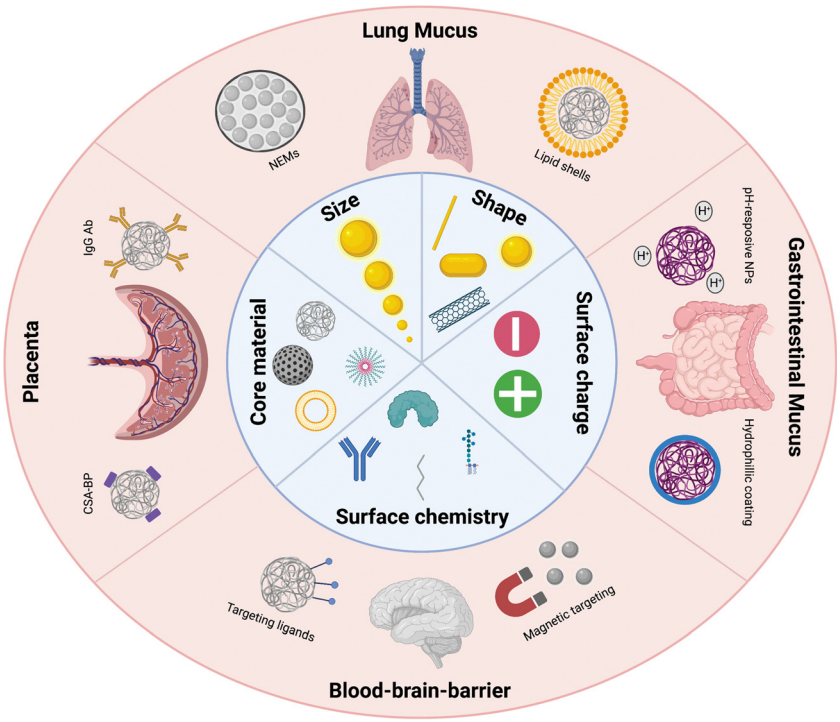

Fig. 1 A representative image of the various biological barriers discussed in this review and some of the successful strategies to overcome these barriers. Illustration was made using https://BioRender.com.

relied (solely) on the enhanced permeability and retention (EPR) effect for passive tumor targeting, where interstitial accumulation of NPs could be achieved due to the leakiness of the tumor vasculature. However, reliance on the EPR effect has not shown promising clinical results and the significance of the EPR role as the main driver of tumor targeting has been challenged.[21–23]

Finally, the third challenge is the presence of physical biological barriers, effectively blocking the passage of cargo-loaded nanoparticles to the organs or regions of interest. The endothelial barrier is the most predominant barrier, impeding translocation over the vascular vessel, when NPs are injected intravenously, or limiting uptake by target endothelial organ cells (barriers of organs). The exact mechanisms underlying vascular crossing or organ uptake are not yet elucidated, but some mechanisms have been suggested. Possible pathways for endothelial uptake include phagocytosis, micropinocytosis, and clathrin- and caveolin-dependent or receptor-mediated endocytosis.[24,25] The NP uptake efficiency by endothelial cells of distinct organs, including liver, lungs, brain and kidney, has been shown to be significantly different, likely due to differences in, among others, surface receptors.[26] Overcoming the vascular endothelial barrier, referred to as extravasation, has been suggested to be possible through dysfunction of the tight junction, for

From left to right: Bella B. Manshian, Vincent Lenders, Xanthippi Koutsoumpou, Stefaan J. Soenen

The group of Bella Manshian (PhD), part of the Translational Cell and Tissue Research Unit, works on translational nanomedicine using advanced 3D precision cut tissue models and engineered nanoformulations for drug delivery. Vincent Lenders and Xanthippi Koutsoumpou (4th year PhD students) have been working in the group on cell based drug delivery systems across biological barriers. They also collaborate closely with the NanoHealth and Optical Imaging Group of Stefaan J. Soenen (PhD), focusing on non-invasive monitoring of nanoparticle distribution in preclinical model systems.

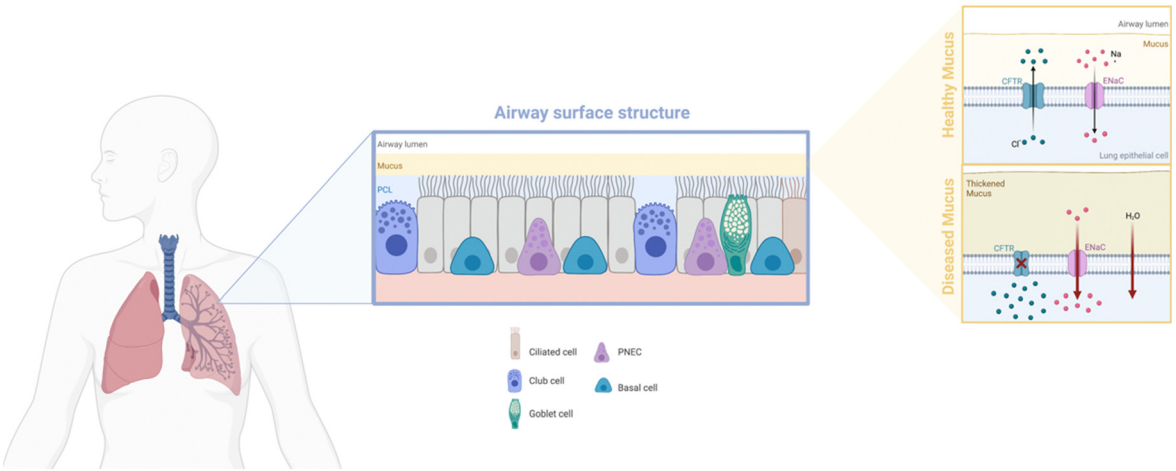

Fig. 2 Schematic depicting the makeup of the airway surface structure, with bronchial mucus in the healthy or diseased state. Illustration was made using **https://BioRender.com**.

example by nanoparticle induced endothelial leakiness (NanoEL). Some NPs can induce micrometer sized gaps in the vascular endothelial barrier, by disrupting the VE-cadherin–VE-cadherin interactions, which eventually leads to the induction of actin remodeling.[27] While this offers a significant opportunity for nanomedicines, a recent study highlights the potential effects it may have on facilitating cancer metastasis.[28]

While many barriers of organs can be considered as an endothelial barrier, there are some special cases where the barrier is complexified. For example, the endothelial blood–brain barrier is generally considered as a stronger barrier compared to the liver or kidney barrier, as brain endothelial cells are non-fenestrated and more tightly packed allowing for more controlled brain protection.[29] Similarly, the placental barrier consists of, next to an endothelial layer, 3 additional barrier layers, which is necessitated by the crucial protection of the developing fetus. Other special barriers include the lung mucus and gastrointestinal barrier, where a superficial mucus layer strengthens control on intake or inhalation of unwanted particles.

As a thorough understanding of the interaction mechanisms of nanomaterials with these physical barriers is critical for better design of nanomedicine-based therapies, we herein offer an overview of the research that has been performed on nano-barrier interactions (Fig. 1). In this review, we have specifically focused on the 4 special barriers of organs discussed earlier. Administration of NPs through inhalation is challenged by the presence of the lung mucus barrier, while the gastro-intestinal mucus barrier is the main physical barrier to be crossed for oral delivery strategies. Within systemic administration, we have focused on the blood–brain barrier, being a major research focus for brain-related diseases and given its non-fenestrated endothelial barrier, and the placental barrier, given its unique role in both maternal and fetal therapeutic strategies and its unique 4-layer barrier composition. Other special systemic barriers, such as the blood–testis barrier and blood–milk barrier, are not discussed given their very limited nanomedical research focus. For each biological barrier, the NP characteristics that can be tuned to enhance or hinder the transport through these barriers are analyzed and advanced technologies to overcome these barriers are discussed. Finally, suggestions are given for improved translatability of barrier-crossing nanomaterials.

2. Lung mucus barrier

The mucus forms a very effective protection layer against injury at multiple sites in (in)direct contact with environmental exposure, such as the intestine, nose and lungs. However, in addition to protection against environmental toxins and microbes,[30] the lung mucus also complexifies administration routes for drug delivery, both for localized lung delivery and for systemic delivery through inhalation. For localized lung delivery, the airway route is one of the most straightforward administration routes, as lungs are easily accessible *via* inhalation.[31] However, major hurdles remain for effective airway drug delivery, mainly due to natural safeguard barriers of the lung, protecting against deep inhalation of large particles or microbe entry. Biological barriers include the typical branched structure of the respiratory tract, the mucus layer, the periciliary layer and alveolar macrophages.[32] These natural protection barriers complicate airway drug delivery by filtration of inhaled agents, restricted permeation and mucociliary clearance, resulting in poor therapeutic efficiencies. In this section, we will describe more in depth the lung mucus as a biological barrier for airway drug delivery and analyze how NP formulation strategies are used to overcome the lung mucus barrier, improving current therapeutic strategies for asthma, cystic fibrosis (CF), chronic obstructive pulmonary disease (COPD), bronchopulmonary dysplasia (BPD) and cancer.[33–35]

2.1. Mucus barrier characteristics

The typical biological features of the lung mucus (Box 1) lead to the formation of a steric filter through a size-exclusion gradient towards the epithelial surface. The molecular mesh tightens towards the cellular surface, so that the particles with a

diameter (d) larger than the local correlation length (ξ) are impeded from reaching the cell surface.[36] The mesh size ranges from 100 to 1000 nm, depending on the airway site. The protective mucus layer progressively reduces in thickness as the alveolar region is approached, decreasing from a thickness of 10–30 μm at the tracheal level to 2–5 μm in the smaller bronchi. At the alveolar level, type II pneumocytes excrete a surfactant, a mixture of phospholipids and proteins, which lines the alveoli with the main function of reducing surface tension.[37] This site-dependent mucus volume, combined with the size-exclusion gradient, is essential in balancing the successful entrapment and removal of particulates, while allowing the passage of small molecules for gas exchange at the lung alveoli.[38]

Box 1: Lung mucus characteristics

Although the basic properties are shared, mucus secretions are adapted to suit their specific mucosal location. In the conducting airways, the main structural trait of bronchial mucus is its 2-layer system: the actual mucus and the underlying periciliary liquid layer (PCL) (Fig. 2). The mucus is a hydrogel consisting of water (90–95%), mucins, lipids, electrolytes, DNA, enzymes and cellular debris, with mucins, secreted by goblet cells, as the main functional components.[40] Mucins are glycoproteins that, through cysteine rich regions, undergo dimerization and subsequent polymerization of the monomers *via* disulfide bonds.[41] This aggregation behavior, further stabilized by weaker hydrophobic and electrostatic interactions, leads to the formation of a gel-like structure.

The PCL has been shown to consist of membrane-spanning mucins and large mucopolysaccharides tethered to the cilia, microvilli and the epithelial cells, providing an effective 'gel-on-brush' system.[36] This structural feature allows for an added dimension to the mucus as an effective biological barrier. Through continuous secretion of mucins by the goblet cells, removal of excessive mucus is facilitated, creating a clearance mechanism. The PCL is less viscous and allows for beating of the cilia as well as lubrication of the cellular layer, allowing for the upwards movement of the mucus in the airways. Clearance of foreign material can be achieved within 15 to 20 minutes after capturing in the mucus. Mucociliary clearance can be further assisted by reflexive coughing if the airways are irritated by foreign matter.[42]

Mucins, containing negatively charged side chains, and mucin-associated compounds such as lipids and DNA, can interact with particulates through electrostatic interactions, hydrophobic interactions and H-bonding. Therefore, the mucus also forms an interaction filter, capable of entrapping small, interacting particles.[39]

Of note, mucus characteristics can change significantly in disease states, depending on the disease type and stage. The thickness of healthy mucus is approximately 30 μm and can easily be transported through ciliary beating. However, a decrease in elasticity or an increase in viscosity and thickness can impede mucus transport.[42] Lung disorders, such as cystic fibrosis (CF), chronic obstructive pulmonary disease (COPD) or primary ciliary dyskinesia, often show defects in ciliary transport.[38] Clearance defects in lung disorders are found to be beneficial for therapy purposes as, due to the slowed or abnormal ciliary beating, retention times of drug-loaded nanoparticles are increased at the mucus site.[43] Although the mechanisms underlying the mucociliary clearing defects are not yet elucidated, the contributing factors are as follows: (i) mucus dehydration: water is crucial in governing the gel-like state of the mucus. For example, exposure to cigarette smoke has been linked to mucus dehydration, leading to an increased mucus concentration. This, in turn, generates a partial osmotic pressure exceeding basal PCL values and eventually reduced mucociliary clearance, aiding in the pathophysiological development of chronic bronchitis.[44,45] Similarly, absence of ion channels, and consequently disruption of the ion streams, after mutation of the cystic fibrosis transmembrane conductance regulator gene, leads to dehydration and acidification of CF airways.[46] (ii) Mucus hypersecretion: upregulation of mucin expression has been associated with chronic airway diseases, with MUC5B becoming dominant in mucus in disease states. Hypersecretion leads to increased mucus concentration, changing the rheological properties of the mucus and hampering mucociliary clearance.[47,48]

2.2. NM engineering for lung mucus penetration

With mucus acting as a multiparametric barrier, airway drug delivery strategies are required to overcome the size exclusion gradient, interaction filter and clearance mechanism of the mucus. Multiple NP formulations and designs have been researched over the years and are commonly referred to as mucus penetrating particles (MPPs); a general overview of these is given in Fig. 3. The details of the most recent strategies are tabulated in Table 1. Strategies not focused on overcoming the lung biological barrier, for example alveolar macrophage targeting therapies, are not considered in the scope of this review.[49]

2.2.1. Core material. The most popular choice of core materials (Fig. 3A) is polymeric materials, in particular poly(lactic-*co*-glycolic acid) (PLGA), due to their use in FDA approved formulations and their ease of synthesis and tunable drug release properties.[80,81] Also, lipid nanoparticles have been researched, as they offer prolonged release, better NP safety due to the avoidance of organic solvents and relatively weak interactions with mucins.[50,82] A few reports have been published on the use of nanocrystals (NCs) for mucus crossing. NCs offer the advantage of having near 100% drug content, improving the chance of delivering the required therapeutic concentration.[83] Only 1 report was published on the use of a carbon-based carrier. Chen *et al.* designed a tetra(piperazino)fullerene epoxide (TPFE) NP providing efficient pulmonary gene delivery. TPFE is mainly attractive because of its excellent DNA compaction and protection properties.[63]

The choice of the core material appears to be mainly driven by the specific application and the drug types to be delivered. Limited research has been performed on the effect of the core material on mucus crossing, probably because most unmodified NPs, especially hydrophobic polymers, fail to penetrate the mucus in a satisfactory manner. The main exception to this is liposomes. Surfactant-mimicking liposomes can be designed,

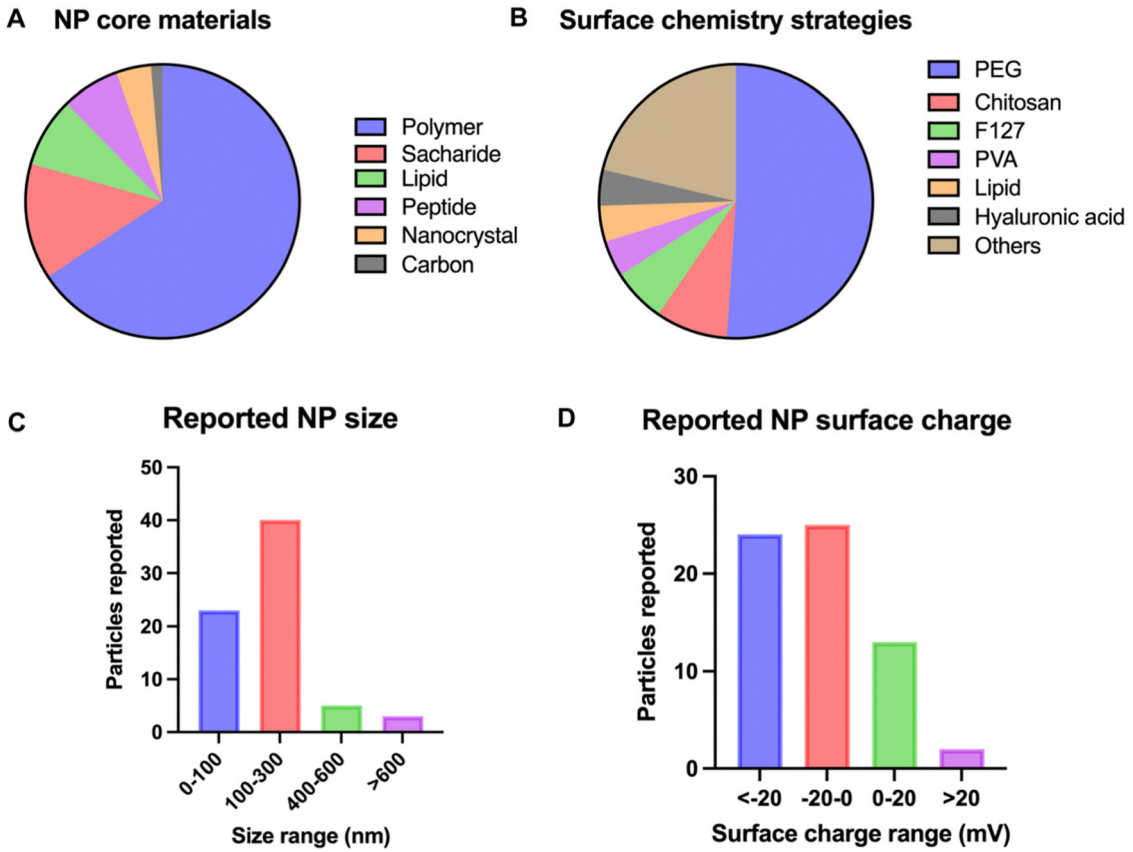

Fig. 3 Overview of NP characteristics used for airway drug delivery. The characteristics of interest are (A) NP core material, (B) NP size, (C) surface chemistry and (D) NP surface charge. Graphs are based on data extracted from the PubMed database of the last 10 years using the search terms 'lung', 'mucus', 'nanoparticle', and 'delivery', identifying 97 manuscripts. 62 articles were used for data insights. Only original research articles and articles within the scope were included.

consisting of dipalmitoyl-phosphatidylcholine (DPPC), a component of the pulmonary surfactant. This biomimetic approach protects the cargo against degradation, improves NP diffusivity and increases lung retention.[51] Furthermore, liposomes offer excellent epithelial cell uptake after mucus penetration, as was shown for pulmonary fibrosis treatment with PGE2.[84] The potential of liposomal formulation is further illustrated by its translation to clinical trials and FDA approval of, for example, Arikayce, a liposomal formulation of amikacin.[85,86]

2.2.2. Size. Given the size exclusion gradient characteristic of the mucus, restricted crossing of larger particles can be expected. The importance of size constraints is illustrated with the majority of reported NPs for barrier crossing having a maximum diameter of 300 nm (Fig. 3B). Illustratively, He *et al.* showed that curcumin nanocrystals (NC) of size ~250 nm exhibit higher diffusion percentages compared to NCs of size ~500 nm, which in turn have higher diffusion percentages compared to NCs of size ~1000 nm.[56] This size exclusion gradient is not linear, as shown in a study by Murgia *et al.*[87] Mechanical dispersion in the mucus of 100, 200 and 500 nm polystyrene (PS) nanoparticles led to, as expected, the entrapment of the largest 500 nm NPs, while the fraction of 100 and 200 nm particles could diffuse in the mucus. However, when the same experiment was performed with aerosol deposition on the mucus layer, only the 100 nm particles were observed to penetrate the mucus, indicating that at the air–mucus interface, smaller pores are present.

Although the size constraints for mucus penetration are widely accepted, mucus penetrating particles have been formulated with sizes up to 800 nm by aspect ratio engineering. For example, Costabile *et al.* made benzothiadiazole nanocrystals of 823 nm that showed diffusion in artificial CF mucus due to their elongated nanorod shape.[58]

2.2.3. Surface engineering. For improving the airway delivery of drug-loaded NPs, muco-adhesive particles (MAPs) have long thought to be one of the most promising design strategies. Muco-adhesion of MAPs is generally mediated by electrostatic attraction of cationic MAPs with negatively charged mucins, although hydrophobic interactions might also be at play for polymeric nanoparticles with hydrophobic regions. However, in an important study performed by Schneider *et al.*, MAPs were directly compared to mucus inert or mucus-penetrating particles (MPPs). Multiple-particle tracking analysis revealed the aggregation and poor airway distribution of MAPs, regardless of size. In contrast, MPPs up to 300 nm showed uniform distribution and improved retention. Additionally, MPPs diffused more rapidly within human mucus.[88]

Table 1 Details of the most recent NP engineering strategies, based on data extracted from the PubMed database of the last 5 years using the search terms 'lung', 'mucus', 'nanoparticle', and 'delivery'. Only original research articles and articles within the scope were included

NM engineering strategy	Surface modification	Core material	Size (nm)	Zeta potential (mV)	Model system	Diseased/healthy state	Comments	Ref.
Core material	/	Stearic acid/F127/Tween 20	90 ± 6	−9.5 ± 1.4	Artificial mucus	Diseased	Zeta potential and size effect were evaluated, favoring a near-zero charge and small size	50
		DPPC	102.6 ± 0.3	−34 ± 10	LPS-induced mouse model	Diseased		51
		DSPC/cholesterol/DSPE-PEG	161 ± 1	−7.9 ± 0.6	Artificial mucus	Healthy		52
		Hyaluronic acid	280	−61 ± 4	Artificial mucus	Healthy		53
		Dextran	200 to 300	−30 to −50	Artificial mucus	Diseased		54
Sizing	/	PLGA	100 to 2500	Around -20	Artificial mucus	Diseased	Smaller NPs (100 nm) have better lung retention and adsorption properties than larger NPs (300, 800 and 2500 nm)	55
		Curcumin (nanocrystal)	246 to 1089	/	Rat model	Healthy	Small NCs show higher dissolution rates. Crossing of the mucus occurs mainly by the free drug form	56
Surface engineering: polymeric coatings	PEG	PBAE	53 ± 2	0.7 ± 0.3	*Scnn1b*-Tg mouse model	Diseased		57
		C190 (nanocrystal)	823 ± 123	-21.2 ± 6.07	Artificial mucus	Diseased	Rod shaped NPs	58
		FLR (peptide)	Around 100	Around 5	Mouse model	Healthy	Effect of the PEGylation rate was evaluated, with 40% the most optimal	59
		PBAE	55 ± 1	1.6 ± 0.3	Orthotopic lung cancer model	Diseased		60
		PLGA	Around 3000	/	Rat model	Healthy	Effect of PEG molecular weight was evaluated, with 2 kDa the most optimal	61
		PHEA-PCL	51.1	−14.4 ± 4.6	Artificial mucus	Healthy	NEM (see nano-embedded microparticles)	62
		TPFE	73.4 ± 0.7	1.3 ± 0.2	*Scnn1b*-Tg mouse model	Diseased		63
		PS	104.6 ± 1.2	−4.9 ± 0.3	Artificial mucus	Healthy + diseased		64
		PLGA	130.9 ± 2.17	1.97 ± 0.1	Bleomycin sulfate-induced mouse model	Diseased		65
		oxi-aCD	254.2 ± 9.5	−32.4 to −37.4	*P. aeruginosa* mouse model	Diseased	Folic acid was added for better cellular uptake	66
	Hyaluronic acid	Poly(b-amino ester)	150	10	LPS-induced mouse model	Diseased		67
		PLGA	228	Around -50	*P. aeruginosa* mouse model	Diseased		68
	Pluronic F127	PLGA	307.5 ± 9.54	−11.3 ± 0.4	/	/	No mucus interaction experiments performed	69
	PVA	PLGA	261 to 282	−0.67 to −0.84	*P. aeruginosa* mouse model	Diseased		70
	CS-A	pDNA/siRNA (CRHC-2/M9)	200 to 400	20 to 25	Mouse model	Healthy		71
	PMeOzi PMeOx	Co-polymer: grafted PHEA and PLA	95 ± 5 78 ± 3	−7.2 ± 4.7 −5.8 ± 4.5	Artificial mucus	Healthy	NEM (see nano-embedded microparticles)	72
Surface engineering: lipid shells	DPPC	PLGA	177.6 ± 9.2	−28.7 ± 1.6	*In vitro* model with mucus-covered Calu-3 cells	Healthy + diseased	Bare lipid shell NPs showed better epithelial internalization compared to PEGylated lipid shell NPs	73
			174 ± 2.03	−29.2 ± 1.58	Artificial mucus	Diseased		74
			238 ± 9	−25 ± 1	Mouse model	Healthy	More neutrally charged lipids DPPC and DPPE led to macrophage uptake inhibition, while negatively	75
	DPPE		230 ± 10	−26 ± 1				

Table 1 (*continued*)

NM engineering strategy	Surface modification	Core material	Size (nm)	Zeta potential (mV)	Model system	Diseased/healthy state	Comments	Ref.
							charged lipids DPPG and DPPS led to increased macrophage uptake	
Surface engineering: peptide coating	Peptide CPSSSREKC	PS	180 ± 3.8	−21.4 ± 1.6	*Ex vivo* human CF sputum + mouse model	Diseased (*ex vivo*) and healthy (*in vivo*)		76
Nano-embedded microparticles	PMeOzi PMeOx	Co-polymer: grafted PHEA and PLA	95 ± 5 78 ± 3	−7.2 ± 4.7 −5.8 ± 4.5	Artificial mucus	Healthy	NEM size: around 4 μm	72
	PEG	PHEA-PCL	51.1	−14.4 ± 4.6	Artificial mucus	Healthy	NEM size: 2 μm	62
Others: redox-responsive NPs	PEG	PLGA	120	−30	Artificial mucus	Healthy		77
Others: enzyme-modified NPs	Papain	Dextran	200	−50	Artificial mucus	Diseased		78
Others: size-shifting NPs	Phosphate ester and octadecylamine	Lipid	126.4 ± 3.5	−27.9 ± 1.3	*In vitro* model with mucus-covered Caco-2 cells	Healthy		79

Consequently, overlooking the reported NP formulations in the past decade, this study shifted design strategies for airway NP delivery towards creating negatively or near-neutrally charged NPs (Fig. 3D), in most cases combined with a hydrophilic coating to limit attraction with mucin glycoproteins through electrostatic and hydrophobic attraction. This effect was also seen in coarse-grained molecular dynamics (CGMD) simulations after modeling the surfactant monolayer translocation behavior of PEG-grafted gold NPs (Fig. 4A).[89] All neutral NPs could penetrate the surfactant, regardless of grafting density or monomer number per chain. Charged NPs with a low monomer number per chain and a high grafting density were impeded from undergoing translocation. Lowering the grafting density or the length of the grafting polymer reallows penetration, likely due to the decrease in surface density. Furthermore, through analyzing the interaction energies between differently charged NPs and the lipid heads, it was observed that positively charged particles take longer to penetrate and adhere to the film after penetration. This phenomenon can be attributed to stronger electrostatic interactions with the lipid heads, as well as stronger van der Waals interactions (Fig. 4B). Reducing the hydrophobicity of the particle surface has also been shown to improve pulmonary biocompatibility *in vivo*.[90]

2.2.3.1. Polymeric coatings. PEG is by far the most used surface modification for this purpose (Fig. 3), and has been shown to improve mucus penetration and therapy effectiveness for cystic fibrosis,[57] inflammation[62] and cancer.[91] Recently, siRNA against *IL11* was co-loaded into PLGA-PEG diblock polymeric NPs with a cationic lipid-like molecule G0-C14, which facilitates transmucosal delivery. Inhalation of these RNAi NPs was shown to effectively inhibit fibrosis in a post-bleomycin challenged mouse model.[65] Surface coating with PEG, however, should be carefully optimized for its surface density and molecular weight. A 5 wt% PEG content is believed to be

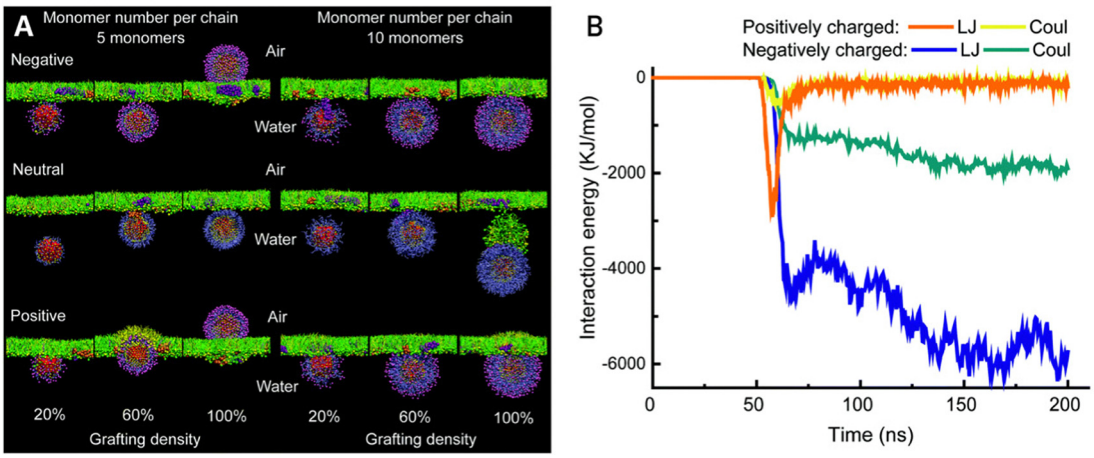

Fig. 4 (A) Snapshots of NPs interacting with a lung surfactant monolayer in a CGMD model. NP variations include monomer number per chain, grafting density and terminal charge. (B) Interaction energy diagram of differently charged NPs with the lipid heads of the surfactant monolayer. Coul stands for electrostatic interactions, and LJ stands for van der Waals interactions. Adapted from ref. 89 with permission from The Royal Society of Chemistry.

needed for effectively shielding the nanoparticle core from mucus interactions.[92] Although some studies have reported on effective bronchial epithelial cell uptake of PEGylated NPs,[93] it is important to note that an increased PEG content or PEG molecular weight may limit cellular uptake and can therefore hamper delivery effectiveness.[94]

Multicomponent coatings have been proposed as a strategy to leverage the transmucosal traits of PEG, while still ensuring uptake by target cells. Wang *et al.* formulated oxy-α-cyclodextrin particles coated with 1,2-distearoyl-*sn*-glycero-3-phosphoethanolamine (DSPE)-PEG and DSPE-PEG-folic acid. While the PEG layer was shown to improve mucus penetration, the use of folic acid improved the uptake by the targeted macrophages, mediated by membrane folate receptors.[66] Another example of multicomponent coatings is related to DNA delivery applications. Dense PEG coating may interfere with DNA compaction, entailing larger NPs with poorer mucus penetrating and cellular characteristics. However, Suk *et al.* reported that using polyethylenimine (PEI)/PEG-PEI or poly-L-lysine (PLL)/PEG-PLL mixtures in optimal ratios can reduce the hydrodynamic size by ~15% compared to particles using PEG-PEI or PEG-PLL coatings only. This approach reduced the mean square displacement ratio $MSD_w/\langle MSD\rangle$ by ~16 fold and ~136 fold for PEI and PLL NPs, respectively, indicating a significant improvement of diffusivity in CF mucus.[95] Finally, non-covalent modification of PEG-NPs with Pluronic F127 has been reported to improve drug activity duration, likely due to an increased colloidal stability of the NP.[96] However, due to its protective nature and possible shielding of mucus interactions, Pluronic F127 alone, without additional PEG shielding, has been reported as a potential, alternative surface engineering strategy for mucus penetration.[69]

Various other hydrophilic coatings have been reported as an alternative to PEG, especially since research indicated possible immune response after repeated administration of PEGylated therapeutics.[97] Casciaro *et al.* have developed PLGA NPs coated with poly(vinyl alcohol) (PVA), which not only reduces NP aggregation, but also provides a neutral, hydrophilic surface. On loading the NPs with an antimicrobial peptide (Esc), an improved efficacy in inhibiting *Pseudomonas aeruginosa* was achieved, proven by a 3-log reduction of pulmonary bacterial burden.[70] In a similar fashion, d'Angelo *et al.* developed colistin loaded PVA-coated PLGA NPs for *Pseudomonas aeruginosa* treatment. Moreover, they tested coating with another hydrophilic polymer, namely chitosan (CS). Although it would be expected that the more positively charged CS-NPs have a higher tendency to interact with mucins, this did not hamper mucus penetration. Instead, CS facilitated mucus penetration to a greater extent than PVA, probably due to the induced collapse of mucus fibers, creating larger mesh pores.[98] The use of cationic chitosan-coated nanoparticles is especially of interest, given their good cell uptake characteristics, as shown for example in asthma treatment, although more mucus interaction studies should be performed to elucidate the dynamics of CS-particles in the mucus.[99]

Alternatively, hyaluronic acid (HA) has recently received attention for its successful creation of a hydrophilic shell and, consequently, improved mucus penetration.[68] For example, Zhu and colleagues designed HA-coated poly(β-amino ester) (BP) NPs successfully penetrating the mucus. Furthermore, once inside the interstitium, uptake by the target interstitial M1 macrophages was achieved.[67] Of note, the radical scavenging property of HA gives, together with any loaded cargo, a synergetic anti-inflammatory benefit, in this case down-regulating TNF-α siRNA.

Improved delivery of siRNA with NPs has also been achieved by using chondroitin sulfate A (CS-A) as hydrophilic coating. Kumari and colleagues recently did indeed show improved mucus penetration for CS-A-coated nanocomplexes, which was further improved by surface conjugation of mannitol, acting as a mucolytic agent. The presence of mannitol reduces mucus viscosity, likely by increasing water influx.[71]

Instead of coating NPs, grafting hydrophilic chains to hydrophobic core materials has been suggested as a design strategy for mucus penetration. Drago and colleagues reported the grafting of the hydrophobic polymer PLA and the hydrophilic chains $PMeO_x$ or PMeOzi on the poly(2-hydroxyethyl acrylate) (PHEA) backbone. The pseudo-polypeptide PO_x structures have similar mucus shielding properties as PEG but can offer the added advantage of faster excretion from the organism.[72] Whether they show similar or better cellular uptake properties as PEG should be evaluated in future work.

2.2.3.2. Peptide coating. While most surface engineering relies on polymeric hydrophilic coatings, the use of peptides as surface coatings was suggested by Leal and colleagues.[76] They developed a peptide-presenting phage library, which can be used for high-throughput screening to identify peptide coatings with the desired mucus inert functionalities. This screening allowed identification of neutral net-charge, hydrophilic sequences (CGGQDLKSC, CSNLTSP*C and CPSSSREKC), mainly composed of glycine, serine, glutamic acid and aspartic acid. CPSSSREKC was shown to be the most promising peptide, as CPSSSREKC-coated PS NPs were more abundantly taken up by cells in a transwell co-culture assay with CF sputum and showed 90% retainment in mouse lungs 24 hours after administration. Interestingly, the peptide-coated PS NPs significantly outperformed PEGylated PS particles (Fig. 5).

2.2.3.3. Lipid shells. A more established surface engineering strategy is the use of lipid shell NPs. While liposomes tend to have several drawbacks in terms of stability and drug release properties, they do offer mucus penetrating traits, as discussed earlier. A lipid shell-enveloped polymeric NP formulation, as reported by Wan *et al.*, combines mucus penetration with sustained drug release from the polymeric core.[100] Conte *et al.* reported a hybrid lipid/polymer NP that effectively achieved gene silencing in an *in vitro* CF model. Moreover, it was demonstrated that bare polymer/lipid nanoparticles, following mucus penetration, are capable of internalization by epithelial cells, whereas epithelial internalization is hampered

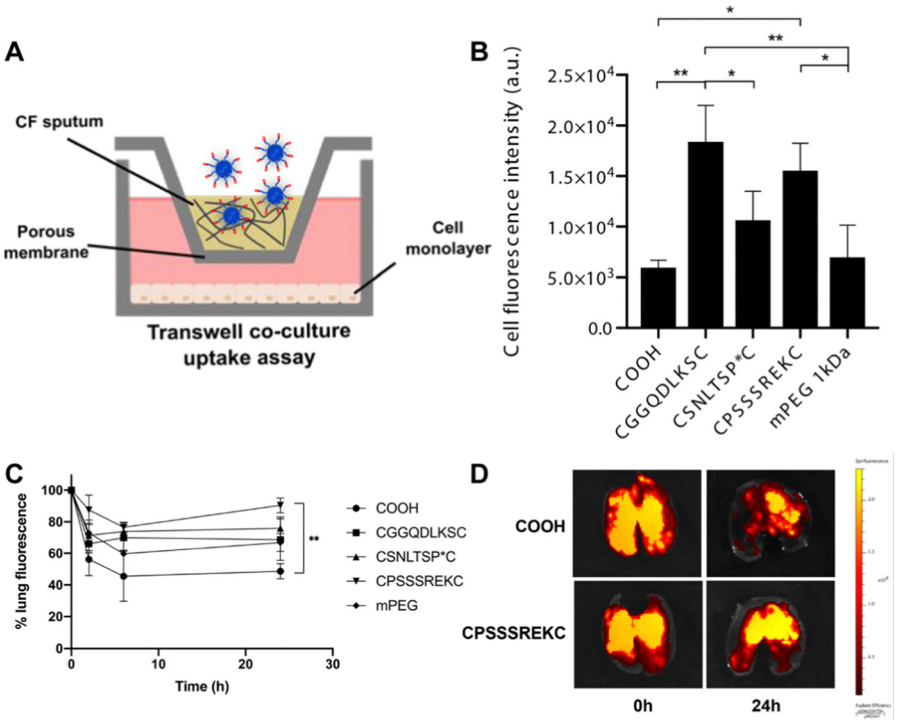

Fig. 5 (A) Schematic of transwell co-culture. (B) Fluorescence intensity of cells after incubation with bare, peptide-coated and mPEG coated PS NPs. (C) NP retention in the lung, measured up to 24 h post-administration. (D) Representative *ex vivo* lung images at time point 0 and 24h. *$p < 0.05$, **$p < 0.01$. Adapted from ref. 76 with permission from Elsevier.

for PEGylated polymer/lipid NPs.[73] The use of lipids for improved mucus penetration and epithelial cellular uptake was also reported by Liu *et al.*, who developed mucus-inert NPs by biomimetic modification with endogenous surfactants, in particular DPPC.[75]

2.2.4. Nano-embedded microparticles. The former examples of NP design strategies illustrate the advantages of nanomaterials for crossing the mucus barrier. However, a major shortcoming of using NPs, especially particles between 100 and 1000 nm, for airway drug delivery is their low deposition efficiency after inhalation, as most NPs are exhaled during inhalation. In contrast, microparticles with aerodynamic diameters of 1 to 5 μm are effectively deposited into the lungs.[101] However, the size exclusion barrier of the mucus, as discussed earlier, and the higher phagocytic rate by macrophages limit the effectiveness of these larger particles. In a successful effort to improve deposition rates, while ensuring mucus penetration, nano-embedded microparticles (NEMs) have been designed.

These formulations consist of mucus penetrating NPs, which are embedded in a microparticle carrier containing an excipient. Once the NEMs reach the mucus, the embedded NPs are released and can spread along and penetrate the mucus (Fig. 6). For example, Craparo *et al.* synthesized rapamycin loaded, PEGylated copolymer nanoparticles embedded in mannitol-based microparticles by spray drying. The NEMs released rapamycin in artificial lung fluid, indicating the successful disintegration of mannitol.[62] Mannitol NEMs have also been successfully designed for gene editing purposes by co-loading siRNA with the cationic lipid dioleoyl-3-trimethylammonium propane (DOTAP) for improving gene silencing properties.[102] Excipients other than mannitol have been researched as well. In an earlier study, lactose was successfully employed as an excipient. Within this study, a comparison was made between PVA and chitosan as a NP stabilizer for antibiotic loaded PLGA NPs. Although both yielded good NEMs, the aerodynamic properties of both

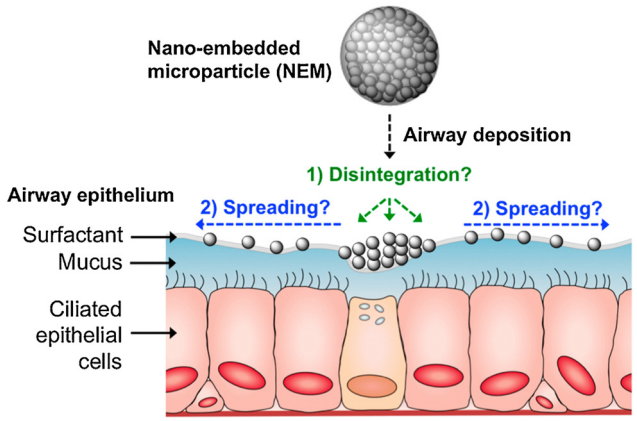

Fig. 6 Schematic overview of the fate of NEMs after deposition on the pulmonary surface. (1) Possible disintegration of the excipient after contact with the mucus. (2) Possible epithelial spreading of the released NP due to ciliary beating movement. Reproduced from ref.104 with permission from Elsevier.

differed as illustrated by the difference in disposition of the NPs. While PVA NPs reached alveoli, chitosan NPs were mainly found in high amounts in the upper airways.[103]

In a study by Porsio *et al.* for the treatment of microbial infections in cystic fibrosis, NEMs were synthesized with either mannitol or PVA, both resulting in NEMs of desired aerodynamic properties. However, mannitol-based NEMs showed better antimicrobial activity and improved CF lung function. The latter was further improved by mixing mannitol with cysteamine.[105] The supremacy of mannitol as an excipient is due to its potential to improve mucus penetration by increasing the fluidity, and thereby the mesh size, of the mucus.[105,106]

Key to the performance of NEMs is the disintegration of mannitol, releasing the embedded NPs. Meticulous analysis of excipient disintegration in an *in vivo*-like environment is thus needed. Torge *et al.* performed a disintegration study under lung-like conditions and showed that exposure to high air humidity is sufficient for mannitol disintegration. However, the disintegration time was significantly influenced by the mannitol content. In their study 20% mannitol content ensured fast release of NPs before clearance.[107] In another study, performed by Ruge *et al.*, the disintegration of NEMs was shown to be only successful when mechanical forces are exerted on the mucus, implicating possible limitations to the use of NEMs for efficient drug delivery.[104] Better models, more closely mimicking the *in vivo* setup, are expected to bring more clarity on this in the future.

2.2.5. Others. Some other advanced strategies to further improve airway drug delivery have been reported. For example, the inclusion of a mucolytic enzyme in the nanoparticles allows for improved mucus permeability. Tran *et al.* illustrated this effect for antibiotic treatment of bronchiectasis, by incorporating papain in the antibiotic-loaded dextran particles, leading to a 1.3-fold reduction of bacterial count compared to papain-free particles.[78] However, for treating bacterial infections, it is crucial to ensure a sustained drug release for prolonged periods to prevent antibiotic resistance. For this purpose, Wan *et al.* developed a D-α-tocopheryl polyethylene glycol 1000 succinate (TPGS) coated PLGA formulation for CF-related *Pseudomonas aeruginosa* infection. TPGS consists of vitamin E and a PEG chain. The hydrophilic PEG chain, exposed outward, ensures mucus and bacterial biofilm inertion. Because of this inertion, it is important to, once inside, avoid escape of the NPs outside the biofilm. Therefore, once the NPs diffuse into the bacterial biofilm, esterases, produced by *P. aeruginosa*, cleave the outer layer of the particle, exposing the lipophilic vitamin E, which anchors the particles in the biofilm.[108]

In an effort to overcome the hampered epithelial cellular uptake of some mucus inert NPs, Conte and colleagues reported a redox-responsive delivery system by creating PEG and PLGA block copolymer NPs, which were synthesized through disulfide bridges between the 2 polymers. This system allows for (i) mucus penetration due to the hydrophilic external PEG layer, (ii) reductive cleavage of the disulfide bond by reducing agents at the cancer cell surface, which reduces the outer PEG layer and improves cellular uptake, and (iii) complete removal of the PEG layer by intracellular GSH, leading to NP breakdown and intracellular drug release (Fig. 7).[77] An alternative strategy for improved absorption has been proposed by Le-Vinh *et al.*, using size-shifting nanocarriers.[79] Solid lipid nanoparticles with a phosphate ester and octadecylamine surfactant provided negatively charged NPs that could penetrate the mucus. However, when in contact with epithelial cells, the membrane bound alkaline phosphatase cleaves and removes the phosphate ester outer layer, exposing the positively charged octadecylamine groups. The lack of negative charge leads to particle aggregation, thereby preventing back-diffusion of particles and thus extending exposure to the absorption membrane.

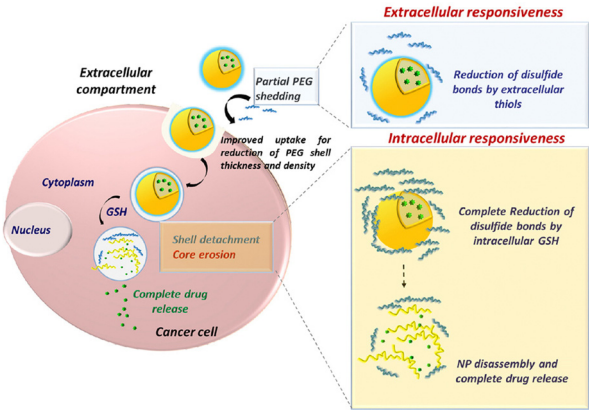

Fig. 7 Improved cellular uptake mechanism using redox-responsive, mucus penetrating nanoparticles for lung cancer therapy. Adapted from ref. 77 with permission from Elsevier.

2.3. Considerations for airway drug delivery

2.3.1. Airway delivery requirements. Pulmonary administration of drugs and their delivery vehicle requires a form of aerosolization. However, multiple parameters during aerosolization can influence the stability of the formulation and thus should be accounted for. We shortly discuss the main considerations; however, a detailed discussion of aerosolized inhalation systems falls outside the scope of this review but has been discussed elsewhere for drug and gene delivery.[109–111]

2.3.1.1. Inhalation devices. The type of nebulizer used has been shown to influence delivery efficiency and should be chosen carefully. Additionally, current nebulizers often fail to achieve deep lung disposition of active pharmaceutical ingredients (APIs).[112] Recent efforts in further improving inhalation devices include mesh nebulizers[113] and smart nebulizers (*e.g.* Akita®Jet).[114] Additionally, computational fluid dynamics tools can be used to analyze and predict the transport and disposition behavior of various formulations in the airways.[115]

2.3.1.2. Formulation considerations. Depending on the nebulization process used, certain formulation constraints are imposed. For example, the aerosolization of liposomes has been a major issue. Tolerance against shear forces during the nebulization process has been shown to depend on surface

characteristics of the liposomes, with positively charged liposomes tending to aggregate and lose the encapsulated cargo during the process.[116] Alternatively, liposomes can be stabilized through membrane addition of cholesterol or phosphatidic acid. Using PEG as a stabilizer is also possible, albeit only at high concentrations.[117] Additionally, to ensure stable shelf-life, lyophilization and subsequent rehydration before nebulization of the lysosomal formulation may be needed. In that case, addition of cryoprotectants can modulate the membrane properties and affect membrane integrity during nebulization.[118] While liposomal NPs may need additional consideration, polymeric nanoparticles have shown to be nebulized without artefacts, for example by employing PVA as a surfactant, shielding the core NP from high shear forces.[119]

2.3.2. Avoidance of the mucus barrier. Given the challenges for airway delivery, alternative administration routes for lung targeting could be considered. Intravenous administration of NPs has shown promising results in the treatment of acute lung sepsis after bacterial infection,[120] chronic bacterial lung infection[121] and lung cancer.[122] However, despite these successful reports, several challenges remain for this administration route. Especially low targeting efficiency and high clearance by the mononuclear phagocyte system (MPS) and renal system have been of concern.[12] Promising strategies for clearance reduction include surface coatings, such as PEGylation,[123] or leveraging the biological inertia and lung targeting properties of circulatory cells, for example by NP hitchhiking on red blood cells (RBC) or mesenchymal stem cells (MSC).[124–126]

Although intravenous administration provides a sound alternative to airway delivery, (dis)advantages of both should be weighed in for every specific formulation or disease type (Table 2). For example, for certain pulmonary diseases, such as COPD or asthma, airway administration of the therapeutic compound is desired as it improves drug delivery to relevant cells.[127] Also for lung carcinoma treatment, intratracheal liposomal administration has been shown to be more therapeutically effective than intravenous administration.[128] However, for other lung disorders, such as bronchopulmonary dysplasia, a systemic approach might still be preferred, given the strong interlink between alveolarization and angiogenesis.[129,130]

2.3.3. Translatability. Translation of nanomedicine-based pulmonary therapies has remained relatively low, with only some lipid-based formulations reaching clinical trials.[131] For improving translatability, future studies could aim for more homogeneous standardization of outcome parameters. For example, only a few studies[96,132] have reported multiple particle tracking analysis results, which offer interstudy comparable parameters for mucus mobility and penetration probability, for example mean square displacement (⟨MSD⟩). Additionally, organ-on-chip technology could provide a valuable model wherein, similar to *in vitro* studies, penetration studies are possible in a more closely *in vivo* mimicking environment.[133,134] Furthermore, only a few studies have performed comparison studies on the effect of mucus penetration in both healthy and disease mucus (Table 1). For example, Chai and colleagues evaluated the diffusion properties of PEG-PS NPs, showing a differing, but still improved, 22-fold and 11-fold faster diffusion in healthy human airway mucus and CF sputum, respectively, for PEG-PS NPs compared to their non-PEGylated counterparts.[64] When evaluating the effect of PEGylation in patient-derived CF sputum, Conte and colleagues found that PEG mainly improved permeation in poorly colonized sputa, while its positive effect was absent for more complex sputa with multiple microbial colonies.[73] This varying effect of the mucus penetration strategy, affected by the health conditions of the patient, has been disregarded and requires further evaluation for all strategies mentioned in this section.

3. Gastrointestinal mucus barrier

3.1. GI mucus characteristics

The gastrointestinal (GI) barrier is coated with mucus in a protective manner that maintains the integrity of the organs from foreign entities. The GI tract is composed of the mouth, pharynx, esophagus, stomach, small and large intestines, colon, and liver amongst others. Delivery to target organs surrounding the GI tract can be achieved *via* localized (direct injection)[135] and systemic (oral) routes of administration.[136] The most common delivery method involves oral administration; however the nanomaterials that follow this route rely on methods that strengthen the stability during transit against drastic pH changes through surface functionality or other modifications. Challenges with orally administered nanomaterials include low proportions absorbed within the gut lumen[137,138] despite taking advantage of higher oral bioavailability.

Table 2 Comparison of advantages and disadvantages of systemic and airway administration

Airway administration	Systemic administration
Advantages	
• Noninvasive administration	• Avoidance of the mucus barrier
• Direct delivery	• Capable of reaching the capillary/alveoli interface
• Low systemic side effects	
Disadvantages	
• Mucus clearance	• Invasive administration
• Formulation restrictions	• Targeting strategy needed
• Specialized administration equipment needed	• Systemic side effects common
• Loss of API by sedimentation in the upper tract or through exhalation	• High clearance by the MPS

Certain disease states like inflammatory bowel diseases also influence the properties of mucus. Irritable bowel disease, Crohn's disease and ulcerative colitis all have similar properties such as inflammation of the GI mucosal tissue that can result in impaired mucus barrier operation.[139] In particular, Crohn's disease can affect all portions of the GI tract in a non-uniform distribution, which can exaggerate immune responses throughout the barrier and compromise its integrity.[140] Specific to the disease state, there are also changes in pH within the GI tract where some patients experiencing Crohn's disease have a colon pH between 5 and 7, whereas ulcerative colitis patients can have a pH of 2.7–5.5; for comparison a healthy patient generally has a colon pH of 6.2–7.4.[141] Notably, the lower pH may present an additional barrier to orally administered drugs, and biologics in particular. Additional characteristics of the GI mucus can be further examined in Box 2. By examining the makeup and physical characteristics of the GI mucosa, it is evident that nanovehicles must be designed with robustness to withstand mucus cycling and acidic pH for effective delivery especially in disease states with more drastic pH shifts.

Within this section, we will examine the current formulations used in targeting the GI tract in regard to physical properties of the nanomaterial as well as potential surface modifications in order to best optimize its translatability.

Box 2: GI mucus characteristics

The gut microbiota of the GI tract maintains the balance of the human flora. Within the secretions of the mucosa, bacteria closely associated to the immune system and tolerated by it must navigate secretory immunoglobulin A that modulates pathogenic access to the intestinal lumen.[142] Goblet cells make up the cell layers that secrete mucin and mucin-associated proteins such as MUC2 and MUC3, which make up the majority of components within the mucus. These proteins have been previously characterized to prevent the adherence of foreign objects and microbes such as *Salmonella enterica* from infiltrating the inner layers of the mouse intestine.[143,144] Bacteria that form the makeup within the mucus facilitate an antimicrobial layer when moving towards the inner layers of the intestinal lumen of the small intestine.[145] With its constant supply of mucus that is secreted and recycled there, researchers have found that the innate protease meprin β plays a role in the detachment of mucus and establishes the adherence of the asymmetrical mucosal outer layer to its inner layer of the colon.[146] Within the colon of the GI tract exists a bilayer of mucus that allows for the passage of endogenous bacterium to maintain the intestinal microbiome balance. Acting as the first line of defense, the mucosal layers inhibit the adherence of foreign pathogens and nanovehicles alike and promote their clearance through the cycling mucus. A brief overview of the human gastrointestinal tract and small intestine makeup is presented in Fig. 8.

Fluid characteristics of the GI tract also play roles in buffering capacity as well as fluid volume that is available for drugs to be dissolved and metabolized. Luminal fluid volume in the GI tract of mice when administered atenolol and/or metoprolol with varying osmolarity indicated varying degrees of permeability.[147] With regard to drugs with poor solubility loaded into polymers, the result is often a lipophilic nanoproduct that has poor adhesion to the mucosal layer and poor aqueous solubility within the GI tract due to the flux in fluid volume across the GI tract.[148]

3.2. NM engineering considerations influencing the interaction with GI mucus

Mucin, the major macromolecule responsible for the gel-like characteristic of mucus, has been found to inhibit the diffusion of various drugs when exposed to a phospholipid vesicle-based permeation assay with stimulated mucin concentrations.[149] In particular, the study determined that drugs would have difficulties diffusing at thicker mucus layered tissues and that the characteristics of the drug–mucin interactions would play a significant role in their diffusibility; lipophilic drugs such as naproxen had reduced diffusion coefficients at higher mucin concentrations similarly to hydrophilic drugs such as atenolol.

Nanomaterials in general have ideal dissolution properties as they have a large surface-to-volume ratio for loaded cargos and quick release of payloads can be achieved to reach saturation.[150] While in theory the nanoscale dimension

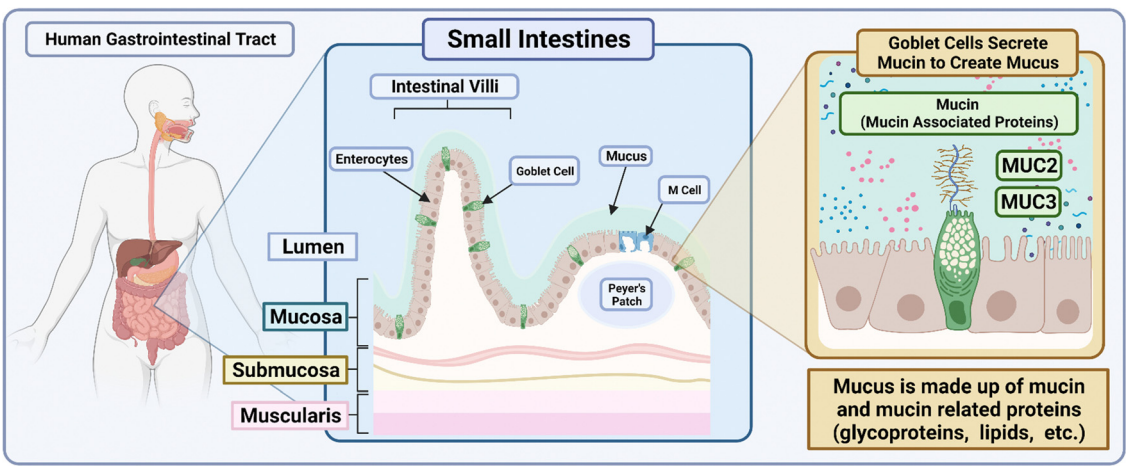

Fig. 8 Schematic depicting the makeup of the small intestines within the human GI tract. The illustration was made using https://BioRender.com.

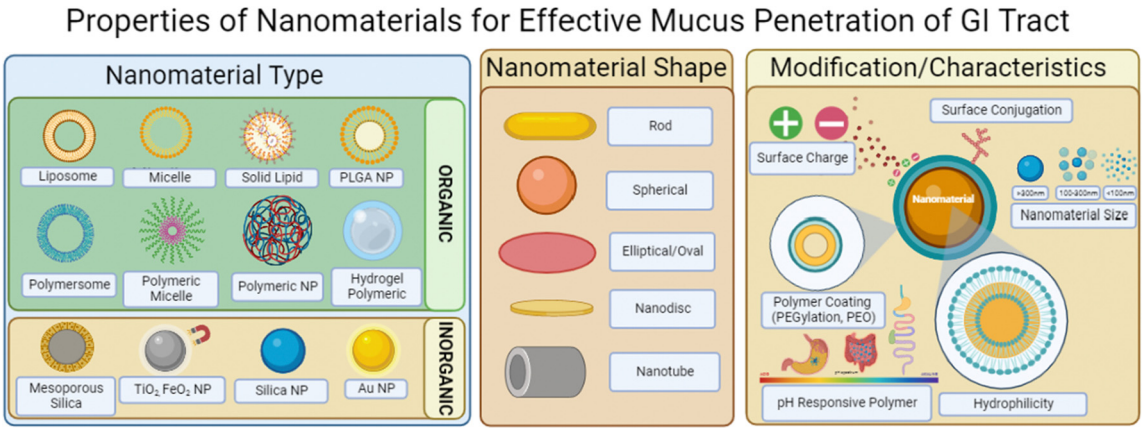

Fig. 9 Image depicting nanomaterial characteristics that influence mucus penetration within the GI tract. Illustrations were made using BioRender.

application seems simple, there exists issues with the biological form of the nanoparticle once taken orally; the outer coating of the nanoparticles once interacting with the mucosal layers can acquire proteins to its surface that alters lipophilicity, size and even different surface charges or moieties.[151,152] This could be due to the protein rich regions of the GI tract as well as any harsh changes in the pH environment such as pH 1–2 in the stomach and up to pH 8 within the intestines and colon. Physical characteristics to keep in mind when formulating nanosystems are delineated in Fig. 9.

When performing a search on PubMed Central to identify physical properties of nano delivery systems that penetrate the GI mucus barrier, a total of 59 studies published within the last 10 years were identified. The search terms included "nanoparticle" AND "gastrointestinal tract" within the abstracts. By excluding studies that did not contain relevance to mammalian GI tracts and reviews, a total of 36 studies of interest were isolated. When examining common sizes of these nanosystems, it was found that over half of the studies had nanoparticles with sizes less than 200 nm (61.11%) and the majority of studies contained nanoparticle systems less than 350 nm (86.11%) as seen in Fig. 10 and detailed in Table 3. Similarly, when examining the zeta potential for reported systems, the majority of studies utilized a negatively charged particle (64%) with approximately half (52%) of the studies designing nanosystems with reported zeta potentials between −10 mV and +10 mV. Polymeric nanomaterials were the most common (70.3%) amongst all studies compared to metal- and lipid-based formulations; polymers observed included PLGA,[153] Eudragit,[154] chitosan,[155] and polystyrene[156] amongst others. Metal-based formulations varied from synthesized to commercial grade and included titanium dioxide,[157] zinc oxide,[158] iron oxide,[159] silver,[160] and gold.[161] Studies using lipids were the least common among those isolated studies and included micelles.[162] When analyzing these data, it can be observed that research has found success in developing nanosystems at smaller sizes and negatively/neutrally charged for optimized mucus permeability.

With considerations to nanosystem design, it is imperative to consider size, shape, hydrophilicity, surface modifications and polymer type in order to optimize mucus permeability and enhance bioavailability of loaded cargos. Studies mimicking the mucus permeability of viruses have modified the surface of the nanomaterials to have hydrophilic properties to reduce mucus adhesion and maintain a neutral surface charge. As research has mainly focused on one property of the nanomaterial for optimization, the best formulation for circumventing the issues that arise with delivery to the mucus GI barrier involves utilizing size, shape, and surface properties as mentioned above. *In silico* simulations have been performed in order to optimize the shape for the drug delivery system. With these considerations in mind, design for mucus penetration can be achieved.

3.2.1. Core material. Within nanomaterials, the core material can influence the interactions of the system with mucin. The material properties of the nanosystem may also influence the mucus barrier's integrity as well as physical characteristics. Broadly, polymeric nanomaterials have seen some success in navigating the ever-changing environment. Alginate as an anionic linear polymer obtained from brown seaweed can be utilized in the formation of nanoparticles for GI tract delivery that may have probiotic benefits.[171,172] As alginate based vehicles have been found to respond to increasing pH levels by swelling in size, the design of any microcapsules should be considered.[173]

Conversely, lipid nanoparticles (LNPs) have been found to have stable release profiles within a large range of pH values which would allow for the delivery through the GI tract. LNPs loaded with siRNA against the luciferase gene were found to effectively achieve gene silencing across a broad pH range.[174] When exposed to pH values ranging from 1 to 8, LNP encapsulation efficiency of the siRNA was insignificantly affected with minimal disturbances to the polydispersity index and zeta potential. In the presence of low levels of mucin, the gene silencing capabilities of LNP siRNA delivery were significantly reduced. Formulating LNPs with increased percentages of PEG was found to improve gene silencing; however, the trade-offs for using high percentages of PEG include smaller diameters and lower encapsulation efficiencies of the siRNA.

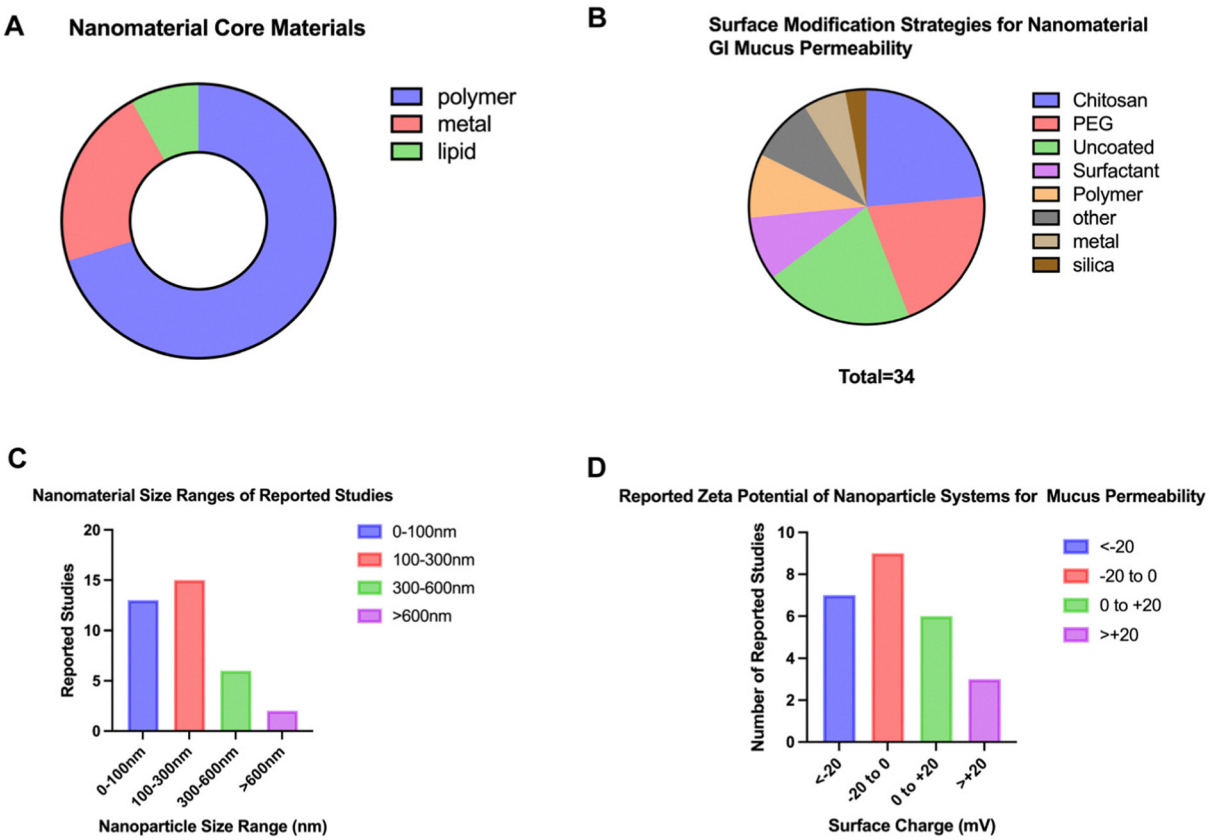

Fig. 10 Characteristics of nanodelivery systems for GI mucus permeation. Among common characteristics of these platforms is (A) the nanomaterial core material, (B) the surface modification, (C) the size ranges and (D) reported surface charges. 37 Pubmed research articles were used to determine common sizes for nano delivery systems in penetrating the mucus barrier of the GI tract. The search terms included 'GI tract', 'mucus', and 'nano' for research articles limited to the last ten years.

Incorporation of chitosan for siRNA delivery is also advantageous for mucosal delivery across the gastric mucosal layer and not the colonic mucus for selective delivery in the treatment of CDX2 gastric lesions;[175] this selectivity resulted from the lowered mucosal adhesion from a lower charge density compared to the colonic mucus.

Within the same category, lipid based micelles have also been modified using a zwitterionic betaine polymer in order to permeate the mucus in a similar manner as viruses in a more efficient approach compared to PEG particles of similar magnitude.[176] The micelles were manufactured using 1,2-distearoyl-*sn*-glycero-3-phosphoethanolamine (DSPE) with poly carboxybetaine (PCB) and were able to transport through cellular tight junctions without opening them and showed increased uptake by Caco-2 cells in order to deliver insulin. This formulation could also achieve a high encapsulation efficiency of 98% and maintain the integrity of the mucus barrier in porcine models.

Apart from lipid and polymer based nanomaterials, the use of metal inorganic systems has also been characterized for GI delivery. Nanoparticles with antimicrobial properties such as those made with titanium oxide have been found to influence the thickness of the mucus layer as well as its composition when exposed to bacteria.[177] In particular, titanium oxide particle treatment for one week was found to result in rats developing oxidative damage to the glycolic proteins within the GI tract mucus in animals receiving nanoparticle treatment over fine particles.[178] Similarly, studies have shown that silver nanoparticles and their interactions with human derived ileal explant tissues indicated different cytokine responses depending on treatment exposure time, the size of the nanoparticle and even depending on the differences in the sex of the derived tissues;[179] tissues derived from human males indicated increased RANTES cytokines compared to those from females which may suggest that males have increased sensitivity to inflammation upon exposure. Within the same study, smaller nanoparticles (10 nm and 20 nm size) could invoke changes in mRNA expression of cell junction genes after nanoparticle treatment. Compared to other inorganic nanoparticle types, cerium oxide nanoparticles manufactured with the sol–gel process have biological modulative effects such as superoxide dismutase and catalase mimicking activity which may suggest a protective effect against ethanol-induced ulcers within the GI tract.[180] Due to the oxidative state of cerium oxide, reactive oxygen species are able to be scavenged by the particles to reduce stress in the local mucosa caused by ethanol. As an intrinsic property of the nanomaterial, antioxidant properties can be dictated by the particle makeup.

Table 3 Selected research studies from PubMed Central Search analysis on gastrointestinal targeted nanocarrier systems according to particle type. Entries were collected from the last 5 years with key words including 'delivery', 'nanomaterial', 'gastrointestinal tract' and 'mucus'. Studies were limited to original research articles and excluded review manuscripts

NM engineering strategy	Surface modification	Core material	Size (nm)	Zeta potential (mV)	Model system	Disease/ normal state	Comments	Ref.
Core material	—	PLGA	200–300	−34 to −33	C57BL/6 intestinal stem cells organoid unit	IBD	PLGA nanoparticles with Matrigel and organoid suspension increase luminal absorption	163
		PHOSPHOLIPON 90G (lipid)	23	—	Premalignant oral epithelial cells (SCC83)	Oral cancer	Lipid micelle delivery targeted drug effectively in a short amount of time (15 minutes)	162
		Chitosan	350	—	Sprague Dawley rats (fasted)	Diabetes mellitus	Mucoadhesive particles adhere within the stomach for prolonged time periods	164
	Iron	Zinc oxide (metal)	100	−40	Balb/c mice	Normal state	Iron embedded zinc oxide nanoparticles improve iron absorption in the gastrointestinal tract in a supplemental manner	158
Surface engineering: polymeric coatings	PEGylation	Chitosan	47	8	Caco-2, HT29-MTX	Normal state	Nanoparticles travel paracellularly through the intestinal epithelium	165
		Coacervate/ catechol	150	—	Sprague Dawley rats	DSS induced colitis	Improved controlled release was achieved as well as improved retention time within the intestines	166
Surface engineering: chitosan	Chitosan	PLGA	350	9.7	Balb/c acute colitis	Acute colitis	CS-PLGA-NP mucoadhesion increased colonic drug delivery in GI	153
	Chitosan	Polylysine-bilirubin	233.9	6.2	Balb/c ethanol induced acute gastric ulcer	Ethanol induced gastric ulcer	Positively charged CS-bilirubin nanoparticles enhance the anti-inflammatory effect	167
	Chitosan, PEG	Hydroxypropyl ethylcellulose phthalate	294	−26.7	Caco-2-cell monolayer, ICR mice	Normal state	HTCC modified chitosan increased mucoadhesion	168
	Chitosan	Chitosan/ fucoidan	300	30	Dialysis bag for nanoparticle release	Normal state	Increased fucoidan composition improves gastrointestinal simulated environments	155
	Chitosan	Tripolyphosphate/ chitosan	700	33.06	Kunming mice	*E. coli* challenged (cow mastitis)	Chitosan encapsulated OmpA protected from acidic pH	169
Surface engineering: pH responsive polymer	Eudragit	PLGA	397.1	—	Gastrointestinal pH simulated conditions	Normal state	Eudragit NP protects the contents from gastric pH	170

Comparatively, the magnetic properties of iron oxide nanoparticles in chitosan-alginate core–shell beads effectively localized the loaded drug to the intestine of rats and increased bioavailability.[181] By taking advantage of the magnetic properties of the iron oxide nanoparticles and incorporating them into the system formulation, there can be improved localization within the targeted areas of the intestines while surpassing first-pass metabolism. In parallel, these systems effect the charge of the NP formulation rendering them more positively charged and thus improving their adsorption properties. Dextran nanoparticles with iron oxide cores provided improved catalytic activity when exposed to the acidic pH to selectively treat oral biofilms.[182]

3.2.2. Porosity and rigidity of the nanomaterial system. Characteristics influencing uptake include the porosity of the formulation as well as its rigidity. Intrinsic properties such as the use of nano cellulose and its porosity allow for gradual enzymatic digestion.[183] An increase in the porosity of the nanomaterial has been linked to improved controlled cargo release and ease in surface functionalization especially in the case of mesoporous silica nanoparticles; passive mechanisms of release have advantages over those such as PLGA or lipid based structures which tend to rely on enzymatic degradation for release of contents.[184] With designing formulations with longevity in mind in order to withstand transport times, increased porosity can be considered to be advantageous for drug release and resilience to mucosal turnover.

With regard to rigidity, the mechanism for cellular uptake is correlated to the formulation. Plant derived nanoparticle-based formulations have a similar rigidity to lipid-based nanoparticles.[185] With PLGA-lipid nanoparticles formulated with varying rigidity, it was found that less rigid particles had lowered penetration into the *trans*-epithelial layer compared to the stiffer ones; it should be noted that functionalization of the Fc neonatal domain binding peptide on the softer nanoparticles increased their uptake in the liver fibrosis model.[186] Physiochemical characteristics of the formulation can be observed as they relate to stability (Fig. 11). Overall, the researchers found that rigidity of the nanoparticles improved mucus penetration over ligand functionalization and/or PEGylation but the most rigid formulation with ligand modification had the best results for transcytosis.

3.2.3. Size/shape of the nanomaterial. Considering the size of the nanosystem is necessary to optimize its bio-distribution

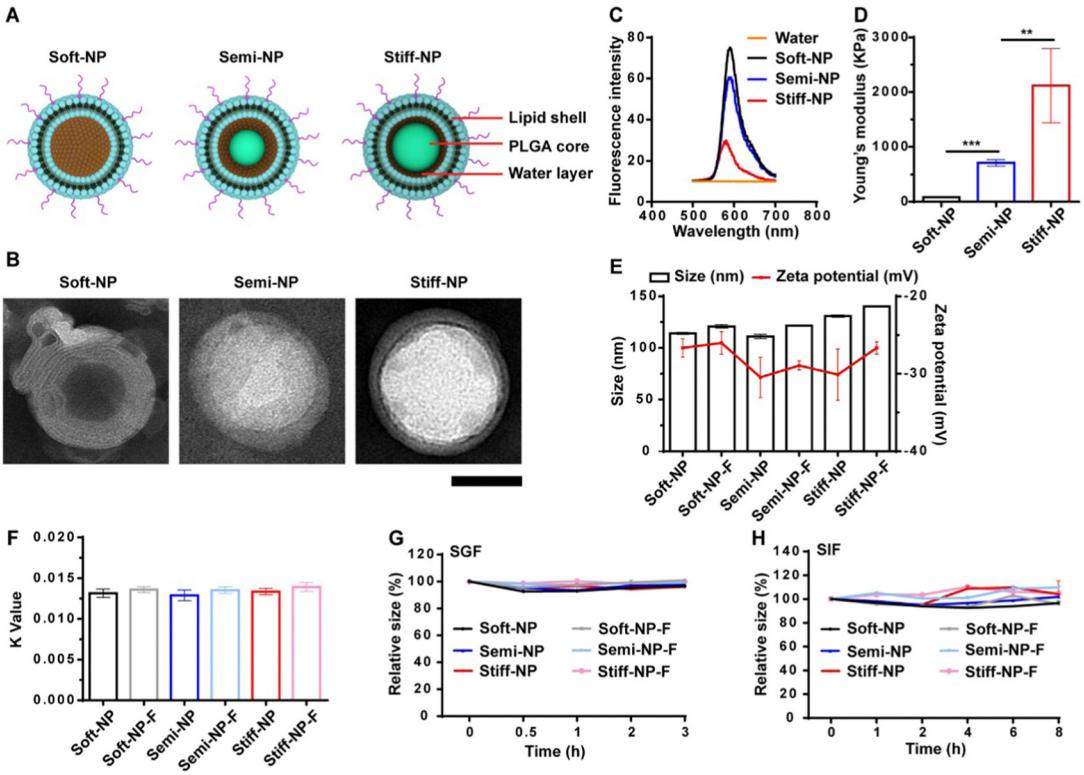

Fig. 11 Characterization of the NP. (A) Schematic illustration of the PLGA-lipid NP. (B) TEM images of the NP. Scar bar: 50 nm. (C) The fluorescence emission spectrum of the rhodamine B-loaded PLGA-lipid NP. (D) The Young's modulus of the PLGA-lipid NP. $^{**}p < 0.01$, $^{***}p < 0.001$. (E) Hydrodynamic diameter and zeta potential of the NP. (F) Hydrophobicity was measured by the rose Bengal method. Stability of the NP in simulated gastric fluid (SGF, G) and simulated intestinal fluid (SIF, H). Data represent mean ± SD (n = 3). Adapted from ref. 186 with permission from Elsevier.

as size dictates its fate (i.e., elimination) in the GI tract. With regard to the nanoparticle size, researchers have found that 100 nm latex beads faced less resistance when traveling through the mucus layer of *ex vivo* porcine mucus compared to larger sized particles (500 nm) which had more restricted access and diffusion within the small intestine.[187] The beads used in the study were tracked using bile salt coated carboxylated latex beads which had portions of immobile beads due to the dynamic two layer mucus system. It was worth noting that nanoparticles greater than 200 nm had the potential of inducing the complement inflammatory response cascade and thus were cleared faster.[188] In a size-dependent manner, these nanosystems that rely on nanoparticle endo/exocytosis for uptake as their method of absorption must be carefully designed in view of their shape as well.[189] When contrasting nanoparticle shape to their uptake efficiency, it was found that carbodiimide crosslinked biotin nanoparticles that were rod shaped had significantly higher uptake compared to spherical and disc shaped ones.[190] Similarly, in the same study, nanoparticles that were smaller (50–200 nm) also had a better cellular uptake within Caco-2/HT-29 intestinal cells. Studies by Zheng *et al.* also confirm that silica nanorods loaded with doxorubicin hydrochloride exhibited augmented cellular uptake in Caco-2 cells with low cytotoxicity compared to nanosphere formulations.[191] As the GI tract relies on M cells and enterocytes as the main components of nanoparticle translocation, smaller nanoparticle sizes tend to indicate more favorable mucosal penetrative properties.[192]

The formulations of nanotube systems have also been advantageous due to their modifiable rigidity and shape.[193] The researchers utilized tubular peptosomes with various levels of rigidity according to the level of α-lactalbumin incorporated into their surface. As the protein assembled tubes had a net negative surface charge, through multiple particle tracking it was found that compared to their spherical counterparts the shorter assembled nanotubes had an advantage in mucosal penetration due to their ability to navigate the shear flow within the intestines and mucus mesh structure. With the highest bioavailability of loaded curcumin, the short nanotube structures indicated good tolerance with no inflammation observable through microscopy of the tissue samples and had the best therapeutic effect compared to longer and more rigid nanotube formulations.

In the comparison of spherical nanoparticles with short and long sized nanorods, spherical nanoparticles were found to have faster clearance in *in vivo* studies.[194] With regard to *in vivo* studies, mesoporous silica nanorods were found to accumulate in a uniform manner along the intestinal villi of rats compared

to spherical nanoparticles which had more difficulty in reaching epithelial cells.[195] Longer nanorods were found to be difficult to eliminate from the mouse GI tract as they achieved a residence time of up to 7 days compared to the other groups with accumulation being observed mostly in the liver and kidney when orally dosed. Additionally with this formulation loaded with camptothecin, mesoporous silica nanorods had up to 2.6-fold higher transportation of the drug compared to the other shaped/control groups. Likewise, the structural rigidity of the nanoparticle system also seems to be instrumental in mucus penetration as well. PLGA nanoparticles that were developed to have a lipid shell in a 'semi-elastic' fashion were able to achieve increased bioavailability of delivered doxorubicin to Caco-2 cells. When the particles were made to be rigid, there were steric effects that hindered deformation; however, soft nanoparticles were found to interact with the hydrogel network and inhibit its permeability.[196] When visualized using microscopy, the nanoparticles were more ellipsoid in shape. Overall, it seemed that rod-shaped and ellipsoid shaped nanoparticles are able to navigate more easily through the mucus compared to nanoparticles of other shapes. Needle shaped nanosystems driven by magnetic properties for gastric mucus penetration were also found to increase drug penetration of doxorubicin;[197] the pepsin bridge structure allows for increased interaction between the nanocapsule needle platform and the mucus itself for improved mucosal adhesion. Utilizing physiochemical properties such as magnetism as well as nanomaterial shape was the key factor in this system's success in improved cellular retention and uptake of the drug.

3.3. NM design strategies and surface engineering

When designing nanomaterials to specifically target the GI tract, it is imperative to address the challenge of pH in the stability of the nanosystem as it travels to its targeted site.[198,199] With this examination, the material to coat the outside of the nanomaterial must be considered. Nanoparticles in general are able to be formulated to encapsulate many pharmaceutically active molecules and are often a popular choice due to their good biodistribution. pH-responsive polymers should be able to change their properties according to their chemical environment such as being dissolvable at higher pH values and insoluble at lower ones.[200]

Considerations to circumvent the issue of early dissolution include coating the particles with a pH-responsive polymer such as Eudragit® and its derivatives,[201] which allows for nanoparticle transport through the GI tract until a specific pH is reached. Eudragit® FS30D was recently incorporated to form zinc oxide nanohybrids which could withstand a stimulated succus entericus environment and achieve an increased release rate from 9.5% to 74.7% with a pH shift from 1 to 6.8.[202] This formulation was also found to remain stable and did not exhibit large physiological changes at 25 °C at 60% humidity for one month. Formulations of Eudragit®-S100 coated PLGA nanoparticles loaded with etoricoxib revealed colon targeting capabilities in healthy human volunteers as a way to treat irritable bowel syndrome.[203]

Strategies incorporating inspirations from *H. pylori* infections within the GI have also found success in biomimetic engineering of nanomaterials. Nucleic acid mimics incorporated using a bacterial cell envelope are also a technique to hybridize *H. pylori* in the treatment of stomach infections allowing for advantageous mucus permeability.[204] With this unique method, antibacterial therapy is achievable through the delivery of antisense oligonucleotides in *in vivo* hybridization. Under this methodology, the cell envelope did not require permeabilization that is generally necessary for cell-membrane based therapeutics. Interestingly, the use of micro propellers to navigate the biological barrier of the GI tract has been implemented to integrate urease to the surface to avoid mucosal degradation.[205] As the bacterium also utilizes the urease mechanism to navigate the mucus by altering the mucus viscosity, systems with magnetized properties with the enzyme on their surface can mobilize through their screw-like shape configuration. In addition, artificial zinc-based micromotors have shown effective travel through acidic gastric conditions for drug retention in the GI.[206] When compared to simple passive diffusion of the free drug, the hydrogen bubble projection allowed for the micromotors to remain stable in low pH environments and retained on the stomach lining in a time-dependent manner for extended retention and drug delivery.

While optimization of nanomaterial delivery platforms is generally done *in vitro*, there are advantages that come with computational simulations; molecular docking technologies are able to provide more insight into the protein–drug interactions for delivery such as the potential effects of metabolism from enzymes and protein coronas that may form. Nanovectors designed for dual encapsulation of evodiamine and curcumin drugs for the treatment of gastric mucosal lesions allowed for improved insight into how the drug formulations would interact in the GI environment in the presence of efflux pumps; this technology allowed researchers to estimate the absorption of the drugs in the supramolecular nanocomplex according to the epithelial cellular uptake models.[207] Similarly, to investigate the gastroprotective effect in a rat model, *in silico* response and contour plots have been used to optimize the globule size of self-nano emulsion particles, where the predicted sizes were similar to the actual value measured (67.7 nm calculated *versus* 64.8 nm actual).[208] Adding automation for the high throughput screening of nanoparticle formulations is necessary to improve optimization speed and predict biological interactions such as solubility and potential penetration capabilities.[209,210]

3.3.1. NM surface modification. Modification of NM is dependent upon the desired interaction of the system; common pathways include mucus adhesion as well as mucus penetration. Mucus adhesion strategies focus on delivery systems that are able to retain NPs longer within the GI mucus. This is accomplished by surface modification that enables sufficient attraction in the mucus layer that can bypass mucosal turnover and displacement.[211] On the other hand, mucus-penetrating strategies focus on hydrophilicity in their characteristics as decreasing adhesive forces between the mucus and the nanomaterial as well as maintaining a neutrally charged surface is

more beneficial.[212] Below some strategies for surface modification are discussed according to mucosal adhesion/penetrating characteristics.

3.3.2. PEGylation. Modification of the surface of nanoparticles can also decrease mucoadhesion to improve uptake and immune system tolerance.[213] Surface coating can consist of decorating the surface through chemical conjugation as well as utilizing polymers to aid in enhanced mucus penetration with increased residence times. In order to better permeate the mucus layer and improve accumulation, surface modifications of nanoparticles can be performed such as PEGylation of PLGA nanoparticles. When attempting to deliver the photosensitizer 5,10,15,20-tetrakis(*m*-hydroxyphenyl)porphyrin (mTHPP) in PLGA nanoparticles for photodynamic therapy in the treatment of gastrointestinal tumors, researchers determined that PEGylation of the nanoparticles resulted in better stimulated transport across a transwell membrane compared to chitosan and non-modified nanoparticles.[214] Studies on the mucus secreting HT-29-MTX cells revealed that the coated nanoparticles indicated low cytotoxicity, quick penetration of the mucosa layer, and ultimately higher accumulation in targeted sites compared to the other systems tested. PEGylation of nanoparticles alters the surface charge of the particles in order to avoid strong interactions with the negatively charged mucin and decrease interactions with the mucus. PEGylation of nanocarriers and its efficiency in mucus permeability also depend on the materials and size of the nanoparticles.[215] When incorporated with the mucolytic agent 4-mercaptobenzoic acid, PLGA-PEG coated nanoparticles were able to release their contents while liposome formulations had a steadier controlled release overall. The incorporation of tea-derived polyphenol coatings into liposomes maintained their anti-bacterial properties and enabled them to swell/lyse under acidic conditions;[216] this system was effective in the targeted treatment of *H. pylori* infections within the stomach to achieve therapeutic efficacy without causing any additional toxicity or inflammation within the body *in vivo*. Alternate studies also reported that utilizing a positively charged surfactant in the incorporation of negatively charged DNA facilitates 10-fold higher transportation of the gene and drug delivery when compared to similarly formed polystyrene nanoparticles which can improve encapsulation of genes for delivery.[217] In general terms of mucus permeability for small molecule drugs, smaller sized, negatively charged/neutrally charged nanocarriers had the highest efficiency which correlates with previously mentioned literature evidence.

In parallel studies, mesoporous silica nano-particles have been modified with poly(lactic acid)-methoxy poly(ethylene glycol) polymers and cysteine modified protamine. While the use of cyteine modified protamine did increase cellular uptake, PEG remained the main factor that contributed to the overall net neutrality of the nanosystem for avoiding mucus inhibition.[218] While the use of cysteine modified protamine did increase cellular uptake, PEG remained the main factor that contributed to the overall net neutrality of the nanosystem for avoiding mucus inhibition. Similar copolymer mixtures of PEG and PLGA linked by a hydrazone bond were able to exhibit increased penetration with high stability in oral insulin delivery;[219] with a surface that can switch from hydrophilic to hydrophobic the researchers found increased nanoparticle reach within the jejunum villi of diabetic rats (Fig. 12).

3.3.3. Chitosan. Particles can be formulated with a core material of chitosan hybrids or utilize it as a surface modification to take advantage of mucus adhesion; chitosan which is derived from the chitin of marine organisms through acetylation is known for its biocompatibility and easy degradation.[220,221] The benefits of using chitosan lie in its formation through ionic gelation which allows for cross linking for tailoring delivery. These techniques involving chitosan hybrid nanoparticles aim to improve the pharmacokinetics of drugs; a lecithin–chitosan nanoparticle system was reported to have improved oral bioavailability with 4.2× increase within female Wistar rats.[222] Within this system there was enhanced uptake in the intestines as the particles were found to be bound to the mucus layer. The physicochemical characteristics of chitosan and its crosslinkers allow for the formation of the amine group at low pH values, which provide strong electrostatic interactions that help the nanoparticle to retain its shape/size whereas at higher pH values the interaction is weakened, resulting in the particle releasing its cargo.[223] Biodistribution of the formulation can be observed in Fig. 13 indicating the highest accumulation in the intestines. Chitosan oligosaccharides for the treatment of gastric ulcers indicated improved electrostatic interactions due to the positively charged amino groups of the nanomaterial and the negatively charged mucin for better mucin-binding as reported by a mucoadhesive strength of 51.22% compared to non-chitosan treated particles.[224]

In a different study, researchers attempting to circumvent the acidic environment that is present in the stomach have modified chitosan-alginate core–shell beads with magnetic nanoparticles and mucoadhesive properties.[225] The beads were able to travel and accumulate in the targeted area through the center of a magnet positioned on the skin. The results delineated that the chitosan coating of the beads improved adhesion to the mucosal membrane layer of the rat jejunum and facilitated drug release.

3.3.4. Hydrophilic surface modification. Other methods to coat nanoparticles with a hydrophilic surface modification involve the use of polyethylene oxide to enhance epithelial cellular uptake.[226] Polyethylene oxide and poloxamer188 coated poly(ε-caprolactone) chain triglyceride hybrid cores were loaded with cabazitaxel and the particles maintained a positive surface and overall had increased oral bioavailability compared to non-coated nanoparticles for the delivery of small molecules.[227] While it was previously mentioned that positively charged nanoparticles could have strong interactions with the mucus and prompt rapid clearance, the researchers found that there was higher mucus permeability with this formulation due to increased localization in the mucus and thus higher chances of permeability while the polyethylene oxide could also weaken mucin interactions by increasing the particle's hydrophilicity. This formulation of the nanoparticle was thought to have a

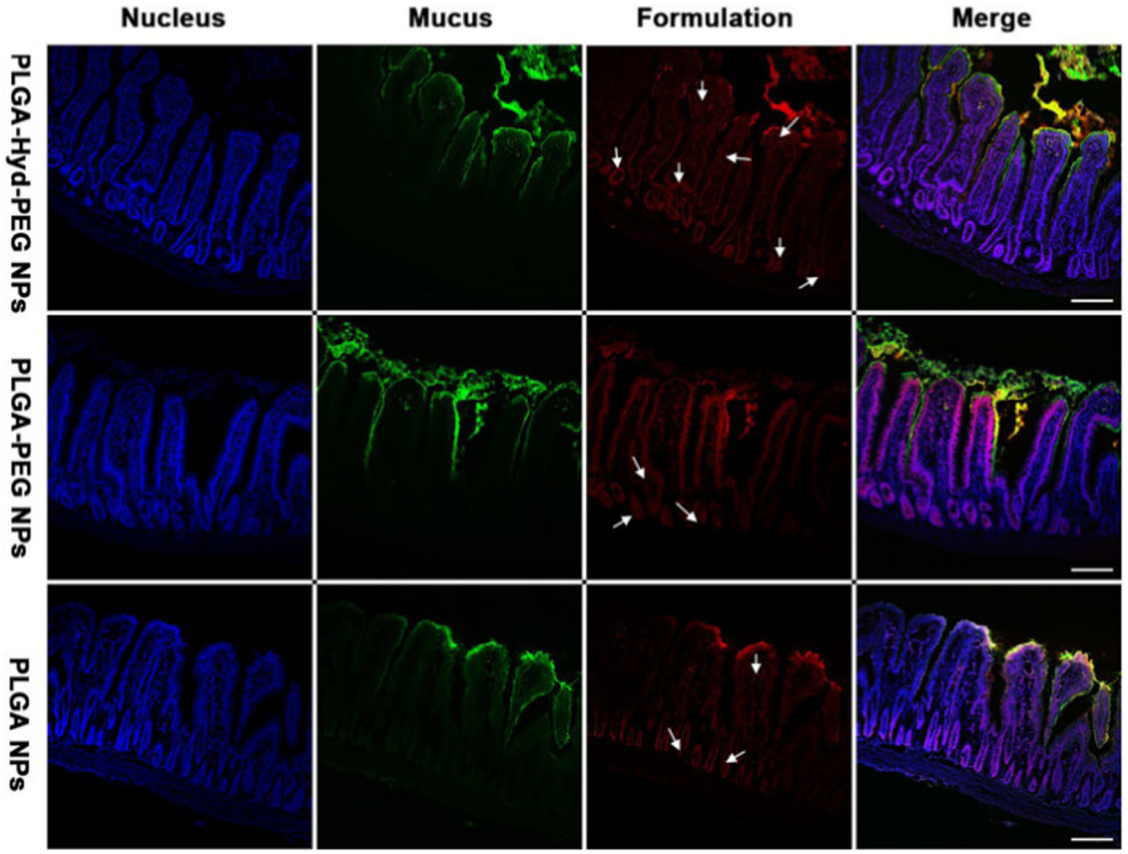

Fig. 12 Confocal micrographs of frozen sections of jejunum villi after 1-h incubation with various formulations. The white arrows indicate representative NPs absorbed into the villi. Scale bars, 100 μm. Adapted from ref. 219 with permission from Elsevier.

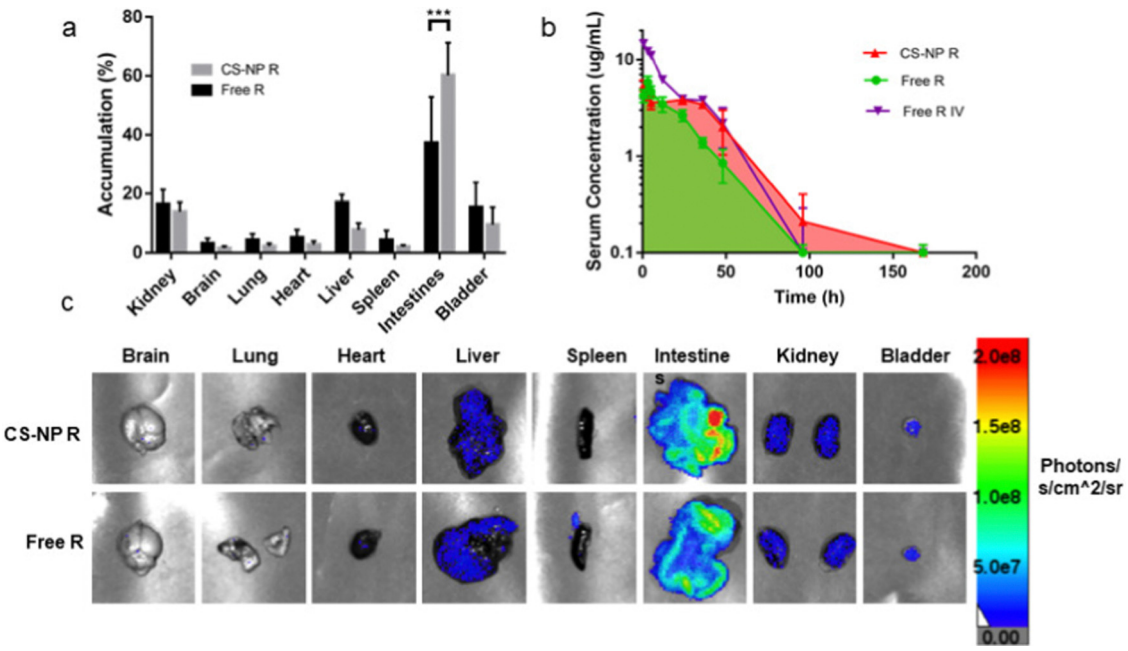

Fig. 13 Semi-quantitative biodistribution of mice treated with 10 mg kg^{-1} rhodamine in 200 μL of CS-NP R and free R 24 h after oral gavage. (a) Comparison of *ex vivo* imaging between rhodamine fluorescence levels showed higher accumulation in the intestines for CS-NP R *vs.* free R 24 h post-oral gavage. (b) Serum fluorescence of CS-NP R shows a greater absolute bioavailability and an extended release profile for the CS-NP formulation for up to 7 days (76.2% for CS-NP R and 47.9% for free R; ***$p \leq 0.001$, $N \geq 4$). (c) Representative *ex vivo* images confirm the highest signal in the intestines in the CS-NP R condition 24 h after oral gavage. Adapted from ref. 223 with permission from Elsevier.

better balance between mucus affinity and mucus penetration capabilities. With this point in mind, defining mucus permeability should consider not only surface charge for interaction with mucin but also hydrophilicity for effective penetration and uptake by inner epithelial cells of the GI tract. With the design of electrostatically neutral mesoporous silica nanoparticles with hydrophilic surface characteristics, the cell-penetrating pentapeptides aim to mimic the virus surface to travel across the intestinal mucus layer.[228] This system had a positive surface charge and was able to effectively lower blood glucose levels in diabetic rats by delivering insulin. By attaching a mix of charged carboxylic groups and KLPVM peptides to the surface, the particle becomes neutral while maintaining hydrophilicity to facilitate transport to the epithelial cells. Similarly, zwitterionic incorporation in porous silica nanoparticles with poly(pyridyl disulfide ethylene phosphate/sulfobetaine) polymers acted in further shielding the nanomaterial and improving mucus diffusion to effectively deliver insulin.[229]

Micelles formed from chitosan–vitamin E succinate copolymers have been previously reported as a self-assembling nanocomplex capable of encapsulation of the hydrophobic drug paclitaxel for intestinal penetration.[230] Bioconjugation of *N*-acetyl-l-cysteine improved mucosal adhesion 2-fold compared to the unconjugated form for improved pharmacokinetic properties. Similar to the nanoparticle formulation, the surface charge, hydrophilicity and physicochemical characteristics of micelles will affect its stability in the mucus environment and affect its mucus penetrating capabilities.[231]

3.4. GI mucus delivery

With these points in mind, the properties of the nanosystem must consider the delivery method such as mucoadhesion or mucus permeability; mucus adhesive nanosystems are optimal for long term drug delivery due to their ability to bypass mucosal clearance when adhered to the mucus while mucus permeability has greater potential for increased protection of sensitive cargos such as proteins due to direct interactions with the epithelium.[211,232] While mucoadhesive nanomaterials are more commonly found within the literature, mucus penetrating systems are also increasingly developed in recent years. As mucoadhesion relies on the exploitation of electrostatic interactions, there exist various molecular interactions that can be artificially engineered for improved delivery system efficiencies such as hydrophobic forces, van der Waals interactions and even non-specific recognition.[233] In parallel, it is imperative to address the properties associated with mucoadhesion within the GI tract with reference to nanomaterials and their efficiency in uptake. Mucins are negatively charged due to their glycosidic moieties and, therefore, positively charged nanomaterials are mucosally adhesive and may prompt swift elimination by the dynamic top layer of the mucus.[234] Mucosally adhesive particles were found to generally accumulate outside the range of the epithelium for absorption whereas non-mucoadhesive mucus particles were able to have a more uniform distribution.[213] It is indicated that for best particle distribution within the GI tract one should formulate their nanosystems according to non-mucoadhesive properties.

3.5. Translatability

3.5.1. *In vitro* and *in vivo* mucus models and translatability. While Caco-2 cells are beneficial in studying the effects of the nanomaterials *in vitro*, it should be noted that the model often has a higher transepithelial electrical resistance compared to *in vivo* models which can affect translational studies;[235] on the other hand human HT29 cells have potential to differentiate into mucus secreting cells for *in vitro* characterization. However, this cell line has been known to have a lower transepithelial resistance used to monitor drug absorption. The authors suggest co-culturing the two cell lines to have a more reliable model that can have more relevance. Likewise, utilizing reconstituted mucus obtained *ex vivo* has been found to contain varying compositions of proteins, lipids, and salts compared to that obtained fresh which will also affect drug absorption studies.[236]

Issues also persist with translatability between animal models to study biodistribution of various delivered nanomaterials: induction of inflammation in nonmammalian and mammalian models based on techniques used as well as the type of inflammation whether long or short term.[237] Mice are commonly used as their intestinal system is similar to humans; however, they can be engineered to display acute or chronic inflammation which may not always fit the origins of the disease state. Similarly, lesions present in humans presenting irritable bowel syndrome differ from those of mice that have been induced to have lesions through chemical irritation/injury. Even structurally in pig models, there is a high concentration of B-cell follicles within Peyer's patches in the intestinal jejunum and a lack of T-cells, which differs from humans.[238] This is despite the fact that pigs and their immune system show more similarities to humans compared to mice models of inflammation.

Mice subject to dextran sulfate sodium (DSS) in order to induce inflammatory colitis must be administered daily in order to maintain the studied disease state which is unlike the progressive conditions experienced by humans;[239] considerations with the model also indicate variability in inflammatory severity according to gender and the living environment. In order to effectively translate biodistribution and inflammation studies to human models, the use of animal models must also be considered with varying degrees of mucus producing capabilities as well as inflammation marker variance. When examining these issues through *in vitro* models like the Caco-2 cell line capable of producing mucus, researchers often get variability between monolayers of different passages and clone variabilities.[240] These issues in combination make studies with human inflammation more difficult in terms of reproducibility and consistency in designing drug delivery systems according to GI mucus characterization.

3.5.2. Targeting to specific GI cell populations. With specific regard to the 'normal' state of GI as opposed to that of the 'diseased' state, personalization of the NM system must consider cell environmental differences that occur between different ailments. Within the 'normal' state of the GI, the naturally thinner mucosal layers surrounding M cells make it an ideal

target for uptake; however in the case of inflammation within the intestines, there is a shift to immune cells and enterocytes accumulating in the area.[241] In the case of IBD, for patients, the physiopathology variables can be altered such as fluid volume and increased presence of immune cells from inflammatory responses along the entire mucus layer.[242] The common route of treatment involves delivery of anti-inflammatory molecules; however confounding factors like variable transit times for the NM formulations also pose considerations for effective delivery.

When determining the formulation for nanomaterial systems, specific cell populations can be considered for more targeted approaches beyond mucus-adhesion and mucus-penetration. In general, these techniques focus on additional surface modifications to target cell receptors within the targeted area.[185] For example, targeting of M-cells within the intestines can be achieved through dapsone and mannosylated solid lipid nanoparticles to target M-cell mannose receptors.[243] Similarly for Peyer's patch M-cell targeting, rifampicin lipid–polymer hybrid nanoparticles had increased adhesion when hydrophobicity was prioritized in the formulation; *in vivo* studies demonstrated increased uptake with Gantrez incorporated nanoparticles for gut-associated lymphoid tissues as M-cells have a thinner layer of mucus and may be easier to deliver.[244]

Immune cell targeting for gut immunity has also found success; in the cases of ulcerative colitis/IBS treatment, galactosylated trimethyl chitosan–cysteine nanoparticles could improve uptake in macrophages for TNF-α production within the colon.[245] Leukocytes localized within the gut were also targeted for siRNA delivery owing to the decorated lipid nanoparticles specific to the α4β7 integrin through a PEG linked mucosal vascular addressin cell-adhesion molecule-1 to its surface.[246]

3.5.3. Translatability into the clinic. Translatability of nano delivery systems into the clinic relies on increasing the bioavailability within oral GI delivery while overcoming the side effects and concerns that come with poorly permeable drugs. Market approved small molecule drugs such as semaglutide (Rybelsus®) deliver a glucagon-like peptide-1 receptor agonist for type 2 diabetes through an ingestible formulation with sodium-*N*-(8-[2-hydroxybenzoyl]amino)caprylate (SNAC);[247] this particular formulation acts to improve solubility and buffers against degradation to be absorbed completely within the stomach of the GI and provides therapeutic relief to patients in glucose metabolism with mild gastrointestinal side effects.[248] Encapsulation of drugs using nano delivery systems like PLGA nanoparticles has shown increased protection against the harsh pH changes and has shown enhanced permeability through Caco-2 cell lines *in vitro*;[249] however it should be noted that studies done *ex vivo* and *in vivo* often struggle to see efficacy through to the clinical level. pH responsive polymers such as Eudragit® have seen some success; however, novel systems should be designed with translatability in mind.

The necessity of surface modification of nanomaterials is advantageous for navigating the changing pH environment within the GI tract but there is an increased chance of off-target effects that challenge effective targeting.[250] As the complexity of the nanosystem increases, the chance for variability also increases due to the intricate biological processes occurring within the GI. Simplicity in formulation and manufacturing allows for the greatest translatability across different organisms from murine cellular studies to human clinical trials.

4. Blood–brain barrier

The blood–brain barrier (BBB) is a critical component of the neurovascular unit, and its characteristics (Box 3) serve important physiological roles, which include (1) the protection of the brain from toxic substances, (2) the modulation of nutrients, (3) the response to different plasma proteins, (4) and the protection of the central nervous system.[251–253] This strong protective barrier function makes the BBB a serious impediment for effective treatment of brain diseases, such as brain tumors or neurodegenerative disorders. Strategies that have been employed for brain drug delivery include among others local drug delivery with convection-enhanced delivery, or drug-loaded polymeric wafer implants.[254,255] However, due to their invasiveness, these methods exhibit a high chance of infection. Other methods include BBB disruption with osmotic agents or ultrasound, but these methods can potentially lead to neurotoxicity.[256]

Systemic administration of nanoparticles, engineered to feature BBB crossing characteristics, is an innovative way for brain targeted drug delivery.[257] Extracellular vesicles, biomimetic NPs and cell-based drug delivery systems are yet other promising strategies employed for crossing the BBB. Therefore, in this section, we elaborate on the characteristics of NPs that influence BBB crossing and the strategies that are employed to penetrate the BBB (Fig. 15). The details of the most recent strategies (published in the last 5 years) are presented in Table 4.

Box 3: BBB characteristics

The BBB separates the vascular space from the brain parenchyma, which consists of brain cells and extracellular (interstitial) space.[251] It is formed by endothelial cells that line the brain microvessels, impeding the paracellular route of large or hydrophilic molecules across the BBB, due to tight junctions (TJ) between the adjacent endothelial cells.[258,259] This barrier is supported by a closely associated basement membrane consisting of type IV collagen, fibronectin and laminin. Additionally, pericyte and astrocyte endfeet are located in the abluminal site and regulate and maintain BBB integrity.[260,261] On the luminal side there is a glycocalyx layer covering the brain endothelial cells, which hinders the passage of anionic macromolecules and substances with sizes over 70 kDa. Molecules can cross the BBB through the paracellular or transcellular pathway.[259,261–264] Paracellular transport, which is the passage between endothelial cells, is highly restricted to small molecules less than 180 Da and is concentration gradient dependent.[263] Larger substances, including NPs, use the transcellular pathway to cross the BBB, travelling through endothelial cells. The transcellular mechanisms include (a) the passive diffusion of lipophilic molecules, (b) receptor-mediated transcytosis, which is used for hydrophilic molecules, (c) carrier-mediated transport, (d) adsorptive-mediated transcytosis and (e) cell-mediated transcytosis (Fig. 14).

Table 4 Selected research studies of the most recent NP engineering strategies, based on data extracted from the PubMed database of the last 5 years using the search terms 'nano' and 'blood brain barrier'. Only original research articles and articles within the scope were included

NM engineering strategy	Surface modification	Core material	Size (nm)	Zeta potential (mV)	Model system	Diseased/normal state	Comments	Ref.
Targeting ligand to low density lipoprotein receptors	Angiopep-2	Ceria	20	+5	*In vitro* (BCECs) and *in vivo* (rat)	Diseased (stroke)		265
		PMLA	4.45	−11.6	*In vivo* (mouse)	Normal		266
		PMLA	9.4	−8.2	*In vivo* (mouse)	Diseased (glioblastoma)	Contrast-enhanced MRI agent	267
		Solid lipid	111.4	−16.4	*In vivo* (mouse)	Diseased (glioblastoma)		268
		PEG-PLL	18.8	+2	*In vitro* (BCECs) and *in vivo* (mouse)	Diseased (brain metastasis of breast cancer)		269
	L-carnosine	PLGA	50	−7.2	*In vitro* (BCECs)	Diseased/normal		270
	Tween 80	Lipid	165	/	*In vivo* (zebrafish)	Normal		271
	Lactoferrin	Lipid	170	−15.9	*In vivo* (mouse)	Normal	+ Lactoferrin receptor binding	272
		Silica	30	−32.3	*In vitro* (HBEC-5i) and 3D U87 tumor spheroids	Diseased/normal		273
		Gold	5	/	*In vivo* (mouse)	Diseased (glioblastoma)	*Oral administration	274
		Gold	5	−26.8	*In vitro* (BMVECs) and *in vivo* (mouse)	Diseased (glioblastoma)	*Oral/i.v. administration	275
	Apolipoprotein E peptide	Polymersome	42–45	+1.06 to +2.02	*In vivo* (mouse)	Diseased (glioma)	*Intranasal administration	276
		Chimeric polymersome	80–86	+1.6	*In vivo* (mouse)	Diseased (glioblastoma)		277
		PBCA	196.4	−8.8	*In vitro* (hCMEC/D3) and *in vivo* (mouse)	Diseased (cryptococcal meningitis)		278
		Polymersome	44	−5.2	*In vivo* (mouse)	Diseased (glioma)	*Intranasal/i.v. administration	279
	Polysorbate 80	PLGA	220	−32.9	*In vivo* (rat)	Diseased (seizures)/normal		280
	Phosphatic acid	HDL	26.4	−7.2	*In vitro* (hCMEC/D3) and *in vivo* (mouse)	Diseased (Alzheimer's disease)		281
Targeting ligand to transferrin receptors	Anti-TfR antibody	PMLA	28.0–28.5	−9.9 to -11.0	*In vivo* (mouse)	Diseased (glioblastoma)		282
	H-ferritin	Iron oxide	6.6	/	*In vitro* (bEnd.3) and *in vivo* (mouse)	Diseased (glioblastoma)/normal		283
	Transferrin targeted peptide	Chitosan-*c*-PGA	132	−38	*In vivo* (mouse)	Diseased (cerebral infarction)		284
Disease targeting ligand	RAP peptide decoration (ligand of RAGE)	PCL-PEG	86.9	−38.3	*In vitro* (bEnd.3) and *in vivo* (mouse)	Diseased (Alzheimer's disease)	In AD lesion sites, the receptor of advanced glycation end products (RAGE) is specifically and highly expressed on the diseased neurovascular unit, including cerebral vascular endothelia l cells, astrocytes and neurons	285
	Diphtheria toxin receptor (DTR) ligand	Poly(ethylene oxide-*co*-propylene oxide)	129–240	−25.6	*In vitro* (hCMEC/D3)	Diseased (glioblastoma)	DTR is up-regulated on the cerebral blood vessels in gliomas, ischemic stroke, and under hypoxic conditions	286
	Neuropilin-1 targeted peptide	Poly(levodopamine)	313	−37.9	*In vivo* (mouse)	Diseased (Glioma)	Neuropilin-1 expressed on neovasculature/glioma cells	287
	Claudin-1 targeted peptide	PEG-Gd	14.5	+7.8	*In vivo* (mouse)	Diseased (aging-induced altered brain)	Claudin-1 is upregulated in aging brain vasculature	288
	cRGD	PEG-*b*-poly-(L-glutamic acid)	29	−2.3	*In vivo* (mouse)	Diseased (glioblastoma)	Affinity of cRGD to Rvβ3 and Rvβ5 integrins that are overexpressed on	289

Table 4 (*continued*)

NM engineering strategy	Surface modification	Core material	Size (nm)	Zeta potential (mV)	Model system	Diseased/normal state	Comments	Ref.
							endothelial cells of tumor angiogenic vessels as well as GBM cells	
	Tryptamine (Try)	Try- Cinnamaldehyde nanoprodrug	200	−0.2	*In vivo* (mouse)	Diseased (glioblastoma)	Try is more easily internalized by gliomas cells *via* the over-expressed 5-HT receptors	290
	CXCR4 targeted anatagonist	PEG-PCL	100	/	*In vivo* (mouse)	Diseased (ischemia)	CXCR4 overexpession in the ischemic brain	291
	VCAM-1 targeted peptide	lanthanide	80	−4	*In vitro* (bEnd.3) and *in vivo* (mouse)	Diseased (ischemia)	VCAM-1 is over-expressed in the cerebral ischemia area	292
	IL13	PEG-PLGA	92	−30.5	*In vitro* (human brain microvascular endothelial cells with human astrocytes and human brain vascular pericytes) and *in vivo* (mouse and rat)	Diseased (glioma)	IL13 binds to the tumor-specific interleukin-13 alpha 2 receptor	293
	iRGD	Solid lipid	300	−8	*In vitro* (hBMEC or mBMEC) and *in vivo* (mouse)	Diseased (glioblastoma)	iRGD: tumor-targeting transcytotic peptide	294
		Zinc phthalocyanine	122	−31.6	*In vitro* (bEnd.3) and *in vivo* (mouse)	Diseased (glioblastoma)		295
	p-Hydroxybenzoic acid (p-HA)	Liposome	123	0.14	*In vivo* (mouse)	Diseased (glioma)	*p*-HA has high affinity for dopamine and sigma receptors which are prominent in the BBB. And over-expressed in brain tumors	296
Targeting ligand: Glucose transporter (GLUT-1)	Cholesterol-undecanoate-glucose conjugate	Liposome	96.2	/	*In vivo* (mouse)	Diseased (malaria)	Better brain targeting *via* i.n. administration	297
	Glycose	PEG-PLL	45	/	*In vivo* (mouse)	Diseased (glycemic conditions, Alzheimer's)		298
Targeting ligand: large neutral amino acid transporter (LAT)-1	L-DOPA	Gold	90	/	*In vitro* (hCMEC/D3 and primary rat brain microvascular endothelial cells)	Normal		299
Targeting ligand: acetylcholine and choline tranbsporters	PMPC	PAMAM dendrimer	8	1.48	*In vivo* (mouse)	Diseased (glioblastoma)		300
	Choline analogue (MPC)	PEGMA	74	0.12	*In vitro* (bEnd.3) and *in vivo* (mouse)	Diseased (glioma)		301
BBB targeting antibody	RG3 single-domain antibody	Liposome	110	/	*In vitro* (bEnd.3) and *in vivo* (mouse)	Diseased (glioma)/ normal		302
	JAM-A targeting antibody	Gold	70	/	*In vivo* (mouse)	Normal	+Increased BBB permeability *via* laser pulse excitation	303
Targeting ligand: folate receptor	Folic acid	Carbon	359.24	−24.7	*In vivo* (mouse)	Diseased (glioblastoma)		304
Targeting ligand: NGF receptor	NGF	MgO micelle	120	−10	*In vivo* (mouse)	Diseased (Parkinson's)		305
Targeting ligand: BBB targeting peptide	TGN	Glycolipid nanomicelle	146.2	+28.2	*In vivo* (rat)	Normal		306
BBB crossing ligand	LysoGM1	PLGA	246.8	−33.2	*In vivo* (zebrafish and mouse)	Diseased (Glioma)/ Normal		307
Extracellular vesicles (EVs)	MSC-derived exosomes	Gold	129.2	−39.9	*In vivo* (mouse)	Diseased (stroke)		308
	Grapefruit EVs	Heparin-based	192	/	*In vitro* (hCMEC/D3) and *in vivo* (mouse)	Diseased (glioma)		309

Table 4 (*continued*)

NM engineering strategy	Surface modification	Core material	Size (nm)	Zeta potential (mV)	Model system	Diseased/normal state	Comments	Ref.
	/	Neuron-2a cell derived exosomes	114		*In vivo* (mouse)	Diseased (Alzheimer's)		310
	MSC-derived exosomes	Gold	100	/	*In vivo* (mouse)	Diseased (stroke, Parkinson's, Alzheimer's, autism)		311
	/	EVs from hiPSC-derived NSCs	145.3	/	*In vivo* (mouse and rat)	Diseased (status epilepticus)	i.n. administration	312
	RGD	EVs from ReN VM cells	100–250	/	*In vivo* (mouse)	Diseased (glioblastoma)		313
	RAW264.7 exosome membrane decorated with cRGD	DSPE-PEG-PEI	152	−20	*In vitro* (bEnd.3) and *in vivo* (mouse)	Diseased (diffuse intrinsic pontine glioma)		314
	CXCR4	NSCs derived EVs decorated with CXCR4	84.3	−24.4	*In vivo* (mouse)	Diseased (glioblastoma)	CXCR4 is a chemokine receptor specific for CXCL12 that is over-expressed in cancer cells, including GBM	315
Combination of targeting ligands	CGN BBB targeting ligand + Tet-1 neuronal targeting ligand	PEG-PDMAEM	70–80	+10	*In vivo* (mouse)	Diseased (Alzheimer's)		316
	Folic acid + Transferrin + Polysorbate 80	PLGA	109.7	−9.38	*In vivo* (rat)	Diseased (Glioma)		317
	Lactoferrin + RGD dimer	Fe3O4/Gd2O3	14.7	/	*In vitro* (HBEC-5i) and *in vivo* (mouse)	Diseased (glioblastoma)/normal		318
Cell mediated delivery	Bone marrow derived macrophages	Iron oxide	190	/	*In vitro* (only transwell inserts) and *in vivo* (rat)	Diseased (glioma)		319
	Bacteria (*Escherichia coli* 25922)	GP-ICG-SiNPs	4.1	/	*In vitro* (human brain microvascular endothelial cells) and *in vivo* (mouse)	Diseased (glioblastoma)		320
	(MOG_{35-55}) T-cells	PLGA-PEG iron oxide	44.1	−40	*In vivo* (mouse)	Diseased (autoimmune encephalomyelitis)/normal		321
Cell membrane coated	Apolipoprotein E peptide-decorated red blood cell membrane	dextran	180	−5	*In vitro* (bEnd.3) and *in vivo* (mouse)	Diseased (glioblastoma)		322
	Angiopep-2-decorated red blood cell membrane	PEI	150–500	−30 × changes with pH	*In vitro* (bEnd.3) and *in vivo* (mouse)	Diseased (glioblastoma)		323
	Macrophage membrane expressing PD-1	PLGA	124.1	−18.9	*In vitro* (bEnd.3) and *in vivo* (mouse)	Diseased (glioblastoma)		324
	/	Hybrid membrane nanocomposites using DC and C6 glioma cell membranes	154	−20 to −33	*In vitro* (bEnd.3) and *in vivo* (mouse)	Diseased (glioma)		325
	Natural killer cell membrane	AIEdots	80	−33.6	*In vitro* (bEnd.3) and *in vivo* (mouse)	Diseased (glioblastoma)		326
	Macrophage membrane	MnO2@PVCL	270	−8.2	*In vitro* (bEnd.3) and *in vivo* (mouse)	Diseased (glioblastoma)		327
Magnetic targeting		BaTiO3 (BTO) @CoFe2O4	20–30	+30	*In vitro* (primary human brain microvascular endothelial cells with human astrocytes and human brain vascular pericytes)	Diseased (HIV)		328

Table 4 (*continued*)

NM engineering strategy	Surface modification	Core material	Size (nm)	Zeta potential (mV)	Model system	Diseased/normal state	Comments	Ref.
		PLGA-MgO/SPIONs	68.4	−33.2	*In vivo* (rat)	Diseased (glioma)		329
	Anti-TfR antibody	Lipid-SPIONs	101.3	/	*In vitro* (C8D1A with bEnd.3)	Diseased (glioblastoma)		330
FUS + micro/nano bubbles	Fluorinated surfactant	Perfluorooctyl bromide (PFOB)	60	/	*In vivo* (mouse)	Normal		331
		Sonosensitive liposome + microbubbles	123.9	/	*In vivo* (mouse)	Diseased (glioblastoma)/normal		332
	PVG peptide	PEG-liposomes + nanobubbles	115.4	+13.6	*In vivo* (mouse)	Normal		333
Others: virus mimicking NPs	Viral envelope (E) protein	Pbs QDs wrapped in TPE-BPA@8CTAB	50	+25	*In vivo* (mouse)	Diseased (inflammation)		334
Others: surface functionalization with cell penetrating peptide	CB5005 peptide	liposome	110	−5	*In vivo* (mouse)	Diseased (glioblastoma)		335
Others: BBB targeting core material	/	Albumin	150.4	−35	*In vitro* (bEnd.3) and *in vivo* (mouse)	Diseased (glioblastoma)	Albumin binding proteins (SPARC) present in glioma	336
		Albumin/PLGA	353–497	−37	*In vivo* (mouse)	Diseased (Parkinson's)	Albumin has the ability to permeate the BBB *via* receptor-mediated pathways	337

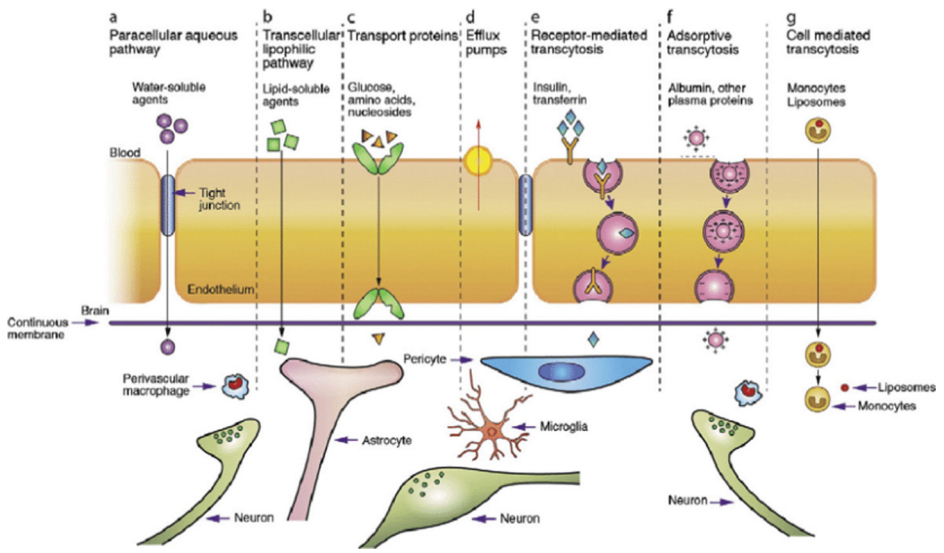

Fig. 14 Transport pathways of substances across the BBB. Reproduced from Ref.1 with permission from Elsevier.

4.1. NM characteristics influencing interaction with the BBB

As the BBB is a strong barrier, BBB crossing requires effective strategies to deliver therapy for brain diseases. Multiple NP formulations and designs have been researched over the years, and a general overview of these is given in Fig. 15. Here, we report an overview of different nanoparticle properties such as size, surface charge, surface chemistry and BBB targeting strategies that showed effective transport through an *in vitro* or *in vivo* BBB model. Please note that while BBB transport has been widely studied using both organic and inorganic NPs, the majority of studies focused on organic NPs (Fig. 15A). Given the large variety of NP types, it is furthermore rather difficult to properly evaluate the influence of the NP core material on BBB crossing ability. We therefore do not address the topic of NP composition directly, but rather indirectly, where specific aspects such as magnetism or NP rigidity will be discussed in view of the specific NP types.

4.1.1. Size. The size of NPs is an important parameter for effective targeting (Fig. 15B). NPs with diameters less than 10 nm are rapidly cleared from the circulation by the

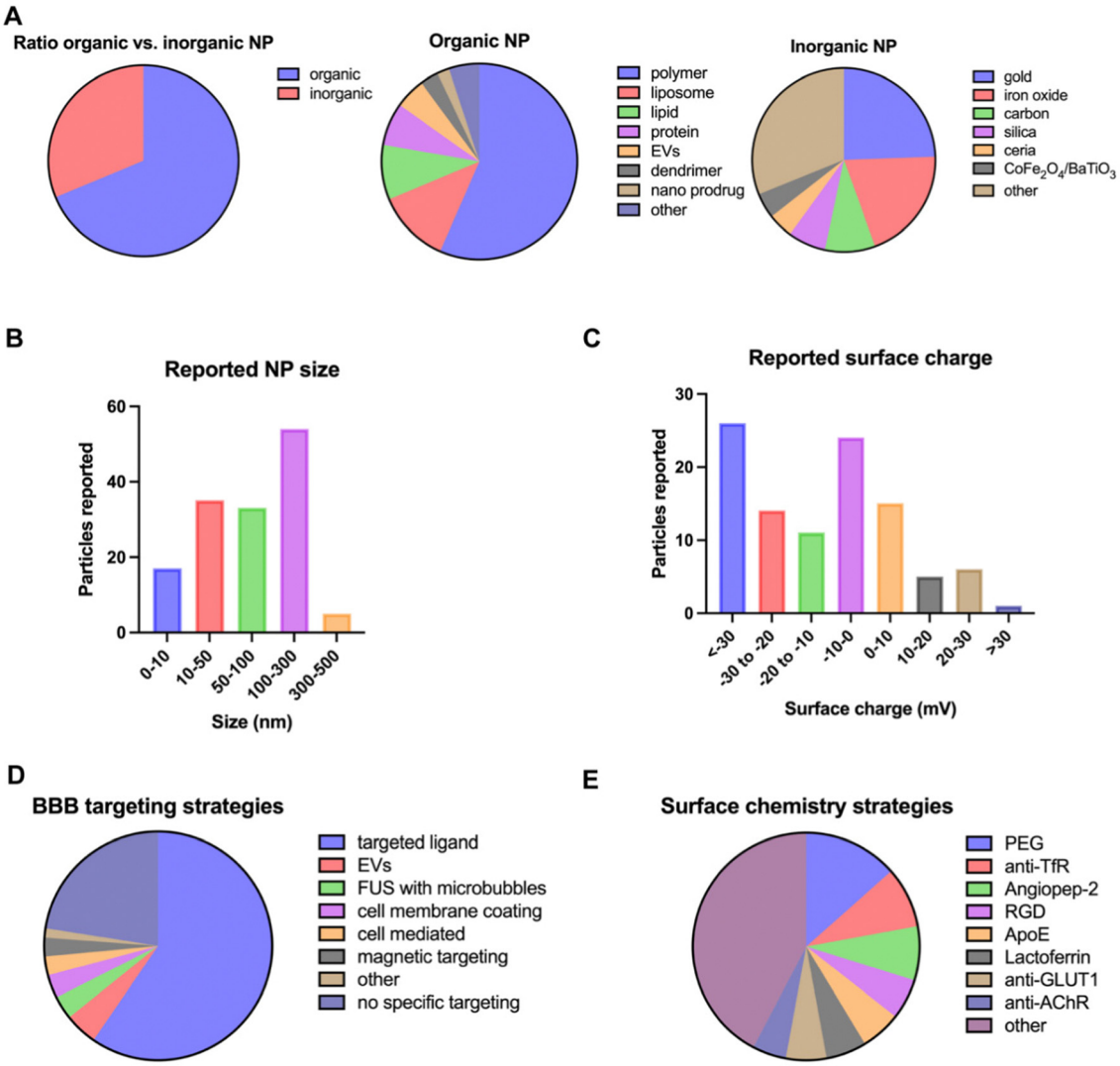

Fig. 15 Overview of NP characteristics and BBB targeting strategies used for brain delivery. Characteristics of interest are (A) core material, (B) size, (C) surface charge, (D) BBB targeting strategies and (E) surface chemistry strategy. Graphs are based on data extracted from the PubMed database of the last 10 years and the search terms 'nano' and 'blood brain barrier', identifying 287 research articles from which 141 articles were selected and used for data insights, with the criteria that show evidence of BBB crossing *in vivo* (animal model) or *in vitro* (Boyden chamber). Only original research articles and articles within the scope were included.

renal system, while NPs larger than 200 nm have a higher chance to be cleared by the reticuloendothelial system (RES).[263] Therefore, NPs in between this range (10–200 nm) are commonly used for *in vivo* targeted delivery. For crossing the BBB, additional size requirements could be expected, but reports have not shown conclusive trends. Shilo and colleagues investigated the effect of Au NP size on the probability to cross the BBB, by quantifying their uptake in bEnd.3 endothelial cells *in vitro*.[338] They incubated Au NPs of various sizes (20, 50, 70 and 110 nm) with the brain endothelial cells and concluded that the 70 nm NPs showed the highest cellular uptake. In a study by C. Li *et al.*, it was revealed that 40 nm Au NPs show an increased endothelial paracellular permeability *in vitro* and an enhanced brain permeability *in vivo* compared to 637 nm Au NPs.[339] The enhanced BBB permeability of the 40 nm NPs was shown to be due to tight junction disassembly and tight junction protein degradation.

Furthermore, there is evidence that size is not a determining factor regarding BBB crossing, if the particles are in an acceptable size range.[263,264] To shed light on the effect of NP physicochemical characteristics on BBB passage, Voigt *et al.* evaluated the influence of size, zeta potential and surfactant composition on BBB transport.[264] For this purpose, they designed fluorescently labeled polybutylcyanoacrylate (PBCA) NPs with a size range from 64 nm to 464 nm and imaged the NP transport through the retina barrier, a model for the BBB barrier, using *in vivo* confocal neuroimaging. Their results indicated that NP size does not influence BBB transport, but the most important parameter proved to be surface chemistry. However, it should be noted that for comparing the effects of

NPs of different sizes, it is not easy to decide how the equivalent injected NP dose will be determined (total mass, NPs mL^{-1}, total surface area) and specifically for fluorescence imaging, bigger NPs will be brighter and hence more easily detected, which may result in biased results.

Additionally, the employed BBB model should be taken into consideration when NP size is investigated. A lot of research on the influence of NP size on BBB permeation has been performed using *in vitro* BBB models, which cannot fully recapitulate the *in vivo* biodistribution clearance mechanisms. For example, in the study of Ohta *et al.*, the size-dependence of Au NP brain delivery, assisted by FUS-induced BBB opening, was investigated.[340] They compared the permeability efficiency of 3 nm, 15 nm and 120 nm Au NPs across an *in vitro* and *in vivo* BBB mouse model. Interestingly, it was shown that the permeability of smaller NPs was higher *in vitro*, while the highest permeability *in vivo* was with the medium sized NPs.

This size-dependence was attributed to competition for permeation through gaps in the BBB and excretion of particles from blood circulation. Of note, the authors determined the equivalent dose of the different NP sized formulation based on the total mass of gold. This means that in their setups, the concentration of NPs mL^{-1} or total surface area for a particular NP size would vary. This is important to take into consideration, in particular upon considering active targeting strategies where at equal ligand densities, the NPs with the highest total surface area will have a higher absolute number of targeting ligands, which may affect receptor binding efficacy and associated transcytosis across the BBB.

4.1.2. Surface charge. Only limited studies have investigated the true effect of surface charge, so conclusive trends cannot be made (Fig. 15C). However, a few interesting studies have reported on the surface charge effect. The BBB and specifically the brain endothelial cell membranes express high levels of phosphatidylinositol and phosphatidylserine on their cell membrane glycocalyx, which results in a more negative surface charge of the brain endothelium, compared to other vascular endothelial cells.[341] This negative charge provides an extra barrier for the penetration of drugs and molecules across the BBB. Zhang *et al.* investigated the permeability of neutral *versus* positively charged NPs across an *in vitro* BBB and showed that positively charged NPs resulted in a 100-fold higher permeability than the neutral ones. Based on their *in vitro* results, the researchers developed an *in silico* BBB model to predict the permeability of NPs due to their charge and size as well as the ion concentration of the surrounding salt solution, and the charge, rigidity, surface tension and viscoelastic properties of the endothelial cell membrane. Their predictions revealed that the charge of the endothelial cell (EC) membrane is fundamental for the transcytosis of NPs. They showed that when EC membranes have no charge, no NPs can cross the *in vitro* BBB. On the other hand, when the EC is negatively charged, there is a higher probability that neutral NPs may pass through transcytosis.[342] The predictions from their *in silico* model could explain the measured permeability data of their *in vitro* results. Positively charged NPs have been shown to cross the BBB easier *in vitro*, but when administered *in vivo*, there are other factors that should be taken into consideration, such as their tendency for rapid formation of a more tightly bound protein corona, which can lead to rapid clearance by the RES, while when administered at high concentration, they may result in BBB toxicity.[341,343] In addition, it is demonstrated that negatively charged and neutral NPs present reduced adsorption of serum proteins and hence an increased circulation half-time.[344]

The work of Lockman *et al.* demonstrated that high concentrations of negatively charged NPs and both high and low concentration of positively charged NPs affected BBB integrity, while neutral NPs had no acute effect.[345] In addition, the researchers showed that neutral NPs and low concentrations of anionic NPs can be delivered safely across the BBB. Therefore, these results indicate that not only the cationic NPs have the potential to cross the BBB, but the neutral and negatively charged NPs do so too.

4.1.3. Shape. Several studies have shown that the shape of nanomaterials affects their *in vivo* biodistribution and their interaction with cell membranes.[344,345] Especially NPs with higher aspect ratios have been shown to interact more with the endothelium.[346,347] Illustratively, Nowak *et al.* used a 3D human BBB microfluidic model to investigate the impact of NP physical parameters on their BBB penetration. The results indicated that the trans-endothelial transport rate of rod-shaped polystyrene NPs across the BBB was higher compared to that of spherical NPs.[348]

On the other hand, there are studies showing that spherical NPs exhibit higher permeation across the brain endothelium than their rod- or star-shaped counterparts. Liu *et al.* investigated the permeabilization of TiO_2 NPs across an *in vitro* as well as an *in vivo* BBB model, and their findings suggest that spherical TiO_2 NPs have higher BBB permeabilization efficiency than rod-shaped particles with similar size.[349] In addition, Enea *et al.* showed that spherical Au NPs internalized more efficiently in BBB endothelial model cells than their counterpart star-shaped NPs.[350]

The discrepancies between the above-mentioned studies regarding the shape effect on BBB permeation can be attributed to variation of other parameters influencing BBB crossing, such as the NP material, BBB model and experimental method used for the validation of BBB permeation. For example, other parameters play a role *in vivo*, such as the sequestration of NPs by macrophages, on the biodistribution and BBB permeation efficiency of NPs. Several studies have shown that NPs with a higher aspect ratio are phagocytosed less efficiently by macrophages, which should be taken into consideration when engineering NPs for BBB targeting through systemic delivery.[351,352]

4.2. Targeted delivery strategies

In the last decade, a plethora of research has been conducted on surface functionalization of NPs with moieties that target components present on the BBB or on chemotaxis exploitation of biological vehicles for enhancing NP passage across the BBB.

In this section we give an overview of the most studied strategies for targeted delivery of NPs (Fig. 16). In most of the studies, the BBB targeting strategy followed is the surface modification of NPs using a targeting ligand (Fig. 16D). In this section we are discussing the main receptors/transporters on the BBB that have been exploited as targets of ligand-functionalized NPs.

4.2.1. Receptor-mediated transcytosis. Receptor-mediated transcytosis is the most extensively studied route for NP-mediated brain targeted delivery. Some of the BBB receptors that have been investigated for delivering therapeutics across the BBB are the low-density lipoprotein receptor (LDLR), transferrin receptor (TfR), insulin receptor, epidermal growth factor receptor (EGFR) and nicotine acetylcholine receptor (nAchR).

4.2.1.1. Low-density lipoprotein receptor (LDLR). LDLR is a transmembrane receptor involved in lipid metabolism and is found in different organs such as the liver, the adrenal cortex, the ovarian corpus luteum and cell structures like neurons and glial cells. The main ligands for LDLR are apolipoproteins in the blood such as apolipoprotein A-I and/or E (ApoE). LDLR has often been used for targeting BBB crossing by NPs.[353–361] It has been shown that the use of surfactants, such as polysorbate 80 and poloxamer 188, enables the adsorption of apolipoproteins from the blood on the NP surface.[339,340] After the adsorption of apolipoproteins on the NP surface, LDL receptor-mediated transcytosis through the BBB becomes possible. Similarly, in a study by Voigt *et al.*, efficient BBB passage was achieved when PBCA-NPs were fabricated with non-ionic surfactants (Tween80, LutensolAT80, Tween20, Brij35) or cationic stabilizers (such as DEAEdextran), but not when anionic compounds were added (SDS).[337] Thus, non-anionic surfactants allow the adsorption of Apo-E from blood, which leads to an efficient BBB passage through the LDL receptor-mediated transcytosis. Additionally, the successful BBB passage of the cationic DEAEdextran NPs suggests that adsorption mediated transcytosis may also play a role. A study by Piazzini *et al.* further confirms the advantages of surfactant usage for BBB crossing. Sterically stabilized liposomes with Tween 80 alone or in combination with didecyldimethylammonium bromide (DDAB) increased the permeability of andrographolide (AG) across hCMEC/D3 monolayer cells. Their results suggest that caveolae-mediated endocytosis is the main mechanism involved in NP uptake.[362] Exploiting the beneficial BBB crossing effect of surfactants, Dal Margo *et al.* proposed a translational NP targeting strategy by using lipid NPs with polysorbate 80 as a surfactant and incubating with recombinant human ApoE4.[363] The ApoE4 decorated NPs showed a 3-fold increased brain accumulation in BALB/c mice, compared to the non-decorated NPs (Fig. 17).

In addition to (indirect) absorption of apolipoproteins on the NP surface, ApoE can be directly coated on the NP surface. For example, Wei *et al.* used a short ApoE peptide, which is less

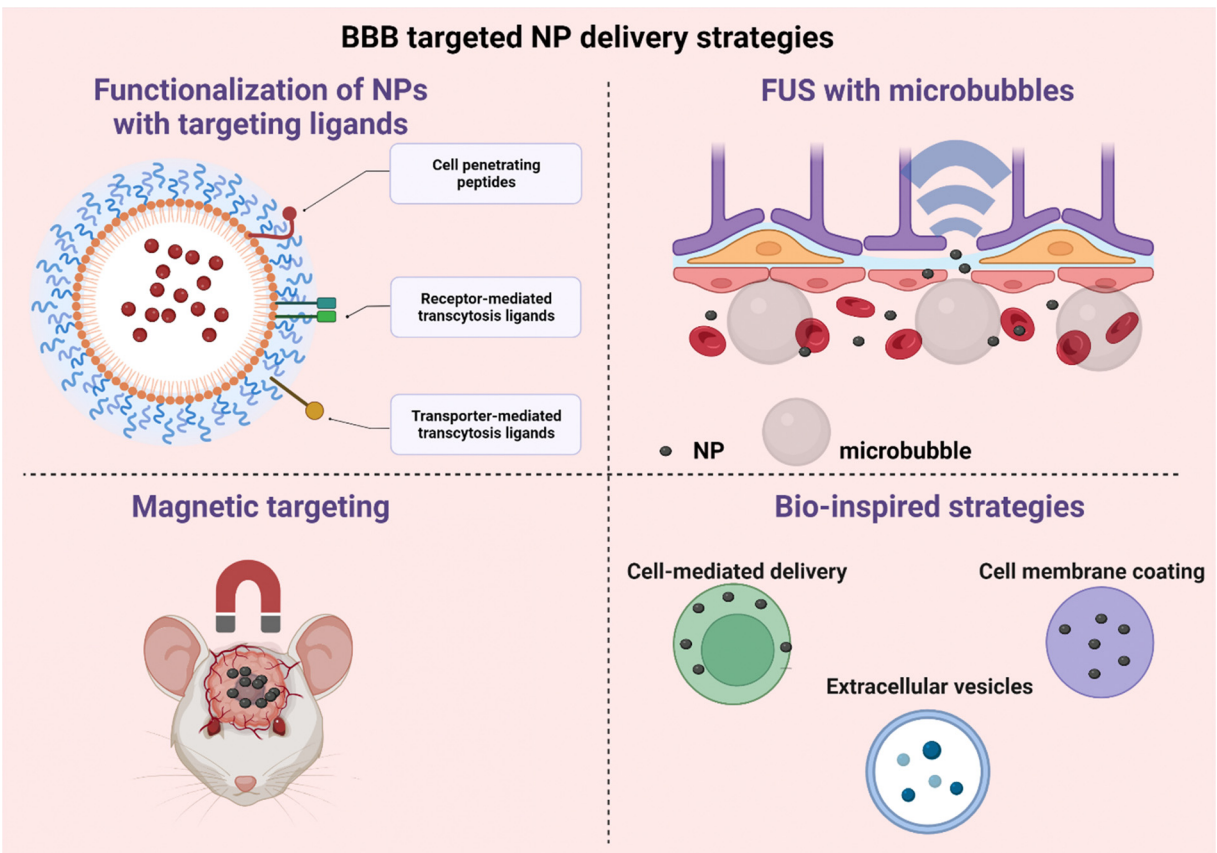

Fig. 16 Schematic representation of the BBB targeted NP delivery strategies. Created with https://BioRender.com.

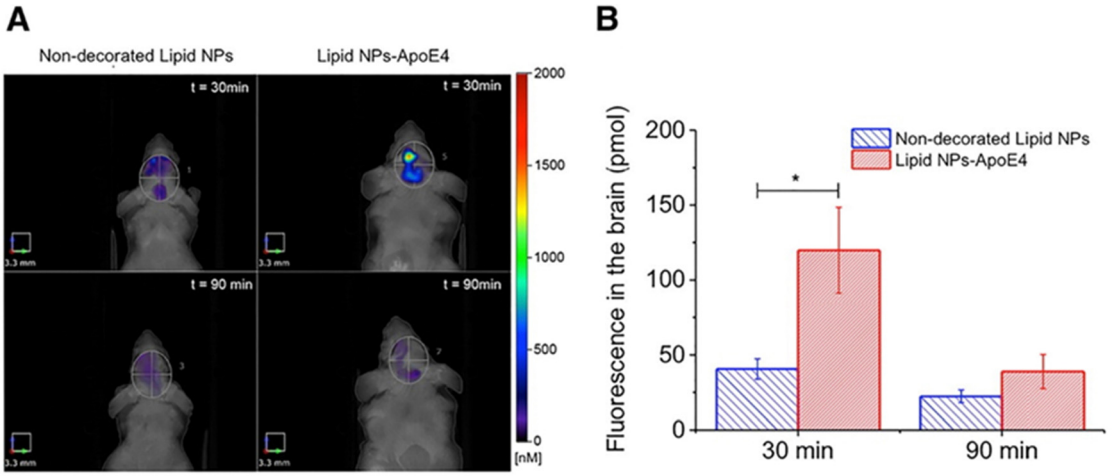

Fig. 17 Comparison of fluorescence of non-decorated and ApoE4-decorated lipid NPs in the brain. (A) Mice were treated with 100 μL of non-decorated lipid NPs or lipid NPs-ApoE4 (ApoE4: 5 μg mL^{-1}) by IV injection and each mouse was analysed 30 min (upper panels) and 90 min (lower panels) after the administration. (B) Quantification of fluorescence (pmol) in the selected region of interest. *$p < 0.01$ by Student's *t*-test. Reproduced from ref. 363 with permission from Elsevier.

immunogenic, easy to synthesize and amenable to chemical modifications than the large apolipoprotein E, to decorate polymersomes for glioma immunotherapy.[364] They used a combination treatment of ApoE-decorated polymersomes loaded with granzyme B, a serine protease granzyme mostly found in natural killer cells and cytotoxic T-cells, or loaded with immunoadjuvants like CpG oligonucleotide (CpG). This combination treatment induced significantly more immunogenic cell death compared with free GrB and non-decorated polymersomes. Additionally, Neves *et al.* functionalized solid lipid nanoparticles with ApoE to assess the advantage of functionalization.[365] Their results showed an increased transcytosis of ApoE modified NPs through an *in vitro* BBB model compared to non-modified NPs, which could be attributed to the interaction between the ApoE ligand and overexpressed LDL receptors in the BBB.

4.2.1.2. Transferrin receptor (TfR). The iron-transport protein transferrin (Tf) is a glycoprotein abundant in plasma, which, upon binding to the transferrin receptor, shuttles iron between cells. Iron binding to transferrin serves three main purposes: (i) it maintains Fe^{3+} in a soluble form under physiologic conditions, (ii) it facilitates iron transport and cellular uptake, and (iii) it maintains Fe^{3+} in a redox-inert state, preventing the generation of toxic free radicals.[366] Two different TfRs have been recognized, TfR1 and TfR2. In the brain, iron deficiency leads to increased translocation of TfR1 to the membrane of microvascular endothelial cells. As TfR is overexpressed at the BBB in diseases such as Alzheimer's disease (AD) and Parkinson's disease (PS) and in brain tumors such as glioblastoma (GBM), TfR-targeted brain drug delivery systems have been extensively explored the recent years.[367–372]

The advantage of using Tf-decorated NPs to target GBM was exploited by Lam *et al.*, who showed that Tf-decorated liposomes co-loaded with temozolomide and bromodomain inhibitor JQ1 resulted in a significantly prolonged survival of U87MG and GL261 glioma mouse models.[373] Similarly, Sun *et al.* showed that the decoration of PTX loaded PEG-PLA micelles with the TfR-T12 peptide presented a prolonged median survival of nude mice bearing glioma.[374]

An important parameter that should be taken into consideration for successful translocation of Tf-NPs from the endothelium into the brain parenchyma is the avidity of Tf-decorated NPs for TfR. In their study, Wiley *et al.* investigated how NP avidity affects their permeation across the BBB into the brain parenchyma.[375] As the avidity of NPs for TfR increases with respect to NP size and Tf content, their study showed that NPs with high binding avidity to TfR resulted in an increased association of the NPs with the brain endothelial cells and thus lower accumulation in the brain parenchyma. NPs with less avidity showed an increased accumulation in the brain parenchyma, which could be attributed to the transcytosis pathway. Continuing this work, a solution for boosting the transcytosis of Tf-NPs across the BBB was proposed by synthesizing 80 nm Au NPs with an acid-cleavable linkage between Tf and NP core.[376] This system exploits the drop in pH during NP transcytosis, so that after the NPs reach the brain, they are free from TfR and can be released into the brain parenchyma.

A second parameter that should be optimized is the density of the TfR antibody on the surface of NPs. A higher density of the TfR antibody has been proven to be more efficient for transmigration of NPs across the BBB, which indicates that there is a lower density limit for successful targeting. However, a higher density comes with the consequence of off-targeted accumulation in the lungs and spleen.[377]

4.2.1.3. Insulin receptor. Insulin receptors (IRs) are highly expressed on the BBB endothelial cells and transport insulin to the brain from the blood through receptor-mediated transcytosis.[378] These receptors can be exploited for the active targeting of the brain using surface functionalized NPs with anti-insulin receptor antibodies. In their study, Ulbrich *et al.*

surface functionalized human serum albumin (HSA) NPs with insulin or an anti-insulin receptor antibody (29B4), with the goal to transfer the drug loperamide into the brain.[379] They tested the antinociceptive effect of the drug through a tail flick test in an ICR (CD-1) mouse model and showed that both insulin and 29B4 surface coated NPs resulted in higher antinociceptive effects compared with the drug alone, while a pre-injection with 29B4 antibody before NP administration inhibited the antinociceptive effects, attributed to saturation of the IRs from the plain antibodies. Furthermore, Kuo *et al.* developed carmustine (BCNU) loaded SLNs grafted with an 83–14 MAb for targeting BBB IRs, which resulted in an improved permeability across an *in vitro* BBB model.[380] Similarly, the study of Shilo *et al.* showed a 5 times greater accumulation of Au NPs in the brain of BALB/c mice when NPs are surface functionalized with insulin compared to non-functionalized NPs.[381]

4.2.1.4. Nicotinic acetylcholine receptor (nAchR). Nicotinic acetylcholine receptors (nAchRs) are receptors for the acetylcholine neurotransmitter and can be found in the peripheral and central nervous system. nAchRs are also expressed on the BBB and BBB permeability can be increased by nicotine treatment.[382] With this in mind, Huey *et al.* conjugated doxorubicin (DOX) loaded PLGA NPs with a 39 amino acid rabies-virus derived peptide (RDP), possessing nAchR binding capability.[383] Their study showed doubled cytotoxicity of RDP-DOX NPs *in vitro*, on SH-SY5Y neural cells, compared to non-decorated DOX-NPs, while nAChR was proven to be essential for RDP uptake. In another study by Hua *et al.*, RVG was used as well, with a 29-amino-acid sequence for an active brain-targeting NP delivery.[384] They developed docetaxel (DTX) loaded RVG29-PEG-PLGA NPs as an anti-glioma targeted therapy and investigated NP biodistribution as well as the anti-glioma effect on a rat glioma model. The results showed that the RVG29 decorated NPs reached the brain with a 2.1 higher concentration than the non-decorated NPs, while the group treated with the RVG decorated NPs had the highest medium survival time.

In a later study, Park *et al.* exploited the RVG brain targeting system for delivery of siRNA for the treatment of Alzheimer's disease.[385] siRNA was loaded in poly(mannitol-*co*-PEI) NP complexes (R-PEG-PMT), showing an increased brain uptake for R-PEG-PMT *in vivo*, while a significant decrease in the expression level of GAPDH mRNA in the brain was noted. Furthermore, R-PEG-PMT/siBACE1 complexes showed significant downregulation of BACE1 in both cortex and hippocampus, whereas PEI, R-PEG-PEI and PEG-PMT/siBACE1 only showed significant down-regulation in the cortex.

Another promising group of peptides with high binding affinity to the nAChR are snake neurotoxins. CDX is a peptide sequence isolated from candoxin, a snake venom, and was investigated by Sepasi *et al.* for its brain delivery potential.[386] CDX-modified chitosan NPs for gene delivery into the brain indeed showed efficient entering of the brain parenchyma. Furthermore, by using ^{D}CDX surface decoration, which is resistant to proteolytic degradation, the integrity of NPs can be maintained. This was shown for CDX-decorated nanoliposomes, which were able to not only target the brain, but also reach the brain in an intact form (Fig. 18).

4.2.2. Transporter-mediated transcytosis. As transporter-mediated transcytosis is a major mechanism for nutrient transport across the BBB, these transporters also have potential for facilitating the transport of nanoformulations across the BBB. The 2 most studied transporters are the glucose and choline transporters.[387]

4.2.2.1. Glucose transporter (GLUT1). The GLUT1 transporter is a sodium-independent transporter which facilitates the transportation of glucose across the BBB and is highly expressed on the microvascular endothelial cells of the BBB, facilitating BBB transport of glucose-modified NPs.[388–390] Using this as a BBB target, Anraku *et al.* developed 30 nm polymeric micelles decorated with multiple glucose molecules with a density of 10%, 25% and 50% glucose.[391] The glucose molecules were linked onto the micelles *via* an ether linkage at the C3 or C6 position of glucose. 25% of glycosylated micelles with the glucose linked at the C6 position accumulated significantly in the brain of mice. However, these results were only obtained for mice that had been fasting for 1 day and after administration of a 20% glucose solution 30 minutes post NP administration, in order to have an elevated blood glucose concentration.

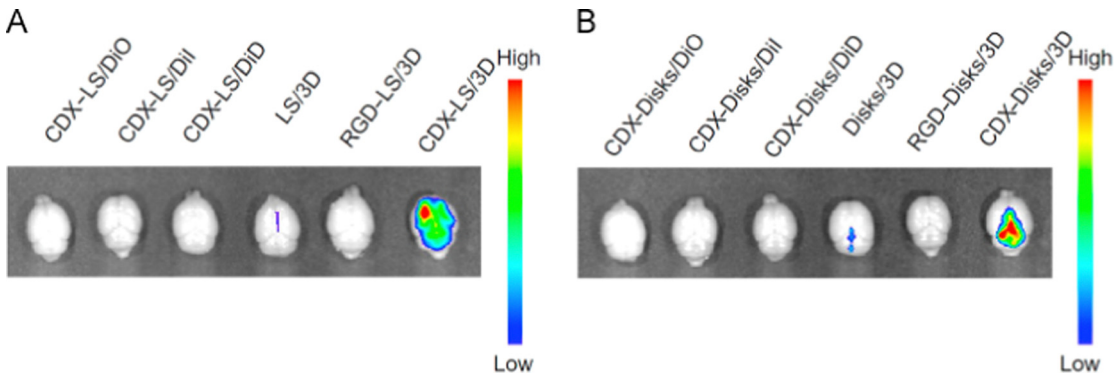

Fig. 18 The *ex vivo* imaging of liposomes (A) and disks (B) in the brains of nude mice bearing an intracranial glioma 15 days post-implantation. The excitation wavelength was 488 nm and the emission filter was 680 nm. C + R, CDX + RGD. Reproduced from ref. 386 (CC BY 4.0).

GLUT1 was also exploited by Zhou *et al.*, to deliver BACE1 siRNA polymeric nanocomplexes into the brain, for the treatment of Alzheimer's disease.[392] D-Galactose modified Cy5-siRNA nanocomplexes were synthesized, which demonstrated a 5.8-fold higher accumulation in the brain of mice and led to restoration of the cognitive performance of AD mice. Again, advantage was taken of GLUT1 recycling by treating the mice after 1 day of fasting and 30 min after 20 wt% injection of glucose solution.

4.2.2.2. Choline transporter (ChT). Similar to GLUT1 exploiting strategies, Wang *et al.* developed anti-PDL1 polymeric nanocapsules (PEGMA) with a choline analogue, 2-methacryloyloxyethyl phosphorylcholine (MPC), for an effective immunotherapy of glioma. Glioma bearing mice treated with the MPC-anti-PDL1-PEGMA nanocapsules presented a prolonged survival compared to the ones treated with anti-PDL1 alone or anti-PDL1-PEGMA nanocapsules without MPC.[393] In another study by Wu *et al.*, MPC was also used for surface decoration of polymeric nanocapsules, successfully delivering protein therapeutics to the brain of mice and non-human primates.[394]

4.2.2.3. Cell-penetrating peptides (CPPs). Cell-penetrating peptides (CPPs) are a group of naturally derived peptides that have been identified with the capability of efficiently crossing cell membranes. They can be classified into three groups: cationic, amphipathic and hydrophobic CPPs.[395] Well-studied CPPs include polyarginine, HIV-1 trans-activator of transcription peptide (TAT), penetratin and mastoparan.[396] The BBB crossing capability of CPPs has not been studied in depth yet, but was explored by Kanazawa *et al.*, who developed MPEG-PCL nanocarriers decorated with TAT. Using intranasal delivery, TAT decorated nanocarriers showed increased brain accumulation compared to naked ones.[397] However, as CPPs can cross various cell membranes, off-target uptake by other organs occurs as well.[396]

4.2.2.4. Considerations on the targeted ligand strategy. It is rather difficult to make solid conclusions about the most efficient targeting ligand for brain NP delivery, as the methods that have been used in the different studies to prove NP targeting efficiency are not comparable. There are very few studies that mention the dose of the encapsulated cargo that reached the brain related to the initial administered dose, while a lot of studies prove their point with qualitative methods such as optical imaging, microscopy or other indirect methods, such as intensity of an encapsulated dye or therapeutic outcome. In the majority of the surface engineering strategy though, NPs are functionalized with a ligand that targets LDL receptors, while in a lot of cases ligands that are related to a specific disease are aimed to be targeted (Table 4). It is worth mentioning that it would be extremely valuable to the field that scientists investigating NP targeting would give quantitative results of the dose that reached the targeted tissue related to the initial administered dose.

4.2.3. Bio-inspired strategies

4.2.3.1. Extracellular vesicles (EVs). Extracellular vesicles (EVs) are small membrane particles produced by cells, loaded with genetic material, lipids and proteins for intercellular communication.[398] EVs are divided into two main groups: (i) EVs formed from the cell's plasma membrane with average sizes of 100–1000 nm, known as microvesicles, ectosomes, or microparticles, and (ii) exosomes, which are smaller than 150 nm and are generated inside multivesicular endosomes or multivesicular bodies.[399] Given their natural property to deliver messages between cells and cross the BBB, they have been exploited as delivery vehicles to deliver therapeutics to the brain.[398] For example, Tsivion-Visbord *et al.* used EVs derived from mesenchymal stem cells (MSCs-EVs), which can home towards sites of injury, in order to improve schizophrenia-like behaviors in a schizophrenia mouse model.[400] Alternatively, Tang *et al.* used neuron-2a cell isolated exosomes loaded with neferine, a compound known for mitigating anxiety, and reported improved motor function and a reduced level of β-amyloid (Aβ) in the brain of an Alzheimer's disease mouse model.[401] Additionally, they found that only exosomes encapsulated with compounds of molecular weight lower than 1109 Da are able to cross the BBB, which is an important finding for future use of exosomes as a brain delivery vehicle.

4.2.3.2. Cell membrane coating. Biomimetic nanomaterials, including cell membranes, have gained considerable attention as delivery vehicles due to their excellent capability of escaping immune recognition. Functionalization of cell membranes with BBB targeting moieties can facilitate passage across the BBB. For example, Duan *et al.* exploited the homotypic targeting capabilities of brain cancer cell membranes for targeting brain tumors for imaging purposes, and used them as a shell for polymeric NPs, loaded with superparamagnetic iron oxide NPs (SPIOs).[402] Additionally, they engineered these cell membranes with cRGD, an endothelial integrin receptor targeting peptide, which is overexpressed in the tumor vasculature, to enhance their targeting efficiency towards glioma. Similarly, Liu *et al.* engineered red blood cell membrane (RBCm) nanovehicles loaded with anti-glioma therapeutic siRNA.[403] The nanovehicles were further decorated with Angiopep-2, resulting in superior anti-tumor efficacy in GBM bearing mice.

Apart from membrane functionalization, fusion of cell membranes to obtain a delivery vehicle with desired properties is a promising alternative strategy. For example, Hao *et al.* prepared hybrid membrane-coated nanosuspensions using the membranes of glioma cancer cells and dendritic cells and loaded them with docetaxel.[404] The exploitation of antigen presentation on the membrane of dendritic cells and the homotypic-targeting mechanism of glioma cells resulted in a delivery system exhibiting the synergistic effects of chemotherapy and immunotherapy, resulting in an enhanced anticancer effect.

4.2.3.3. Cell-mediated delivery. Cells as a whole have also been used for delivery purposes, with immune cells, such as monocytes, macrophages, dendritic cells, lymphocytes, neutrophils and stem cells, exhibiting both homing properties to sites of injury, inflammation or cancer and BBB crossing

capabilities. Immune cells have the capability of crossing the BBB in response to cytokines produced in neuroinflammation or cancer, *via* changing their shape through a process called diapedesis.[405] NPs can be attached on the cell membrane with covalent or ligand–receptor coupling, the so-called cell–NP hitchhiking system, or be internalized inside the cell cytoplasm, the so called 'Trojan Horse method'.[406] Ayer M. *et al.* exploited the migration capability of activated CD4+ T-cells across the BBB and used them for delivering NPs conjugated to the membranes of these cells for enhancing their brain targeting.[407] Alternatively, Tong H. *et al.* used SPIO internalized bone marrow derived monocytes to target the inflamed brain of mice.[408] Transiently disrupting the BBB using mannitol, bradykinin and serotonin further increased the transmigration efficiency of monocytes into the inflamed brain tissues (1.3–1.8-fold increase). In addition, Wu M. *et al.* exploited the chemotactic ability of neutrophils to inflamed tissues and used them as Trojan horses of doxorubicin loaded core–shell magnetic mesoporous silica nanoparticles to increase NP delivery into an incomplete resected U87 glioma model that mimics postsurgical glioma. This strategy enabled MRI diagnosis of the residual tumor as well as an improved survival rate and delayed glioma relapse.[409]

Besides its potential, engineering of live cells *ex vivo* also has limitations, such as the risk of mitigating cell transmigration abilities, reduced cell viability and fast degradation of the cargos before reaching their target, high cost and insufficient quantities of harvested cells.[410,411] An emerging strategy is the *in vivo* hitchhiking of immune cells with NPs which give them an 'eat me' signal in order to exploit their migratory abilities to the diseased tissue. For example, Li M. *et al.* cloaked cisplatin loaded NPs with bacteria-secreted outer membrane vesicles so as to be recognized by neutrophils upon intravenous administration and internalized by them. Following NP internalization, neutrophils targeted residual s.c. microtumors after photothermal therapy, released their cargo and eradicated the residual tumors.[411] In another example, Gao C. *et al*. intravenously injected bacteria-mimetic gold NPs in a melanoma mouse model, which were internalized by immune cells in circulation and converted to gold aggregates with a photothermal effect inside the cell cytoplasm. Next, the intracellular gold nanoaggregates were transferred to melanoma tissue *via* inflammatory tropism and showed highly effective antitumor PTT/immunotherapy.[412] These strategies show great potential for NP targeted delivery and still need to be explored for their potential to cross the BBB.

4.3. Combination strategies

4.3.1. Focused ultrasound with microbubbles. Focused ultrasound (FUS) coupled with IV administration of microbubbles is a non-invasive method for localized opening of the BBB. The mechanism of action of the localized opening of the BBB is based on the oscillation of the circulating microbubbles at the preferred location, due to their FUS exposure. This oscillation causes mechanical effects on the blood vessel walls, opening them temporarily without tissue damage.[413] Combination of nano-based delivery systems with FUS using microbubbles is therefore a promising strategy to overcome the BBB impediment. Bérard *et al.* developed perfluorooctyl bromide (PFOB) nanodroplets loaded with a hydrophobic molecule of interest (dye or drug) and administered them in healthy mice, combined with FUS-mediated BBB disruption using microbubbles.[414] Their results showed BBB permeabilization and delivery of nanodroplets to the FUS exposed hemisphere only (Fig. 19). Similarly, Moon *et al.* showed that sonosensitive liposomes, loaded with doxorubicin, combined with FUS using microbubbles showed an increased accumulation at the tumor site of a murine GBM model.[415]

Apart from co-administration of NPs with microbubbles, several studies have shown more sufficient BBB crossing when NPs are linked to the microbubbles. For example, Burke *et al.* demonstrated that 5-fluorouracil (5FU) loaded PLGA NPs, covalently linked to microbubbles with FUS activation, significantly increased NP delivery to C6 glioma subcutaneous tumors compared to PLGA NPs alone or PLGA NPs co-administrated with microbubbles.[416] Similarly, Aslund *et al.* showed that poly(butyl cyanoacrylate) (PBCA) NPs used together with casein could be self-assembled into microbubbles (NPMBs).[417] Application of FUS after intravenous administration of the NPMBs resulted in a reversible BBB disruption allowing NP delivery across the BBB.

4.3.2. Magnetic targeting. A final strategy to overcome the BBB and increase brain drug delivery is by the use of external magnetic forces and magnetic nanoparticles. Iron oxide NPs have been extensively investigated as magnetic carriers, due to their intrinsic magnetic properties as well as their biocompatibility. Below a critical size ($\sim$30 nm) iron oxide nanoparticles exhibit superparamagnetic properties, meaning that their magnetization appears to be zero, on average, at physiological temperatures, while being easily magnetized by an external magnetic field. This trait makes them ideal candidates for magnetic targeting, magnetic hyperthermia treatment, magnetic resonance imaging (MRI) and magnetic particle imaging (MPI).[418] For example, Huang *et al.* used Tween-80-SPIOs or PEI/PEG-SPIOs to target the brain of rats using an external magnetic field.[419] The presence of iron in the frontal cortex of the rats increased the BBB permeability of Tween-SPIOs combined with magnetic targeting, while the magnetic force could not increase the BBB permeability of PEI/PEG-SPIOs, indicating that both Tween 80 and the external magnetic field play a role in BBB permeability. Similarly, Kong *et al.* administered iron oxide loaded polystyrene NPs in mice and observed that after a one-hour long application of an external magnetic field on the skull of mice, a 25-fold increase in the brain retention of the NPs was achieved.[420]

4.4. Considerations for BBB delivery

Apart from the commonly chosen intravenous administration route for brain delivery of NPs, other routes of administration have been investigated. Nose-to-brain delivery is considered a non-invasive way to bypass the BBB, by delivering therapeutics directly from the nasal cavity, *via* the olfactory and trigeminal

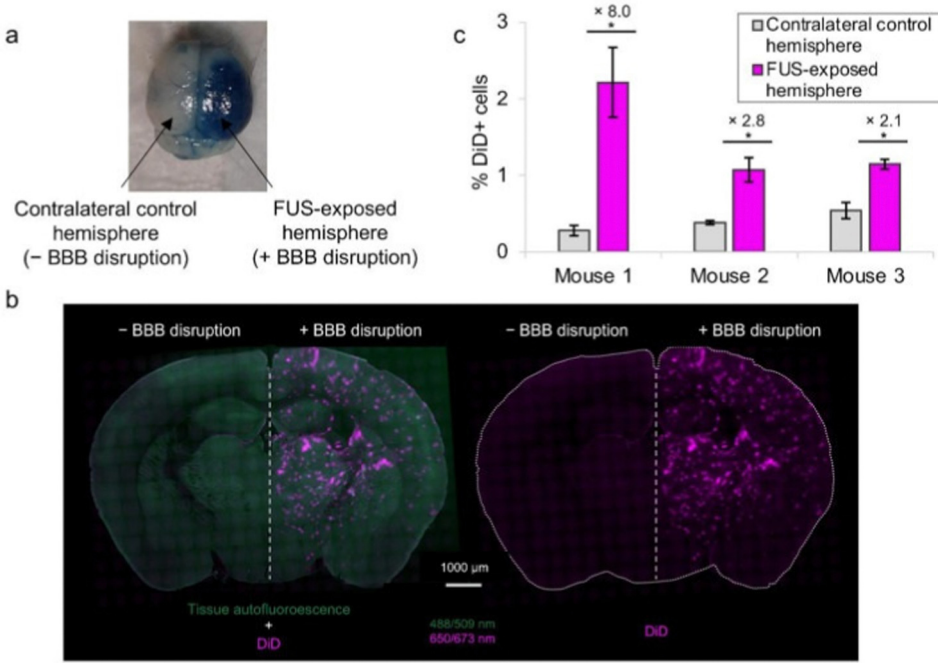

Fig. 19 *In vivo* intracerebral accumulation of nanodroplets after BBB disruption. (a) Evans blue coloration in the sonicated hemisphere after FUS exposure to 0.33 MPa acoustic pressure. (b) Fluorescence microscopy imaging of coronal brain slices after retro-orbital i.v. administration with STE (pale blue-purple) and hemisphere FUS procedure application. (c) Fluorescence-activated cell-sorting analysis of DiD positive cells in sonicated and non-sonicated (control) brain hemispheres after retro-orbital i.v. administration with STE and hemisphere FUS procedure application (n = 3 areas for each hemisphere, *$p < 0.05$, student's t-test). Adapted from ref. 414 (CC BY 4.0).

neural pathways, to the central nervous system. Comparing the delivery of dendrimers to the brain after intranasal or intravenous administration, studies have showed an increased brain accumulation after intranasal administration (Fig. 20).[421]

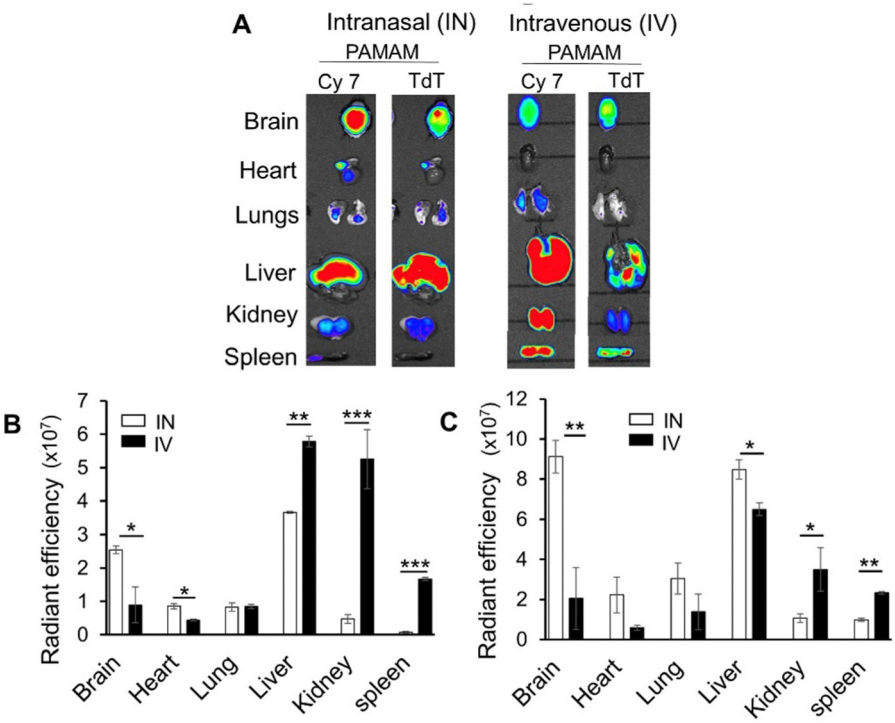

Fig. 20 PAMAM NPs with labeled with cy7 and complexed with the Td tomato plasmid were delivered IN or IV. The mice were sacrificed 72 h post administration. (A) *Ex vivo* images of the explanted organs. (B and C) Histograms representing the level of Cy7 fluorescence (B) and RFP fluorescence (C). Reproduced from Ref. 421 with permission from Elsevier.

Furthermore, Wei *et al.* compared the immunotherapy effects of (ApoE)-directed polymersomes CpG NPs in LCPN glioma bearing mice after intravenous or intranasal administration.[247] Both administration routes showed an effective glioma immunotherapy, with the intranasal administered group showing around 45 days overall survival *versus* 55 days overall survival for the intravenous administered group. While promising, intranasal delivery has some intrinsic drawbacks, as there is a limited volume and surface area of the olfactory mucosa and mucociliary clearance resulting in low drug concentrations reaching the brain. In their extensive review, D. Lee and T. Minko give the details of the pharmacokinetics and physicochemical properties of NPs that play an important role for an effective nose-to-brain delivery. We advise the readers to refer to their review for more details on nose-to-brain NP delivery.[422]

For NM to cross the BBB, a clear distinction must be made in the disease state that will be targeted. In neurodegenerative diseases, the BBB may be affected, but its integrity overall will not change too much. In invasive tumors such as glioblastoma, the effects on BBB integrity can be far more outspoken. However, it is difficult to assess the extent of it in all conditions and how to relate this to NM delivery efficacy. Preclinical imaging setups such as dynamic contrast-enhanced MRI or PET imaging are indispensable tools in this, but these are not available to all researchers. While various strategies are employed to enhance NM delivery across the BBB, as for other 'tissue barriers', one unique concept of the BBB is to purposefully break down the BBB to allow for transfer of blood-borne components to enter the brain more easily. These transient pores, generated through ablation or focused ultrasound, serve as a special tool to allow the researcher or clinician to open up small delivery portals through the barrier. As such, the excellent filtration capacity of the BBB becomes less of a direct issue, but more information is needed on the safety and efficacy of generating these pores.

Other administration routes for brain delivery include delivery by the lymphatic system, which has been shown to be more effective than iv administration,[278] and oral delivery, which is often considered the most convenient administration route, because of the ease of administration and patient compliance. However oral delivery requires formulations to cross both the intestinal barrier and the BBB to reach the brain.[279] Nevertheless, Kim *et al.* have reported the accumulation of gold (Au) NPs in the brain of glioma bearing mice after oral administration, by surface functionalizing the NPs with lactoferrin, which is expressed in the GI tract, BBB and GBM.[280]

4.5. Translatability

Despite a wealth of promising research in nanomedicine for targeting the brain and in the use of nanoparticle-mediated delivery across the BBB, only a limited number of these discoveries have made it to clinical trials. Most studies focused on tumor models such as GBM, where, due to the invasive nature of the tumor, the integrity of the BBB itself may have been compromised facilitating the delivery of the investigated nano-therapeutics across the BBB. An initial study (phase I; NCT00734682) examined the pharmacokinetics of a liposomal irinotecan derivative in patients with recurrent, high-grade gliomas. While the trial stopped in 2014, no follow-up trial was set up, likely indicating the poor brain delivery. A second trial (phase II; NCT02340156) studied the efficacy of temozolomide together with p53 cDNA encapsulated in cationic liposomes. This study was, however, terminated due to the low number of participants that could be enrolled. A first-in-human trial was concluded in 2022 (NCT03020017) where patients were given NU-0129, a gold nanoparticle coated with nuclear acids that target Bcl2L12, where the primary objective was to study safety and delivery into the brain. The study indicated that most patients had not suffered any side effects, but a low percentage did indicate changes in lymphocytes, platelets and vascular disorders. It remains unclear whether these studies will be continued and whether the delivery was sufficiently high to reach therapeutic efficacy. Another ongoing trial was set up (phase I/II) in 2022, where polysiloxane Gd-chelates based nanoparticles (AGuIX) are tested together with radiotherapy and concomitant temozolomide in the treatment of newly diagnosed glioblastoma (NCT04881032). The study will be a combined dose escalation (phase I) and randomized (phase II) trial to study the recommended dose and therapeutic efficacy, next to pharmacokinetic properties. While the number of trials is low, it is important to notice as well that none of the formulations mentioned make any modifications to enhance the delivery of their nanoparticles across the BBB. They rely on the intrinsic ability of some nanoparticles to cross the BBB, albeit at low efficacy, while simultaneously expecting some BBB damage that would help the nanoparticles to cross more efficiently. It is, therefore, important to note that most strategies described here are preclinical and would need to be tested in human settings. If they could efficiently promote BBB transfer, this would have a strong impact on future clinical trials. Other settings, such as the transient opening of the BBB using external stimuli, have been more widely researched (NCT03712293; NCT02474966; NCT03744026; NCT04440358; NCT04417088; NCT04614493; NCT04417088... a total of 58 studies were found on ClinicalTrials.gov), but have thus far not been combined with nanotherapies; instead they have been used in combination with classical chemotherapies. Therefore, more preclinical studies are needed which are based on patient derived tissues and cells for precision medicine and to facilitate the translation of discoveries in the nanomedicine and nano targeting field into the clinic.

5. Placental barrier

During intrauterine life, the fetus is protected from environmental factors by the mother and the placenta. The latter functions both as a barrier and a central metabolic organ where the two main pathways (maternal–fetal and fetal–maternal transport) enable fetal protection, detoxification, growth and development. Optimizing treatment and minimizing side effects through targeted drug delivery are therefore of critical importance for maternal diseases that co-occur in pregnant

women, for example cancer, pregnancy-related complications, for example preeclampsia, or specific fetal diseases. Although major therapeutic advancements have been implemented, such as antenatal corticosteroid use for improved fetal outcome and flecainide administration for fetal supraventricular tachycardia,[423,424] true custom-made therapies for mothers and fetuses are rare. This can, at least in part, be attributed to the abovementioned presence of the placenta as a biological barrier. The placental barrier plays a dual role, as it allows and facilitates transport of nutrients/waste to and from the fetus, and also protects the fetus by impeding exposure to damaging substances, making tuned antenatal drug delivery more complex (Box 4).

In this section, we analyze how nanomaterials have been employed for crossing the placental barrier and improving prenatal medicine. The latter can be subdivided into fetal, maternal or placental disorders and each category poses specific challenges for targeted therapeutics. Fetal therapeutics are needed for diseases such as fetal tachycardia and genetic diseases, but also for lung maturation acceleration in case of expected preterm delivery.[425] The aim of these fetal therapeutics should be to target the fetus by enabling the crossing of the placental barrier, while avoiding maternal side effects, for example in the case of pregnancy-related diabetes after antenatal corticosteroid therapy.[426] For maternal therapeutics, for example in the case of cancer, the therapeutic agent should be targeted towards the tumor while the crossing of the placenta, with potential fetal exposure, should be avoided. The third category are the placental therapeutics, for example for pre-eclampsia management, for which only the placenta should be targeted and side effects in both the fetus and the mother should be minimized.

Box 4: Placental barrier characteristics

The placenta is composed of both maternal, derived from the endometrium, and fetal tissue, derived from the chorionic sac. In between the two regions, the intervillous space is characterized by the villous structures containing fetal blood vessels. These vessels transport oxygenated blood from the microvilli to the umbilical vein, while deoxygenated fetal blood is returned from the fetus to the placental microvilli *via* the umbilical arteries. Nutrients, waste and oxygen are then interchanged with maternal blood, which flows through the intervillous space.[427] Blood perfusion of the villi and maternal–fetal exchange are not established until the end of the first trimester and abnormal vascular development has been linked to preeclampsia onset.[428] In humans, fetal and maternal blood are separated by 3 layers: the syncytiotrophoblast, connective tissue and the vascular endothelium of fetal blood vessels. These 3 layers form the placental membrane or barrier. Molecules larger than ~600 Da do not cross the human placenta, unless through active energy-dependent pathways, as is the case for IgG antibodies.[429,430] However, this size exclusion can vary over time as the placenta is a dynamic structure, developing right after blastocyst implantation up to expulsion right after birth. Multiple changes in the placenta can be noted during pregnancy: (i) the syncytiotrophoblast (STB) develops from a primitive to a layer with apical–basal polarity (Fig. 21A); (ii) continued regeneration of the STB by differentiation and fusion of cytotrophoblasts (Fig. 21B); (iii) thinning of the placental barrier, as the cytotrophoblast layer is depleted, from 50–100 μm to 2–4 μm at term; and (iv) changes in placental transporters at the placental surface.[2,427] Of note, important differences in the placental structure exist between species, so interspecies extrapolation has its limits.

5.1. NM design strategies for placental interaction

5.1.1. (Not) crossing the placenta barrier. (Nano)particles have been shown to cross the placenta, with studies mainly focusing on fetal toxicity concerns after maternal exposure to, for example, ambient black carbon particles or multiwalled carbon nanotubes.[431,432] Unfortunately, to date, only a limited number of studies have been reported on crossing the placenta for fetal therapy purposes, despite the need for better side effect management as well as improved therapeutic dosage attainment at the fetal site. For instance, promising antenatal drugs, such as sildenafil, have been shown to have a very low transplacental transfer (2.9%) and could benefit from a fetal targeted nanomedicine approach, allowing transplacental transport.[433] Contrarily, valproic acid, an antiepileptic drug occasionally given during pregnancy if there are no other effective options, crosses the placenta but has been associated with detrimental fetal side effects. Encapsulation of valproic acid in liposomes significantly reduces fetal exposure compared to free drug administration.[434]

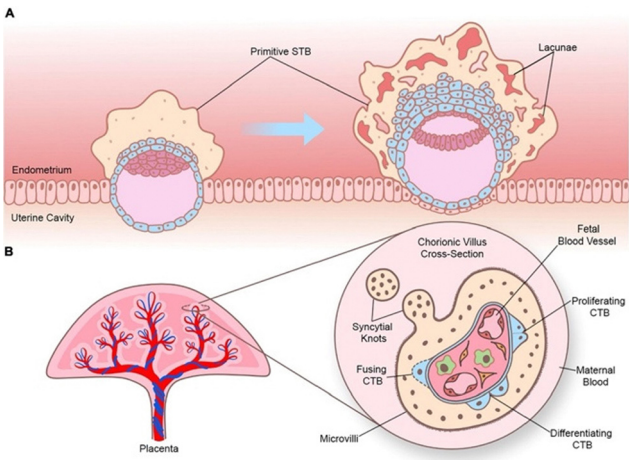

Fig. 21 Placental structure during pregnancy. (A) Formation of the primitive syncytiotrophoblast (STB) from GD 7–8 to 8–9. First formation of lacunae. (B) Well-developed chorionic villus in late pregnancy. Reproduced from ref. 2 (CC BY 4.0).

Evidently, simply encapsulating drugs in NPs does not suffice for (avoiding) placental crossing. As with any barrier, multiple parameters can determine whether nanoparticles can cross the placental barrier. While sizing of NPs is considered to play a role, reports vary significantly. For example, small inorganic nanoparticles, such as titanium dioxide and silver NPs, show high (toxic) fetal concentrations after maternal exposure.[435,436] On the other hand, polystyrene nanoparticles

up to 500 nm have been reported to cross the placenta, albeit at significantly lower concentrations.[437] Furthermore, a study by Huang and colleagues in an *in vivo* mouse model showed that 20 nm PS NPs showed significantly less placental uptake than 40 nm PS NPs, suggesting a non-linear size exclusion mechanism for placental uptake.[438] Small NPs may even be impeded from undergoing translocation, as was shown for Cu NPs with a size of 15 nm.[439] Likely, the varying effect can, at least partly, be attributed to differing material compositions. Of note, the lack of placental translocation does not exclude possible fetal side effects. Maternal exposure to Cu NPs did lead to strong immunomodulatory effects in the offspring.

The non-linear size exclusion implies the involvement of active transportation of particles. In a study by Grafmueller and colleagues, it was shown that passive diffusion, through concentration equilibration, was indeed not the main driver of placental translocation and, therefore, active transport pathways are involved in NP transport.[440] Various active transport pathways have later been described to play a role. Through selective inhibition of the caveolae-mediated endocytosis pathways, barrier crossing *in vitro* of pullulan acetate (PA) NPs was reduced by 55%, indicating that active caveolae-mediated transport has an important role in NP transport (Fig. 22A). Inhibition of macropinocytosis and clathrin-mediated endocytosis reduced transport as well, but by only. 24.2% and 23.9% respectively.[441] With the role of active transporters in mind, Jiang and colleagues developed folate-conjugated pullulan acetate (FPA) NPs, which showed placental translocation *in vitro*, by leveraging folate receptor-mediated transport.[442]

The role of surface charge is still unclear, but studies have showed its impact on placental transport, with negatively charged NPs tending to show better barrier penetration compared to positively charged NPs.[443] However, highly negatively charged nanoparticles, for example through COOH-surface groups, show less placental translocation.[338] Neutrally charged NPs, for example NPs coated with PEG, have been shown to pass in higher quantity compared to negatively charged particles in *ex vivo* human placenta models.[444] However, the precise effect of PEGylation on placental crossing remains unclear, as other reports have suggested impeding of placental translocation by particle PEGylation.[443,445]

Finally, in a recent study by Tse and colleagues, inspiration was taken from the maternal–fetal transfer of passive immunity for their design of IgG-modified chitosan nanoparticles.[446] IgG antibodies are known to be transported across the placental barrier through involvement of Fc receptors.[447] Based on this, IgG-NPs were shown to be translocated across the placenta *in vitro* (Fig. 22B).

5.1.2. Targeting the placental barrier. Most strategies for increased placental retention of nanoparticles use antibody/peptide surface functionalization for increased interaction with a specific placental target. A popular placental target is chondroitin sulfate A (CSA), which is present on syncytiotrophoblast cells, and which has been shown to be a target of malaria infected red blood cells. The specific binding regions have been identified through phage selection as VAR2CSA regions, also called CSA-binding domains (CSA-BP).[448] By mimicking malaria infected RBCs, Zhang and colleagues developed CSA-BP coated NPs which showed specific binding to trophoblast cells, increasing placental methotrexate (MTX) concentrations more than 3-fold compared to non-functionalized MTX-NPs. Furthermore, both renal and hepatic maternal toxicity was reduced compared to free MTX treatment and no detectable placental crossing of the NPs was observed.[449] Meanwhile, the potential of CSA-BP guided placental targeting has been underlined by successful reports on choriocarcinoma treatment using CSA-BP modified dendrimers and preeclampsia management by siRNA delivery with CSA-BP modified PEG-PLA NPs.[450,451] An alternative placental targeting strategy is the use of tumor-homing peptides. As the highly dynamic placenta

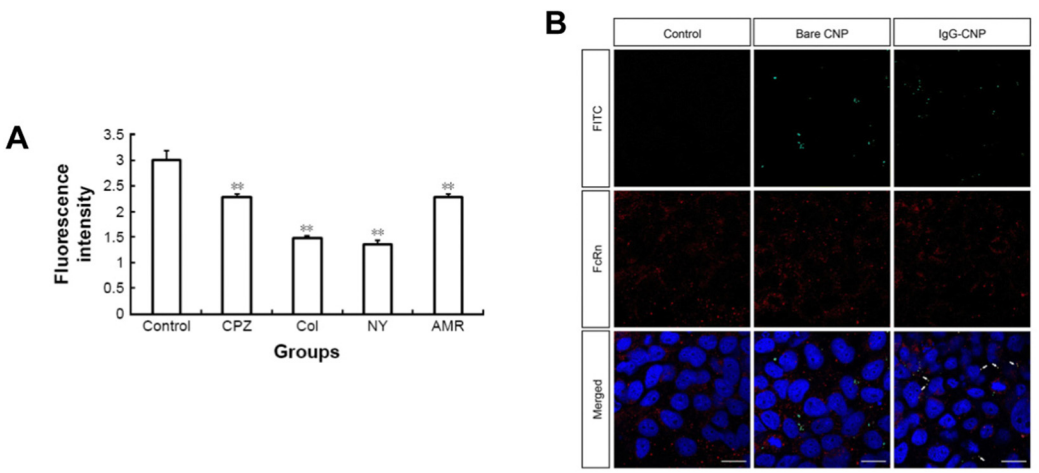

Fig. 22 (A) Fluorescence intensity of BeWo after uptake of PA-FITC NPs in the presence of the endocytic inhibitor chlorpromazine (CPZ), colchicine (Col), nystatin (NY) or amiloride (AMR). $^{**}p < 0.01$. Adapted from ref. 441 with permission from Dove Medical Press Limited. (B) Confocal microscopy images of BeWo cells and FITC-labelled CNPs or IgG-CNPs (green) with immunostaining for FcRn (red) and counterstaining with DAPI (blue). Co-localization (yellow; white arrows) of the IgG-CNPs with FcRn was observed. Scale bars = 20 μm. Adapted from ref. 456 with permission from the Royal Society of Chemistry.

shares physiologic and biochemical similarities to solid tumors, the placenta could be considered as a well-controlled tumor and thus, King and colleagues hypothesized that well-developed tumor targeting nanomedicine strategies could potentially be used for placental therapies as well.[452] CGKRK or cyclic iRGD peptide functionalization of liposomes did indeed show specific homing towards the placenta, accumulating within the syncytiotrophoblast layer of both mouse and human placentas, while avoiding fetal exposure. Administration of IGF-2 loaded iRGD-liposomes improved placental growth and fetal weight of growth-restricted mice. However, further evaluation of this targeting strategy is needed to ensure safety in women with undiagnosed malignancies. Other peptide surface functionalizations include arginine-glycine-aspartic acid (RGD) peptides, which specifically target highly expressed integrin $\alpha v\beta 3$ on the placenta, or epidermal growth factor receptor (EGFR) targeting peptides.[453,454]

Besides active targeting strategies, tuning nanoparticle properties can improve placental targeting, although available studies are scarce. A study by Ho and colleagues reported positively charged PEI-PGMA with significant higher retention proportions than plain PGMA particles.[429] Additionally, Swingle and colleagues recently reported on a systematic study in which they screened lipid NPs with differing ionizable lipid components for both their mRNA loading and their placental targeting.[455] While lipid NPs have commonly been used for liver accumulation for, among others, vaccination purposes, oxygen-containing lipids were found to significantly increase extrahepatic delivery towards the placenta. In a similar fashion, systematically varying the molar ratios of C12–200, DOPE, cholesterol and PEG allowed optimal lipid NP design for maximizing placental accumulation.[456]

5.2. Considerations for antenatal drug delivery

5.2.1. Administration route. Maternal administration for fetal therapies is evidently the least invasive but also less effective mode of administration. Placental or fetal targeting can also be achieved through invasive methods. Invasive procedures have mainly been used for prenatal diagnostic tests, such as amniocentesis and chorionic villus sampling, but principles can be extrapolated for targeted drug delivery as well.[457] For example, a study by Ellah and colleagues reported IGF-1 plasmid DNA loaded polymeric NPs with effective and trophoblast specific transgene expression after direct murine placental injection.[458]

Fetal targeting can be invasively enhanced, for example by intra-amniotic administration of PAMAM dendrimer-based therapeutics.[459] Alternatively, administration *via* the umbilical vein was recently reported in clinical settings for enzyme-replacement therapy for infantile-onset Pompe's disease.[460] However, it should be noted that more invasive procedures pose risks to the unborn child and mother; however recent studies indicate that risk mitigation might be feasible.[461,462]

5.2.2. Research gaps. Nanomedicine has only recently infiltrated the field of antenatal medicine and research gaps are to be expected. Despite the promising research described above and the conceptual potential of nanomedicine to address current shortcomings in prenatal medicine, the current limited knowledge of the influence of NP characteristics on placental barrier crossing and its associated mechanisms is the cause for concern. Thorough methodological experimental designs are needed to better understand NP–placenta interactions. For this, placenta-on-chip tools could be of assistance, as they provide a dynamic model considering placental differentiation over time, as well as shear stress induced by maternal blood flow.[463] Validation of transport studies with the already well-integrated *ex vivo* human placenta models is therefore essential. Additionally, only a few studies have looked at NP biodistribution at different gestational ages, as *ex vivo* human placentas are usually late gestational ones.[464]

5.2.3. Translatability. As the placenta is different at the histological level and functional level in many of the common lab species (mouse, rat, sheep, *etc.*) compared to humans, the extrapolation of data from animal studies is challenging.[465]

Furthermore, clinical applications of therapeutics during pregnancy are subjected to significant constraints which make translationability cumbersome. Ethical considerations regarding fetal therapies need to balance harm and benefits for both mother and child and may change depending on the gestational age.[466] These considerations further impact clinical trial designs, where exclusion of pregnant women has been common practice. Illustratively, only 5% of available medicines have been tested and labeled for use in pregnancy.[467] Given the proven differences of changing drug pharmacokinetics during pregnancy, translationability and clinical use of new drugs and advanced drug delivery technologies for pregnancy-related complications remain a gray area.[468]

6. Conclusions and final remarks

The biological barriers described in this review portrait a unique challenge, where each individual barrier requires tailormade engineering of nanomaterials to modulate their translocation. While we provide an overview of key parameters, and their respective effect on barrier penetration, a general lack of systematic studies impedes in-depth analysis of the relative contribution of these different parameters to (un)successful barrier crossing and subsequent interactions with the target cells. We reckon that future studies should include homogeneous standardization, for example, in the case of mucus penetration by including multiple particle tracking analysis, offering interstudy comparable parameters for penetration probability. Such standardized systematic studies may not only allow better translational research, but they will also aid in our fundamental understanding of the bio-nano interface and the *in vivo* fate of these nanoformulations.[469] While this review has mainly focused on 4 special, yet highly relevant, cases of organ barriers, the insights on nanoformulation engineering are transferable to other physical barriers, albeit with a significant required effort on specific barrier customization.

Upcoming technologies that may aid in the execution of these standardized studies include precision-cut-tissue slices and organ-on-chip technologies, providing a tool wherein, similar to *in vitro* studies, barrier penetration studies are possible but in a more closely *in vivo* mimicking environment.[470] Additionally, mathematical modelling tools can aid in screening relevant nanoparticles and calculating their barrier crossing probability.[471–473]

Despite the knowledge gap on fundamental bio-nano interactions, advanced strategies have been discussed in this review showing potential to efficiently transport the cargo across the barriers. For systemic barriers, such as the blood–brain barrier and placental barrier, initial reports on, for example, cell-based nanoformulations show a very promising outlook and are expected to drastically improve biodistribution control and barrier translocation efficiency.[474,475] On the other hand, for mucus-based barriers, intelligent or switchable nanoparticles are expected to drive formulation efficiency, not only in terms of mucus penetration, but also for subsequent target cell interactions. These intelligent nanoparticles can be redox-responsive, pH-responsive or ROS-triggered and, subsequently, may change their size, charge or shape accordingly.[77,476,477] Other NP types, such as Janus NPs, may serve as hyper-engineered platforms, leveraging the strengths of different crossing strategies or allow dual-drug treatment with simultaneous delivery in multifunctional NPs.[478,479] While simplicity in formulation has often been regarded as having the greatest translatability from preclinical studies to human clinical trials, these recently suggested engineered formulations may hold the greatest promise for effectively penetrating the barriers of organs.

In conclusion, the current review has demonstrated that ample efforts have been made to improve the transport of engineered NPs across biological barriers. While the efficacy of nanomedicine strategies has remained, generally, rather low, the introduction of more advanced engineered nanomaterials is expected to be the foundation for future clinical success.

Conflicts of interest

There are no conflicts to declare.

Acknowledgements

This work was supported by the European Commission under the Horizon 2020 framework for ERC (ERC StG 750973), KU Leuven Internal Funds C2 (C24/18/101) and Fonds Wetenschappelijk Onderzoek (G0B2919N).

References

1 Y. Chen and L. Liu, *Adv. Drug Deliv. Rev.*, 2012, **64**, 640–665, DOI: 10.1016/j.addr.2011.11.010.
2 A. Jaremek, M. J. Jeyarajah, G. Jaju Bhattad and S. J. Renaud, *Front. Cell Dev. Biol.*, 2021, **9**, 674162, DOI: 10.3389/fcell.2021.674162.
3 V. Lenders, X. Koutsoumpou, A. Sargsian and B. B. Manshian, *Nanoscale Adv.*, 2020, **2**, 5046–5089, DOI: 10.1039/d0na00478b.
4 Z. Zhao, K. Powers, Y. Hu, M. Raleigh, P. Pentel and C. Zhang, *Biomaterials*, 2017, **123**, 107–117, DOI: 10.1016/j.biomaterials.2017.01.038.
5 Y. Gao, A. Sarode, N. Kokoroskos, A. Ukidve, Z. Zhao, S. Guo, R. Flaumenhaft, A. S. Gupta, N. Saillant and S. Mitragotri, *Sci. Adv.*, 2020, **6**, eaba0588.
6 H. Naatz, B. B. Manshian, C. Rios Luci, V. Tsikourkitoudi, Y. Deligiannakis, J. Birkenstock, S. Pokhrel, L. Madler and S. J. Soenen, *Angew. Chem., Int. Ed.*, 2020, **59**, 1828–1836, DOI: 10.1002/anie.201912312.
7 M. Van Woensel, N. Wauthoz, R. Rosière, V. Mathieu, R. Kiss, F. Lefranc, B. Steelant, E. Dilissen, S. W. Van Gool, T. Mathivet, H. Gerhardt, K. Amighi and S. De Vleeschouwer, *J. Controlled Release*, 2016, **227**, 71–81, DOI: 10.1016/j.jconrel.2016.02.032.
8 M. Van Woensel, T. Mathivet, N. Wauthoz, R. Rosière, A. D. Garg, P. Agostinis, V. Mathieu, R. Kiss, F. Lefranc, L. Boon, J. Belmans, S. W. Van Gool, H. Gerhardt, K. Amighi and S. De Vleeschouwer, *Sci. Rep.*, 2017, **7**, 1217, DOI: 10.1038/s41598-017-01279-1.
9 A. Gauthier, A. Fisch, K. Seuwen, B. Baumgarten, H. Ruffner, A. Aebi, M. Rausch, F. Kiessling, M. Bartneck, R. Weiskirchen, F. Tacke, G. Storm, T. Lammers and M. G. Ludwig, *Biomaterials*, 2018, **178**, 481–495, DOI: 10.1016/j.biomaterials.2018.04.006.
10 A. C. Anselmo and S. Mitragotri, *Bioeng. Transl. Med.*, 2021, **6**, e10246, DOI: 10.1002/btm2.10246.
11 S. M. Stavis, J. A. Fagan, M. Stopa and J. A. Liddle, *ACS Appl. Nano Mater.*, 2018, **1**, 4358–4385, DOI: 10.1021/acsanm.8b01239.
12 S. Wilhelm, A. Tavares, Q. Dai, S. Ohta, J. Audet, H. Dvorak and W. Chan, *Nat. Rev. Mater.*, 2016, **1**, 16014.
13 Y. Hayashi, M. Takamiya, P. B. Jensen, I. Ojea-Jimenez, H. Claude, C. Antony, K. Kjaer-Sorensen, C. Grabher, T. Boesen, D. Gilliland, C. Oxvig, U. Strahle and C. Weiss, *ACS Nano*, 2020, **14**, 1665–1681, DOI: 10.1021/acsnano.9b07233.
14 C. A. Ruge, U. F. Schaefer, J. Herrmann, J. Kirch, O. Canadas, M. Echaide, J. Perez-Gil, C. Casals, R. Muller and C. M. Lehr, *PLoS One*, 2012, **7**, e40775, DOI: 10.1371/journal.pone.0040775.
15 J. Yoo, K. Kim, S. Kim, H. H. Park, H. Shin and J. Joo, *Nanoscale*, 2022, **14**, 14482–14490, DOI: 10.1039/d2nr02995b.
16 J. S. Suk, Q. Xu, N. Kim, J. Hanes and L. M. Ensign, *Adv. Drug Deliv. Rev.*, 2016, **99**, 28–51, DOI: 10.1016/j.addr.2015.09.012.
17 Z. Zhao, A. Ukidve, V. Krishnan, A. Fehnel, D. C. Pan, Y. Gao, J. Kim, M. A. Evans, A. Mandal, J. Guo, V. R. Muzykantov and S. Mitragotri, *Nat. Biomed. Eng.*, 2021, **5**, 441–454, DOI: 10.1038/s41551-020-00644-2.
18 C. Gao, Q. Wang, J. Li, C. H. T. Kwong, J. Wei, B. Xie, S. Lu, S. M. Y. Lee and R. Wang, *Sci. Adv.*, 2022, **8**, eabn1805.

19 L. Liu, T. K. Hitchens, Q. Ye, Y. Wu, B. Barbe, D. E. Prior, W. F. Li, F. C. Yeh, L. M. Foley, D. J. Bain and C. Ho, *Biochim. Biophys. Acta*, 2013, **1830**, 3447–3453, DOI: 10.1016/j.bbagen.2013.01.021.

20 M. P. Nikitin, I. V. Zelepukin, V. O. Shipunova, I. L. Sokolov, S. M. Deyev and P. I. Nikitin, *Nat. Biomed. Eng.*, 2020, **4**, 717–731, DOI: 10.1038/s41551-020-0581-2.

21 S. Sindhwani, A. M. Syed, J. Ngai, B. R. Kingston, L. Maiorino, J. Rothschild, P. MacMillan, Y. Zhang, N. U. Rajesh, T. Hoang, J. L. Y. Wu, S. Wilhelm, A. Zilman, S. Gadde, A. Sulaiman, B. Ouyang, Z. Lin, L. Wang, M. Egeblad and W. C. W. Chan, *Nat. Mater.*, 2020, **19**, 566–575, DOI: 10.1038/s41563-019-0566-2.

22 F. Danhier, *J. Controlled Release*, 2016, **244**, 108–121, DOI: 10.1016/j.jconrel.2016.11.015.

23 M. Izci, C. Maksoudian, F. Goncalves, L. Aversa, R. Salembier, A. Sargsian, I. Perez Gilabert, T. Chu, C. Rios Luci, E. Bolea-Fernandez, D. Nittner, F. Vanhaecke, B. B. Manshian and S. J. Soenen, *J. Nanobiotechnol.*, 2022, **20**, 518, DOI: 10.1186/s12951-022-01727-9.

24 Y. X. Li, Y. Wei, R. Zhong, L. Li and H. B. Pang, *Pharmaceutics*, 2021, **13**, 552, DOI: 10.3390/pharmaceutics13040552.

25 T. Kang, X. Gao, Q. Hu, D. Jiang, X. Feng, X. Zhang, Q. Song, L. Yao, M. Huang, X. Jiang, Z. Pang, H. Chen and J. Chen, *Biomaterials*, 2014, **35**, 4319–4332, DOI: 10.1016/j.biomaterials.2014.01.082.

26 A. Aliyandi, S. Satchell, R. E. Unger, B. Bartosch, R. Parent, I. S. Zuhorn and A. Salvati, *Int. J. Pharm.*, 2020, **587**, 119699, DOI: 10.1016/j.ijpharm.2020.119699.

27 M. I. Setyawati, C. Y. Tay, B. H. Bay and D. T. Leong, *ACS Nano*, 2017, **11**, 5020–5030, DOI: 10.1021/acsnano.7b01744.

28 F. Peng, M. I. Setyawati, J. K. Tee, X. Ding, J. Wang, M. E. Nga, H. K. Ho and D. T. Leong, *Nat. Nanotechnol.*, 2019, **14**, 279–286, DOI: 10.1038/s41565-018-0356-z.

29 G. W. Liu, E. B. Guzman, N. Menon and R. S. Langer, *Pharm. Res.*, 2023, **40**, 3–25, DOI: 10.1007/s11095-023-03471-7.

30 C. R. Bakshani, A. L. Morales-Garcia, M. Althaus, M. D. Wilcox, J. P. Pearson, J. C. Bythell and J. G. Burgess, *npj Biofilms Microbiomes*, 2018, **4**, 14, DOI: 10.1038/s41522-018-0057-2.

31 A. M. Shen and T. Minko, *J. Controlled Release*, 2020, **326**, 222–244, DOI: 10.1016/j.jconrel.2020.07.011.

32 K. S. LeMessurier, M. Tiwary, N. P. Morin and A. E. Samarasinghe, *Front. Immunol.*, 2020, **11**, 3, DOI: 10.3389/fimmu.2020.00003.

33 A. Gie, Y. Regin, A. Mersanne and J. Toelen, *JoVE*, 2021, e61982, DOI: 10.3791/61982.

34 C. C. Campa, R. L. Silva, J. P. Margaria, T. Pirali, M. S. Mattos, L. R. Kraemer, D. C. Reis, G. Grosa, F. Copperi, E. M. Dalmarco, R. C. P. Lima-Junior, S. Aprile, V. Sala, F. Dal Bello, D. S. Prado, J. C. Alves-Filho, C. Medana, G. D. Cassali, G. C. Tron, M. M. Teixeira, E. Ciraolo, R. C. Russo and E. Hirsch, *Nat. Commun.*, 2018, **9**, 5232, DOI: 10.1038/s41467-018-07698-6.

35 P. J. Kuehl, C. S. Tellez, M. J. Grimes, T. H. March, M. Tessema, D. A. Revelli, L. M. Mallis, W. W. Dye, T. Sniegowski, A. Badenoch, M. Burke, D. Dubose, D. T. Vodak, M. A. Picchi and S. A. Belinsky, *Br. J. Cancer*, 2020, **122**, 1194–1204, DOI: 10.1038/s41416-020-0765-2.

36 B. Button, L.-H. Cai, C. Ehre, M. Kesimer, D. B. Hill, J. K. Sheehan, R. C. Boucher and M. Rubinstein, *Science*, 2012, **337**, 937–941, DOI: 10.1126/science.1223012.

37 E. Hermans, M. S. Bhamla, P. Kao, G. G. Fuller and J. Vermant, *Soft Matter*, 2015, **11**, 8048–8057, DOI: 10.1039/c5sm01603g.

38 C. Karamaoun, B. Sobac, B. Mauroy, A. Van Muylem and B. Haut, *PLoS One*, 2018, **13**, e0199319, DOI: 10.1371/journal.pone.0199319.

39 J. Witten, T. Samad and K. Ribbeck, *Curr. Opin. Biotechnol*, 2018, **52**, 124–133, DOI: 10.1016/j.copbio.2018.03.010.

40 F. Taherali, F. Varum and A. W. Basit, *Adv. Drug Deliv. Rev.*, 2018, **124**, 16–33, DOI: 10.1016/j.addr.2017.10.014.

41 R. Bansil and B. S. Turner, *Curr. Opin. Colloid Interface Sci.*, 2006, **11**, 164–170, DOI: 10.1016/j.cocis.2005.11.001.

42 S. Ren, W. Li, L. Wang, Y. Shi, M. Cai, L. Hao, Z. Luo, J. Niu, W. Xu and Z. Luo, *Sci. Rep.*, 2020, **10**, 2030, DOI: 10.1038/s41598-020-58922-7.

43 S. M. Vanaki, D. Holmes, K. Suara, P. G. Jayathilake and R. Brown, *Comput. Biol. Med.*, 2020, **117**, 103595, DOI: 10.1016/j.compbiomed.2019.103595.

44 W. H. Anderson, R. D. Coakley, B. Button, A. G. Henderson, K. L. Zeman, N. E. Alexis, D. B. Peden, E. R. Lazarowski, C. W. Davis, S. Bailey, F. Fuller, M. Almond, B. Qaqish, E. Bordonali, M. Rubinstein, W. D. Bennett, M. Kesimer and R. C. Boucher, *Am. J. Respir. Crit. Care Med.*, 2015, **192**, 182–190, DOI: 10.1164/rccm.201412-2230OC.

45 V. Y. Lin, N. Kaza, S. E. Birket, H. Kim, L. J. Edwards, J. LaFontaine, L. Liu, M. Mazur, S. A. Byzek, J. Hanes, G. J. Tearney, S. V. Raju and S. M. Rowe, *Eur. Respir. J.*, 2020, **55**, 1900419, DOI: 10.1183/13993003.00419-2019.

46 A. L. Garland, W. G. Walton, R. D. Coakley, C. D. Tan, R. C. Gilmore, C. A. Hobbs, A. Tripathy, L. A. Clunes, S. Bencharit, M. J. Stutts, L. Betts, M. R. Redinbo and R. Tarran, *Proc. Natl. Acad. Sci. U. S. A.*, 2013, **110**, 15973–15978, DOI: 10.1073/pnas.1311999110.

47 S. Yuan, Q. Liu, Z. Hu, Z. Zhou, G. Wang, C. Li, W. Xie, G. Meng, Y. Xiang, N. Wu, L. Wu, Z. Yu, L. Bai and Y. Li, *Cell Death Dis.*, 2018, **9**, 450, DOI: 10.1038/s41419-018-0472-6.

48 B. A. Helling, A. N. Gerber, V. Kadiyala, S. K. Sasse, B. S. Pedersen, L. Sparks, Y. Nakano, T. Okamoto, C. M. Evans, I. V. Yang and D. A. Schwartz, *Am. J. Respir. Cell Mol. Biol.*, 2017, **57**, 91–99, DOI: 10.1165/rcmb.2017-0046OC.

49 I. R. Scolari, X. Volpini, M. L. Fanani, B. La Cruz-Thea, L. Natali, M. M. Musri and G. E. Granero, *Mol. Pharm.*, 2021, **18**, 807–821, DOI: 10.1021/acs.molpharmaceut.0c00692.

50 G. Alp and N. Aydogan, *Eur. J. Pharm. Biopharm.*, 2020, **149**, 45–57, DOI: 10.1016/j.ejpb.2020.01.017.

51 S. Arber Raviv, M. Alyan, E. Egorov, A. Zano, M. Y. Harush, C. Pieters, H. Korach-Rechtman, A. Saadya, G. Kaneti,

I. Nudelman, S. Farkash, O. D. Flikshtain, L. N. Mekies, L. Koren, Y. Gal, E. Dor, J. Shainsky, J. Shklover, Y. Adir and A. Schroeder, *J. Controlled Release*, 2022, **346**, 421–433, DOI: **10.1016/j.jconrel.2022.03.028**.

52 R. M. Derbali, V. Aoun, G. Moussa, G. Frei, S. F. Tehrani, J. C. Del'Orto, P. Hildgen, V. G. Roullin and J. L. Chain, *Mol. Pharm.*, 2019, **16**, 1906–1916, DOI: **10.1021/acs.molpharmaceut.8b01256**.

53 C. I. Camara, L. Bertocchi, C. Ricci, R. Bassi, A. Bianchera, L. Cantu, R. Bettini and E. Del Favero, *Int. J. Mol. Sci.*, 2021, **22**, 10480, DOI: **10.3390/ijms221910480**.

54 T. T. Tran, C. Vidaillac, H. Yu, V. F. L. Yong, D. Roizman, R. Chandrasekaran, A. Y. H. Lim, T. B. Low, G. L. Tan, J. A. Abisheganaden, M. S. Koh, J. Teo, S. H. Chotirmall and K. Hadinoto, *Int. J. Pharm.*, 2018, **547**, 368–376, DOI: **10.1016/j.ijpharm.2018.06.017**.

55 Q. Liu, X. Zhang, J. Xue, J. Chai, L. Qin, J. Guan, X. Zhang and S. Mao, *J. Controlled Release*, 2022, **347**, 435–448, DOI: **10.1016/j.jconrel.2022.05.006**.

56 Y. He, Y. Liang, J. C. W. Mak, Y. Liao, T. Li, R. Yan, H.-F. Li and Y. Zheng, *Colloids Surf., B*, 2020, **186**, 110703, DOI: **10.1016/j.colsurfb.2019.110703**.

57 N. Kim, G. Kwak, J. Rodriguez, A. Livraghi-Butrico, X. Zuo, V. Simon, E. Han, S. K. Shenoy, N. Pandey, M. Mazur, S. E. Birket, A. Kim, S. M. Rowe, R. Boucher, J. Hanes and J. S. Suk, *Thorax*, 2022, **77**, 812–820, DOI: **10.1136/thoraxjnl-2020-215185**.

58 G. Costabile, R. Provenzano, A. Azzalin, V. C. Scoffone, L. R. Chiarelli, V. Rondelli, I. Grillo, T. Zinn, A. Lepioshkin, S. Savina, A. Miro, F. Quaglia, V. Makarov, T. Coenye, P. Brocca, G. Riccardi, S. Buroni and F. Ungaro, *Nanomedicine*, 2020, **23**, 102113, DOI: **10.1016/j.nano.2019.102113**.

59 G. Osman, J. Rodriguez, S. Y. Chan, J. Chisholm, G. Duncan, N. Kim, A. L. Tatler, K. M. Shakesheff, J. Hanes, J. S. Suk and J. E. Dixon, *J. Controlled Release*, 2018, **285**, 35–45, DOI: **10.1016/j.jconrel.2018.07.001**.

60 Y. C. Kim, H. T. Hsueh, N. Kim, J. Rodriguez, K. T. Leo, D. Rao, N. E. West, J. Hanes and J. S. Suk, *Adv. Ther.*, 2020, **3**, 2000013, DOI: **10.1002/adtp.202000013**.

61 J. Li, H. Zheng, E. Y. Xu, M. Moehwald, L. Chen, X. Zhang and S. Mao, *Acta Biomater.*, 2021, **123**, 325–334, DOI: **10.1016/j.actbio.2020.12.061**.

62 E. F. Craparo, S. E. Drago, F. Quaglia, F. Ungaro and G. Cavallaro, *Drug Deliv. Transl. Res.*, 2022, **12**, 1859–1872, DOI: **10.1007/s13346-021-01102-5**.

63 D. Chen, S. Liu, D. Chen, J. Liu, J. Wu, H. Wang, Y. Su, G. Kwak, X. Zuo, D. Rao, H. Cui, C. Shu and J. S. Suk, *Angew. Chem., Int. Ed.*, 2021, **60**, 15225–15229, DOI: **10.1002/anie.202101732**.

64 G. Chai, A. Hassan, T. Meng, L. Lou, J. Ma, R. Simmers, L. Zhou, B. K. Rubin, Q. T. Zhou, P. W. Longest, M. Hindle and Q. Xu, *Nanomedicine*, 2020, **29**, 102262, DOI: **10.1016/j.nano.2020.102262**.

65 X. Bai, G. Zhao, Q. Chen, Z. Li, M. Gao, W. Ho, X. Xu and X.-Q. Zhang, *Sci. Adv.*, 2022, **8**, eabn7162.

66 Y. Wang, Q. Yuan, W. Feng, W. Pu, J. Ding, H. Zhang, X. Li, B. Yang, Q. Dai, L. Cheng, J. Wang, F. Sun and D. Zhang, *J. Nanobiotechnol.*, 2019, **17**, 103, DOI: **10.1186/s12951-019-0537-4**.

67 J. Zhu, M. Guo, Y. Cui, Y. Meng, J. Ding, W. Zeng and W. Zhou, *ACS Appl. Mater. Interfaces*, 2022, **14**, 5090–5100, DOI: **10.1021/acsami.1c23069**.

68 J. Wu, T. Zhai, J. Sun, Q. Yu, Y. Feng, R. Li, H. Wang, Q. Ouyang, T. Yang, Q. Zhan, L. Deng, M. Qin and F. Wang, *J. Colloid Interface Sci.*, 2022, **624**, 307–319, DOI: **10.1016/j.jcis.2022.05.121**.

69 V. Puri, K. R. Chaudhary, A. Singh and C. Singh, *Curr. Res. Pharmacol. Drug Discov.*, 2022, **3**, 100084, DOI: **10.1016/j.crphar.2022.100084**.

70 B. Casciaro, I. d'Angelo, X. Zhang, M. R. Loffredo, G. Conte, F. Cappiello, F. Quaglia, Y. P. Di, F. Ungaro and M. L. Mangoni, *Biomacromolecules*, 2019, **20**, 1876–1888, DOI: **10.1021/acs.biomac.8b01829**.

71 A. Kumari, S. Pal, B. R. G, F. P. Mohny, N. Gupta, C. Miglani, B. Pattnaik, A. Pal and M. Ganguli, *Mol. Pharm.*, 2022, **19**, 1309–1324, DOI: **10.1021/acs.molpharmaceut.1c00770**.

72 S. E. Drago, E. F. Craparo, R. Luxenhofer and G. Cavallaro, *Nanomedicine*, 2021, **37**, 102451, DOI: **10.1016/j.nano.2021.102451**.

73 G. Conte, G. Costabile, D. Baldassi, V. Rondelli, R. Bassi, D. Colombo, G. Linardos, E. V. Fiscarelli, R. Sorrentino, A. Miro, F. Quaglia, P. Brocca, I. d'Angelo, O. M. Merkel and F. Ungaro, *ACS Appl. Mater. Interfaces*, 2022, **14**, 7565–7578, DOI: **10.1021/acsami.1c14975**.

74 M. Comegna, G. Conte, A. P. Falanga, M. Marzano, G. Cernera, A. M. Di Lullo, F. Amato, N. Borbone, S. D'Errico, F. Ungaro, I. d'Angelo, G. Oliviero and G. Castaldo, *Sci. Rep.*, 2021, **11**, 6393, DOI: **10.1038/s41598-021-85549-z**.

75 Q. Liu, J. Xue, X. Zhang, J. Chai, L. Qin, J. Guan, X. Zhang and S. Mao, *Acta Biomater.*, 2022, **147**, 391–402, DOI: **10.1016/j.actbio.2022.05.038**.

76 J. Leal, X. Peng, X. Liu, D. Arasappan, D. C. Wylie, S. H. Schwartz, J. J. Fullmer, B. C. McWilliams, H. D. C. Smyth and D. Ghosh, *J. Controlled Release*, 2020, **322**, 457–469, DOI: **10.1016/j.jconrel.2020.03.032**.

77 C. Conte, F. Mastrotto, V. Taresco, A. Tchoryk, F. Quaglia, S. Stolnik and C. Alexander, *J. Controlled Release*, 2018, **277**, 126–141, DOI: **10.1016/j.jconrel.2018.03.011**.

78 T. T. Tran and K. Hadinoto, *Colloids Surf., B*, 2020, **193**, 111095, DOI: **10.1016/j.colsurfb.2020.111095**.

79 B. Le-Vinh, C. Steinbring, R. Wibel, J. D. Friedl and A. Bernkop-Schnurch, *Eur. J. Pharm. Biopharm.*, 2021, **163**, 109–119, DOI: **10.1016/j.ejpb.2021.03.012**.

80 L. Gomes Dos Reis, W. H. Lee, M. Svolos, L. M. Moir, R. Jaber, N. Windhab, P. M. Young and D. Traini, *Pharmaceutics*, 2019, **11**, 12, DOI: **10.3390/pharmaceutics11010012**.

81 N. Varga, V. Hornok, L. Janovak, I. Dekany and E. Csapo, *Colloids Surf., B*, 2019, **176**, 212–218, DOI: **10.1016/j.colsurfb.2019.01.012**.

82 N. Nafee, A. Husari, C. K. Maurer, C. Lu, C. de Rossi, A. Steinbach, R. W. Hartmann, C. M. Lehr and M. Schneider, *J. Controlled Release*, 2014, **192**, 131–140, DOI: **10.1016/j.jconrel.2014.06.055**.

83 C. P. Hollis, H. L. Weiss, M. Leggas, B. M. Evers, R. A. Gemeinhart and T. Li, *J. Controlled Release*, 2013, **172**, 12–21, DOI: 10.1016/j.jconrel.2013.06.039.
84 V. Ivanova, O. B. Garbuzenko, K. R. Reuhl, D. C. Reimer, V. P. Pozharov and T. Minko, *Eur. J. Pharm. Biopharm.*, 2013, **84**, 335–344, DOI: 10.1016/j.ejpb.2012.11.023.
85 B. P. H. Wittgen, P. W. A. Kunst, K. van der Born, A. W. van Wijk, W. Perkins, F. G. Pilkiewicz, R. Perez-Soler, S. Nicholson, G. J. Peters and P. E. Postmus, *Clin. Cancer Res.*, 2007, **13**, 2414–2421, DOI: 10.1158/1078-0432.Ccr-06-1480.
86 X. Jin, J. Oh, J.-Y. Cho, S. Lee and S.-J. Rhee, *Antibiotics*, 2020, **9**, 784.
87 X. Murgia, P. Pawelzyk, U. F. Schaefer, C. Wagner, N. Willenbacher and C. M. Lehr, *Biomacromolecules*, 2016, **17**, 1536–1542, DOI: 10.1021/acs.biomac.6b00164.
88 C. S. Schneider, Q. Xu, N. J. Boylan, J. Chisholm, B. C. Tang, B. S. Schuster, A. Henning, L. M. Ensign, E. Lee, P. Adstamongkonkul, B. W. Simons, S.-Y. S. Wang, X. Gong, T. Yu, M. P. Boyle, J. S. Suk and J. Hanes, *Sci. Adv.*, 2017, **3**, e1601556.
89 X. Bai, M. Li and G. Hu, *Nanoscale*, 2020, **12**, 3931–3940, DOI: 10.1039/c9nr09251j.
90 M.-C. Jones, S. A. Jones, Y. Riffo-Vasquez, D. Spina, E. Hoffman, A. Morgan, A. Patel, C. Page, B. Forbes and L. A. Dailey, *J. Controlled Release*, 2014, **183**, 94–104, DOI: 10.1016/j.jconrel.2014.03.022.
91 Q. Zhong, B. V. Humia, A. R. Punjabi, F. F. Padilha and S. R. P. da Rocha, *Eur. J. Pharm. Sci.*, 2017, **109**, 86–95, DOI: 10.1016/j.ejps.2017.07.030.
92 Q. Xu, L. M. Ensign, N. J. Boylan, A. Schon, X. Gong, J.-C. Yang, N. W. Lamb, S. Cai, T. Yu, E. Freire and J. Hanes, *ACS Nano*, 2015, **9**, 9217–9227.
93 O. B. Garbuzenko, N. Kbah, A. Kuzmov, N. Pogrebnyak, V. Pozharov and T. Minko, *J. Controlled Release*, 2019, **296**, 225–231, DOI: 10.1016/j.jconrel.2019.01.025.
94 X. Huang, J. Chisholm, J. Zhuang, Y. Xiao, G. Duncan, X. Chen, J. S. Suk and J. Hanes, *Proc. Natl. Acad. Sci. U. S. A.*, 2017, **114**, E6595–E6602, DOI: 10.1073/pnas.1705407114.
95 J. S. Suk, A. J. Kim, K. Trehan, C. S. Schneider, L. Cebotaru, O. M. Woodward, N. J. Boylan, M. P. Boyle, S. K. Lai, W. B. Guggino and J. Hanes, *J. Controlled Release*, 2014, **178**, 8–17, DOI: 10.1016/j.jconrel.2014.01.007.
96 A. Popov, L. Schopf, J. Bourassa and H. Chen, *Int. J. Pharm.*, 2016, **502**, 188–197, DOI: 10.1016/j.ijpharm.2016.02.031.
97 J. J. Verhoef, J. F. Carpenter, T. J. Anchordoquy and H. Schellekens, *Drug Discov. Today*, 2014, **19**, 1945–1952, DOI: 10.1016/j.drudis.2014.08.015.
98 I. d'Angelo, B. Casciaro, A. Miro, F. Quaglia, M. L. Mangoni and F. Ungaro, *Colloids Surf., B*, 2015, **135**, 717–725, DOI: 10.1016/j.colsurfb.2015.08.027.
99 A. S. Morris, S. C. Sebag, J. D. Paschke, A. Wongrakpanich, K. Ebeid, M. E. Anderson, I. M. Grumbach and A. K. Salem, *Mol. Pharm.*, 2017, **14**, 2166–2175, DOI: 10.1021/acs.molpharmaceut.7b00114.
100 F. Wan, T. Nylander, S. N. Klodzinska, C. Foged, M. Yang, S. G. Baldursdottir and H. M. Nielsen, *ACS Appl. Mater. Interfaces*, 2018, **10**, 10678–10687, DOI: 10.1021/acsami.7b19762.
101 J. Heyder, *Proc. Am. Thorac. Soc.*, 2004, **1**, 315–320, DOI: 10.1513/pats.200409-046TA.
102 D. K. Jensen, L. B. Jensen, S. Koocheki, L. Bengtson, D. Cun, H. M. Nielsen and C. Foged, *J. Controlled Release*, 2012, **157**, 141–148, DOI: 10.1016/j.jconrel.2011.08.011.
103 F. Ungaro, I. d'Angelo, C. Coletta, R. d'Emmanuele di Villa Bianca, R. Sorrentino, B. Perfetto, M. A. Tufano, A. Miro, M. I. La Rotonda and F. Quaglia, *J. Controlled Release*, 2012, **157**, 149–159, DOI: 10.1016/j.jconrel.2011.08.010.
104 C. A. Ruge, A. Bohr, M. Beck-Broichsitter, V. Nicolas, N. Tsapis and E. Fattal, *Colloids Surf., B*, 2016, **139**, 219–227, DOI: 10.1016/j.colsurfb.2015.12.017.
105 B. Porsio, M. G. Cusimano, D. Schillaci, E. F. Craparo, G. Giammona and G. Cavallaro, *Biomacromolecules*, 2017, **18**, 3924–3935, DOI: 10.1021/acs.biomac.7b00945.
106 Z. Wang, J. L. Cuddigan, S. K. Gupta and S. A. Meenach, *Int. J. Pharm.*, 2016, **512**, 305–313, DOI: 10.1016/j.ijpharm.2016.08.047.
107 A. Torge, P. Grutzmacher, F. Mucklich and M. Schneider, *Eur. J. Pharm. Sci.*, 2017, **104**, 171–179, DOI: 10.1016/j.ejps.2017.04.003.
108 F. Wan, S. S. Bohr, S. N. Klodzinska, H. Jumaa, Z. Huang, T. Nylander, M. B. Thygesen, K. K. Sorensen, K. J. Jensen, C. Sternberg, N. Hatzakis and H. Morck Nielsen, *ACS Appl. Mater. Interfaces*, 2020, **12**, 380–389, DOI: 10.1021/acsami.9b19644.
109 M. Y. T. Chow, R. Y. K. Chang and H. K. Chan, *Adv. Drug Deliv. Rev.*, 2021, **168**, 217–228, DOI: 10.1016/j.addr.2020.06.001.
110 A. Yildiz-Pekoz and C. Ehrhardt, *Pharmaceutics*, 2020, 12, DOI: 10.3390/pharmaceutics12100911.
111 J. G. Chan, J. Wong, Q. T. Zhou, S. S. Leung and H. K. Chan, *AAPS PharmSciTech*, 2014, **15**, 882–897, DOI: 10.1208/s12249-014-0114-y.
112 A. Ari, *Pediatr. Pulmonol.*, 2019, **54**, 1735–1741, DOI: 10.1002/ppul.24449.
113 K. H. Chang, S. H. Moon, S. K. Yoo, B. J. Park and K. C. Nam, *Pharmaceutics*, 2020, 12, DOI: 10.3390/pharmaceutics12080721.
114 W. B. van den Bosch, S. F. Kloosterman, E. R. Andrinopoulou, R. Greidanus, M. W. H. Pijnenburg, H. Tiddens and H. M. Janssens, *J. Asthma*, 2022, **59**, 2223–2233, DOI: 10.1080/02770903.2021.1996597.
115 L. Shachar-Berman, S. Bhardwaj, Y. Ostrovski, P. Das, P. Koullapis, S. Kassinos and J. Sznitman, *Pharmaceutics*, 2020, 12, DOI: 10.3390/pharmaceutics12030230.
116 B. Lehofer, F. Bloder, P. P. Jain, L. M. Marsh, G. Leitinger, H. Olschewski, R. Leber, A. Olschewski and R. Prassl, *Eur. J. Pharm. Biopharm.*, 2014, **88**, 1076–1085, DOI: 10.1016/j.ejpb.2014.10.009.
117 J. Szabova, O. Misik, M. Havlikova, F. Lizal and F. Mravec, *Colloids Surf., B*, 2021, **204**, 111793, DOI: 10.1016/j.colsurfb.2021.111793.
118 M. Zaru, S. Mourtas, P. Klepetsanis, A. M. Fadda and S. G. Antimisiaris, *Eur. J. Pharm. Biopharm.*, 2007, **67**, 655–666, DOI: 10.1016/j.ejpb.2007.04.005.

119 M. Beck-Broichsitter, P. Kleimann, T. Gessler, W. Seeger, T. Kissel and T. Schmehl, *Int. J. Pharm.*, 2012, **422**, 398–408, DOI: 10.1016/j.ijpharm.2011.10.012.
120 Y. Yang, Y. Ding, B. Fan, Y. Wang, Z. Mao, W. Wang and J. Wu, *J. Controlled Release*, 2020, **321**, 463–474, DOI: 10.1016/j.jconrel.2020.02.030.
121 Y. Gao, J. Wang, M. Chai, X. Li, Y. Deng, Q. Jin and J. Ji, *ACS Nano*, 2020, **14**, 5686–5699, DOI: 10.1021/acsnano.0c00269.
122 W. Zhang, W. Xu, Y. Lan, X. He, K. Liu and Y. Liang, *Int. J. Nanomed.*, 2019, **14**, 5287–5301, DOI: 10.2147/IJN.S203113.
123 F. Guo, J. Wu, W. Wu, D. Huang, Q. Yan, Q. Yang, Y. Gao and G. Yang, *J. Nanobiotechnol.*, 2018, 16, DOI: 10.1186/s12951-018-0384-8.
124 V. Lenders, R. Escudero, X. Koutsoumpou, L. Armengol Álvarez, J. Rozenski, S. J. Soenen, Z. Zhao, S. Mitragotri, P. Baatsen, K. Allegaert, J. Toelen and B. B. Manshian, *J. Nanobiotechnol.*, 2022, **20**, 0, DOI: 10.1186/s12951-022-01544-.
125 X. Wang, H. Chen, X. Zeng, W. Guo, Y. Jin, S. Wang, R. Tian, Y. Han, L. Guo, J. Han, Y. Wu and L. Mei, *Acta Pharm. Sin. B*, 2019, **9**, 167–176, DOI: 10.1016/j.apsb.2018.08.006.
126 Z. Zhao, A. Ukidve, Y. Gao, J. Kim and S. Mitragotri, *Sci. Adv.*, 2019, **5**, eaax9250.
127 A. Kuzmov and T. Minko, *J. Controlled Release*, 2015, **219**, 500–518, DOI: 10.1016/j.jconrel.2015.07.024.
128 O. B. Garbuzenko, M. Saad, S. Betigeri, M. Zhang, A. A. Vetcher, V. A. Soldatenkov, D. C. Reimer, V. P. Pozharov and T. Minko, *Pharm. Res.*, 2009, **26**, 382–394, DOI: 10.1007/s11095-008-9755-4.
129 L. Bonadies, P. Zaramella, A. Porzionato, G. Perilongo, M. Muraca and E. Baraldi, *J. Clin. Med.*, 2020, 9, DOI: 10.3390/jcm9051539.
130 S. H. Abman, *Am. J. Respir. Crit. Care Med.*, 2001, **164**, 1755–1756, DOI: 10.1164/rccm2109108.
131 A. De Soyza, T. Aksamit, T.-J. Bandel, M. Criollo, J. S. Elborn, E. Operschall, E. Polverino, K. Roth, K. L. Winthrop and R. Wilson, *Eur. Respir. J.*, 2018, **51**, 1702052, DOI: 10.1183/13993003.02052-2017.
132 B. S. Schuster, J. S. Suk, G. F. Woodworth and J. Hanes, *Biomaterials*, 2013, **34**, 3439–3446, DOI: 10.1016/j.biomaterials.2013.01.064.
133 M. A. U. Khalid, Y. S. Kim, M. Ali, B. G. Lee, Y.-J. Cho and K. H. Choi, *Biochem. Eng. J.*, 2020, 155, DOI: 10.1016/j.bej.2019.107469.
134 D. Baptista, L. Moreira Teixeira, D. Barata, Z. Tahmasebi Birgani, J. King, S. van Riet, T. Pasman, A. A. Poot, D. Stamatialis, R. J. Rottier, P. S. Hiemstra, A. Carlier, C. van Blitterswijk, P. Habibovic, S. Giselbrecht and R. Truckenmuller, *ACS Biomater. Sci. Eng.*, 2022, **8**, 2684–2699, DOI: 10.1021/acsbiomaterials.1c01463.
135 G. Cafri, J. J. Gartner, T. Zaks, K. Hopson, N. Levin, B. C. Paria, M. R. Parkhurst, R. Yossef, F. J. Lowery, M. S. Jafferji, T. D. Prickett, S. L. Goff, C. T. McGowan, S. Seitter, M. L. Shindorf, A. Parikh, P. D. Chatani, P. F. Robbins and S. A. Rosenberg, *J. Clin. Invest.*, 2020, **130**, 5976–5988, DOI: 10.1172/JCI134915.
136 J. Byrne, H.-W. Huang, J. C. McRae, S. Babaee, A. Soltani, S. L. Becker and G. Traverso, *Adv. Drug Delivery Rev.*, 2021, **177**, 113926, DOI: 10.1016/j.addr.2021.113926.
137 A. Pietroiusti, E. Bergamaschi, M. Campagna, L. Campagnolo, G. De Palma, S. Iavicoli, V. Leso, A. Magrini, M. Miragoli, P. Pedata, L. Palombi and I. Iavicoli, *Part. Fibre Toxicol.*, 2017, **14**, 47, DOI: 10.1186/s12989-017-0226-0.
138 J. K. Patra, G. Das, L. F. Fraceto, E. V. R. Campos, M. D. P. Rodriguez-Torres, L. S. Acosta-Torres, L. A. Diaz-Torres, R. Grillo, M. K. Swamy, S. Sharma, S. Habtemariam and H.-S. Shin, *J. Nanobiotechnol.*, 2018, **16**, 71, DOI: 10.1186/s12951-018-0392-8.
139 J. Sun, X. Shen, Y. Li, Z. Guo, W. Zhu, L. Zuo, J. Zhao, L. Gu, J. Gong and J. Li, *Nutrients*, 2016, **8**, 44, DOI: 10.3390/nu8010044.
140 O. Hartwig, M. A. Shetab Boushehri, K. S. Shalaby, B. Loretz, A. Lamprecht and C.-M. Lehr, *Adv. Drug Delivery Rev.*, 2021, **175**, 113828, DOI: 10.1016/j.addr.2021.113828.
141 E.-M. Collnot, H. Ali and C.-M. Lehr, *J. Controlled Release*, 2012, **161**, 235–246, DOI: 10.1016/j.jconrel.2012.01.028.
142 G. P. Donaldson, S. M. Lee and S. K. Mazmanian, *Nat. Rev. Microbiol.*, 2016, **14**, 20–32, DOI: 10.1038/nrmicro3552.
143 M. Zarepour, K. Bhullar, M. Montero, C. Ma, T. Huang, A. Velcich, L. Xia and A. Vallance Bruce, *Infect. Immun.*, 2013, **81**, 3672–3683, DOI: 10.1128/IAI.00854-13.
144 J.-F. Sicard, G. Le Bihan, P. Vogeleer, M. Jacques and J. Harel, *Front. Cell. Infect. Microbiol.*, 2017, **7**, 387.
145 M. Herath, S. Hosie, J. C. Bornstein, A. E. Franks and E. L. Hill-Yardin, *Front. Cell. Infect. Microbiol.*, 2020, **10**, 248.
146 R. Wichert, A. Ermund, S. Schmidt, M. Schweinlin, M. Ksiazek, P. Arnold, K. Knittler, F. Wilkens, B. Potempa, B. Rabe, M. Stirnberg, R. Lucius, J. W. Bartsch, S. Nikolaus, M. Falk-Paulsen, P. Rosenstiel, M. Metzger, S. Rose-John, J. Potempa, G. C. Hansson, P. J. Dempsey and C. Becker-Pauly, *Cell Rep.*, 2017, **21**, 2090–2103, DOI: 10.1016/j.celrep.2017.10.087.
147 Y. Tanaka, T. Goto, M. Kataoka, S. Sakuma and S. Yamashita, *J. Pharm. Sci.*, 2015, **104**, 3120–3127, DOI: 10.1002/jps.24433.
148 L. M. Ensign, R. Cone and J. Hanes, *Adv. Drug Delivery Rev.*, 2012, **64**, 557–570, DOI: 10.1016/j.addr.2011.12.009.
149 M. Falavigna, P. C. Stein, G. E. Flaten and M. P. di Cagno, *Pharmaceutics*, 2020, **12**, 168, DOI: 10.3390/pharmaceutics12020168.
150 V. Muraleetharan, J. Mantaj, M. Swedrowska and D. Vllasaliu, *RSC Adv.*, 2019, **9**, 40487–40497, DOI: 10.1039/C9RA08403G.
151 A. Berardi and F. Baldelli Bombelli, *Expert Opin. Drug Delivery*, 2019, **16**, 563–566, DOI: 10.1080/17425247.2019.1610384.
152 Y. Wang, M. Li, X. Xu, W. Tang, L. Xiong and Q. Sun, *J. Agric. Food Chem.*, 2019, **67**, 2296–2306, DOI: 10.1021/acs.jafc.8b05702.
153 J. Zhang, A. Ou, X. Tang, R. Wang, Y. Fan, Y. Fang, Y. Zhao, P. Zhao, D. Chen, B. Wang and Y. Huang, *J. Nanobiotechnol.*, 2022, **20**, 389, DOI: 10.1186/s12951-022-01598-0.

154 B. J. Müller, A. V. Zhdanov, S. M. Borisov, T. Foley, I. A. Okkelman, V. Tsytsarev, Q. Tang, R. S. Erzurumlu, Y. Chen, H. Zhang, C. Toncelli, I. Klimant, D. B. Papkovsky and R. I. Dmitriev, *Adv. Funct. Mater.*, 2018, **28**, 1704598, DOI: **10.1002/adfm.201704598**.

155 A. I. Barbosa, S. A. Costa Lima and S. Reis, *Molecules*, 2019, **24**, 346, DOI: **10.3390/molecules24020346**.

156 K. S. Kim, K. Suzuki, H. Cho, Y. S. Youn and Y. H. Bae, *ACS Nano*, 2018, **12**, 8893–8900, DOI: **10.1021/acsnano.8b04315**.

157 E. Baranowska-Wójcik, K. Gustaw, D. Szwajgier, P. Oleszczuk, B. Pawlikowska-Pawlęga, J. Pawelec and J. Kapral-Piotrowska, *Foods*, 2021, **10**, 939, DOI: **10.3390/foods10050939**.

158 P. Kiełbik, A. Jończy, J. Kaszewski, M. Gralak, J. Rosowska, R. Sapierzyński, B. Witkowski, Ł. Wachnicki, K. Lawniczak-Jablonska, P. Kuzmiuk, P. Lipiński, M. Godlewski and M. M. Godlewski, *Pharmaceuticals*, 2021, **14**, 859, DOI: **10.3390/ph14090859**.

159 G. M. DeLoid, Y. Wang, K. Kapronezai, L. R. Lorente, R. Zhang, G. Pyrgiotakis, N. V. Konduru, M. Ericsson, J. C. White, R. De La Torre-Roche, H. Xiao, D. J. McClements and P. Demokritou, *Part. Fibre Toxicol.*, 2017, **14**, 40, DOI: **10.1186/s12989-017-0221-5**.

160 S. Nallanthighal, C. Chan, D. J. Bharali, S. A. Mousa, E. Vásquez and R. Reliene, *NanoImpact*, 2017, **5**, 92–100, DOI: **10.1016/j.impact.2017.01.003**.

161 G. K. Hinkley, P. Carpinone, J. W. Munson, K. W. Powers and S. M. Roberts, *Part. Fibre Toxicol.*, 2015, **12**, 9, DOI: **10.1186/s12989-015-0085-5**.

162 L. Cosby, K. H. Lee, T. Knobloch, C. Weghorst and J. Winter, *Int. J. Nanomed.*, 2020, **15**, 8217–8230, DOI: **10.2147/IJN.S259202**.

163 Z. Davoudi, N. Peroutka-Bigus, B. Bellaire, M. Wannemuehler, T. A. Barrett, B. Narasimhan and Q. Wang, *J. Biomed. Mater. Res., Part A*, 2018, **106**, 876–886, DOI: **10.1002/jbm.a.36305**.

164 N. SreeHarsha, C. Ramnarayanan, B. E. Al-Dhubiab, A. B. Nair, J. G. Hiremath, K. N. Venugopala, R. T. Satish, M. Attimarad and A. Shariff, *BioMed Res. Int.*, 2019, **2019**, 3950942, DOI: **10.1155/2019/3950942**.

165 J. C. Imperiale, I. Schlachet, M. Lewicki, A. Sosnik and M. M. Biglione, *Polymers*, 2019, **11**, 1862, DOI: **10.3390/polym11111862**.

166 P. Zhao, X. Xia, X. Xu, K. K. C. Leung, A. Rai, Y. Deng, B. Yang, H. Lai, X. Peng, P. Shi, H. Zhang, P. W. Y. Chiu and L. Bian, *Nat. Commun.*, 2021, **12**, 7162, DOI: **10.1038/s41467-021-27463-6**.

167 Z. Huang, Y. Shi, H. Wang, C. Chun, L. Chen, K. Wang, Z. Lu, Y. Zhao and X. Li, *Int. J. Nanomed.*, 2021, **16**, 8235–8250, DOI: **10.2147/IJN.S344805**.

168 Z. Zhang, H. Li, G. Xu and P. Yao, *Drug Delivery*, 2018, **25**, 1224–1233, DOI: **10.1080/10717544.2018.1469685**.

169 X. Liu, W. Sun, N. Wu, N. Rong, C. Kang, S. Jian, C. Chen, C. Chen and X. Zhang, *Vaccines*, 2021, **9**, 304, DOI: **10.3390/vaccines9030304**.

170 A. Larrea, M. Arruebo, C. A. Serra and V. Sebastián, *Micromachines*, 2022, **13**, 878, DOI: **10.3390/mi13060878**.

171 C. L. Okolie, B. Mason, A. Mohan, N. Pitts and C. C. Udenigwe, *Food Biosci.*, 2020, **37**, 100672, DOI: **10.1016/j.fbio.2020.100672**.

172 M. A. Oshi, J. Lee, J. Kim, N. Hasan, E. Im, Y. Jung and J.-W. Yoo, *Pharmaceutics*, 2021, **13**, 1412, DOI: **10.3390/pharmaceutics13091412**.

173 L. G. Gómez-Mascaraque, M. Martínez-Sanz, S. A. Hogan, A. López-Rubio and A. Brodkorb, *Carbohydr. Polym.*, 2019, **223**, 115121, DOI: **10.1016/j.carbpol.2019.115121**.

174 R. L. Ball, P. Bajaj and K. A. Whitehead, *Sci. Rep.*, 2018, **8**, 2178, DOI: **10.1038/s41598-018-20632-6**.

175 A. Sadio, J. K. Gustafsson, B. Pereira, C. P. Gomes, G. C. Hansson, L. David, A. P. Pêgo and R. Almeida, *PLoS One*, 2014, **9**, e99449, DOI: **10.1371/journal.pone.0099449**.

176 X. Han, Y. Lu, J. Xie, E. Zhang, H. Zhu, H. Du, K. Wang, B. Song, C. Yang, Y. Shi and Z. Cao, *Nat. Nanotechnol.*, 2020, **15**, 605–614, DOI: **10.1038/s41565-020-0693-6**.

177 R. Limage, E. Tako, N. Kolba, Z. Guo, A. García-Rodríguez, C. N. H. Marques and G. J. Mahler, *Small*, 2020, **16**, 2000601, DOI: **10.1002/smll.202000601**.

178 N. Krivova, O. Zaeva, T. Misina and N. Kuvshinov, *Key Eng. Mater.*, 2016, **683**, 447–453, DOI: **10.4028/www.scientific.net/KEM.683.447**.

179 K. Gokulan, K. Williams, S. Orr and S. Khare, *Int. J. Mol. Sci.*, 2021, **22**, 9, DOI: **10.3390/ijms22010009**.

180 V. Prasad, R. Davan, S. Jothi, P. Ayalasomayajula and D. B. Raju, *Nano Biomed. Eng.*, 2013, 5, DOI: **10.5101/nbe.v5i1.p46-49**.

181 A. Seth, D. Lafargue, C. Poirier, T. Badier, N. Delory, A. Laporte, J.-M. Delbos, V. Jeannin, J.-M. Péan and C. Ménager, *Eur. J. Pharm. Sci.*, 2017, **100**, 25–35, DOI: **10.1016/j.ejps.2016.12.022**.

182 P. C. Naha, Y. Liu, G. Hwang, Y. Huang, S. Gubara, V. Jonnakuti, A. Simon-Soro, D. Kim, L. Gao, H. Koo and D. P. Cormode, *ACS Nano*, 2019, **13**, 4960–4971, DOI: **10.1021/acsnano.8b08702**.

183 L. Liu and F. Kong, *J. Food Eng.*, 2021, **292**, 110346, DOI: **10.1016/j.jfoodeng.2020.110346**.

184 M. P. Sarparanta, L. M. Bimbo, E. M. Mäkilä, J. J. Salonen, P. H. Laaksonen, A. M. K. Helariutta, M. B. Linder, J. T. Hirvonen, T. J. Laaksonen, H. A. Santos and A. J. Airaksinen, *Biomaterials*, 2012, **33**, 3353–3362, DOI: **10.1016/j.biomaterials.2012.01.029**.

185 C. Yang and D. Merlin, *Int. J. Nanomed.*, 2019, **14**, 8875–8889, DOI: **10.2147/IJN.S210315**.

186 Y. Yu, L. Xing, L. Li, J. Wu, J. He and Y. Huang, *J. Controlled Release*, 2022, **341**, 215–226, DOI: **10.1016/j.jconrel.2021.11.026**.

187 B. H. Bajka, N. M. Rigby, K. L. Cross, A. Macierzanka and A. R. Mackie, *Colloids Surf., B*, 2015, **135**, 73–80, DOI: **10.1016/j.colsurfb.2015.07.038**.

188 N. Hoshyar, S. Gray, H. Han and G. Bao, *Nanomedicine*, 2016, **11**, 673–692, DOI: **10.2217/nnm.16.5**.

189 M. J. Mitchell, M. M. Billingsley, R. M. Haley, M. E. Wechsler, N. A. Peppas and R. Langer, *Nat. Rev. Drug Discovery*, 2021, **20**, 101–124, DOI: **10.1038/s41573-020-0090-8**.

190 A. Banerjee, J. Qi, R. Gogoi, J. Wong and S. Mitragotri, *J. Controlled Release*, 2016, **238**, 176–185, DOI: **10.1016/j.jconrel.2016.07.051**.

191 N. Zheng, J. Li, C. Xu, L. Xu, S. Li and L. Xu, *Artif. Cells, Nanomed., Biotechnol.*, 2018, **46**, 1132–1140, DOI: **10.1080/21691401.2017.1362414**.

192 S.-j Cao, S. Xu, H.-m Wang, Y. Ling, J. Dong, R.-d Xia and X.-h Sun, *AAPS PharmSciTech*, 2019, **20**, 190, DOI: 10.1208/s12249-019-1325-z.
193 C. Bao, B. Liu, B. Li, J. Chai, L. Zhang, L. Jiao, D. Li, Z. Yu, F. Ren, X. Shi and Y. Li, *Nano Lett.*, 2020, **20**, 1352–1361, DOI: 10.1021/acs.nanolett.9b04841.
194 Y. Zhao, Y. Wang, F. Ran, Y. Cui, C. Liu, Q. Zhao, Y. Gao, D. Wang and S. Wang, *Sci. Rep.*, 2017, **7**, 4131, DOI: 10.1038/s41598-017-03834-2.
195 M. Yu, J. Wang, Y. Yang, C. Zhu, Q. Su, S. Guo, J. Sun, Y. Gan, X. Shi and H. Gao, *Nano Lett.*, 2016, **16**, 7176–7182, DOI: 10.1021/acs.nanolett.6b03515.
196 M. Yu, L. Xu, F. Tian, Q. Su, N. Zheng, Y. Yang, J. Wang, A. Wang, C. Zhu, S. Guo, X. Zhang, Y. Gan, X. Shi and H. Gao, *Nat. Commun.*, 2018, **9**, 2607, DOI: 10.1038/s41467-018-05061-3.
197 X. Cai, Y. Xu, L. Zhao, J. Xu, S. Li, C. Wen, X. Xia, Q. Dong, X. Hu, X. Wang, L. Chen, Z. Chen and W. Tan, *Nano Today*, 2021, **36**, 101032, DOI: 10.1016/j.nantod.2020.101032.
198 A. A. Date, J. Hanes and L. M. Ensign, *J. Controlled Release*, 2016, **240**, 504–526, DOI: 10.1016/j.jconrel.2016.06.016.
199 Y. Mu, L. Gong, T. Peng, J. Yao and Z. Lin, *OpenNano*, 2021, **5**, 100031, DOI: 10.1016/j.onano.2021.100031.
200 L. Liu, W. Yao, Y. Rao, X. Lu and J. Gao, *Drug Delivery*, 2017, **24**, 569–581, DOI: 10.1080/10717544.2017.1279238.
201 A. Sood, A. Dev, S. J. Mohanbhai, N. Shrimali, M. Kapasiya, A. C. Kushwaha, S. Roy Choudhury, P. Guchhait and S. Karmakar, *ACS Appl. Nano Mater.*, 2019, **2**, 6409–6417, DOI: 10.1021/acsanm.9b01377.
202 F. Luo, M. Wang, L. Huang, Z. Wu, W. Wang, A. Zafar, Y. Tian, M. Hasan and X. Shu, *ACS Omega*, 2020, **5**, 11799–11808, DOI: 10.1021/acsomega.0c01216.
203 E. El-Maghawry, M. Tadros, S. Elkheshen and A. Abd-Elbary, *Int. J. Nanomed.*, 2020, **15**, 3965–3980, DOI: 10.2147/IJN.S244124.
204 R. S. Santos, G. R. Dakwar, R. Xiong, K. Forier, K. Remaut, S. Stremersch, N. Guimarães, S. Fontenete, J. Wengel, M. Leite, C. Figueiredo, S. C. De Smedt, K. Braeckmans and N. F. Azevedo, *Mol. Ther. – Nucleic Acids*, 2015, 4, DOI: 10.1038/mtna.2015.46.
205 D. Walker, B. T. Käsdorf, H.-H. Jeong, O. Lieleg and P. Fischer, *Sci. Adv.*, 2015, **1**, e1500501, DOI: 10.1126/sciadv.1500501.
206 W. Gao, R. Dong, S. Thamphiwatana, J. Li, W. Gao, L. Zhang and J. Wang, *ACS Nano*, 2015, **9**, 117–123, DOI: 10.1021/nn507097k.
207 Y. Chen, M. Zhang, H. Zhao, Y. Liu, T. Wang, T. Lei, X. Xiang, L. Lu, Z. Yuan, J. Xu and J. Zhang, *Nanoscale*, 2022, **14**, 8967–8977, DOI: 10.1039/D2NR01469F.
208 M. F. Radwan, M. A. El-Moselhy, W. M. Alarif, M. Orif, N. K. Alruwaili and N. A. Alhakamy, *Dose-Response*, 2021, **19**, 15593258211013655, DOI: 10.1177/15593258211013655.
209 J. N. Chu and G. Traverso, *Nat. Rev. Gastroenterol. Hepatol.*, 2022, **19**, 219–238, DOI: 10.1038/s41575-021-00539-w.
210 B.-H. Mao, Y.-K. Luo, B. Wang, Jr., C.-W. Chen, F.-Y. Cheng, Y.-H. Lee, S.-J. Yan and Y.-J. Wang, *Part. Fibre Toxicol.*, 2022, **19**, 6, DOI: 10.1186/s12989-022-00447-0.
211 D. A. Subramanian, R. Langer and G. Traverso, *J. Nanobiotechnol.*, 2022, **20**, 362, DOI: 10.1186/s12951-022-01539-x.
212 M. Liu, J. Zhang, W. Shan and Y. Huang, *Asian J. Pharm. Sci.*, 2015, **10**, 275–282, DOI: 10.1016/j.ajps.2014.12.007.
213 K. Maisel, L. Ensign, M. Reddy, R. Cone and J. Hanes, *J. Controlled Release*, 2015, **197**, 48–57, DOI: 10.1016/j.jconrel.2014.10.026.
214 L. Mahlert, J. Anderski, D. Mulac and K. Langer, *Eur. J. Pharm. Sci.*, 2019, **133**, 28–39, DOI: 10.1016/j.ejps.2019.03.010.
215 V. Bourganis, T. Karamanidou, E. Samaridou, K. Karidi, O. Kammona and C. Kiparissides, *Eur. J. Pharm. Biopharm.*, 2015, **97**, 239–249, DOI: 10.1016/j.ejpb.2015.01.021.
216 G. Deng, Y. Wu, Z. Song, S. Li, M. Du, J. Deng, Q. Xu, L. Deng, H. S. Bahlol and H. Han, *ACS Appl. Mater. Interfaces*, 2022, **14**, 13001–13012, DOI: 10.1021/acsami.1c23342.
217 M. Dawson, E. Krauland, D. Wirtz and J. Hanes, *Biotechnol. Prog.*, 2004, **20**, 851–857, DOI: 10.1021/bp0342553.
218 X. Tan, N. Yin, Z. Liu, R. Sun, J. Gou, T. Yin, Y. Zhang, H. He and X. Tang, *Mol. Pharmaceutics*, 2020, **17**, 3177–3191, DOI: 10.1021/acs.molpharmaceut.0c00223.
219 J. Li, H. Qiang, W. Yang, Y. Xu, T. Feng, H. Cai, S. Wang, Z. Liu, Z. Zhang and J. Zhang, *J. Controlled Release*, 2022, **341**, 31–43, DOI: 10.1016/j.jconrel.2021.11.020.
220 I. Younes and M. Rinaudo, *Mar. Drugs*, 2015, **13**, 1133–1174, DOI: 10.3390/md13031133.
221 J. Xie, A. Li and J. Li, *Macromol. Rapid Commun.*, 2017, **38**, 1700413, DOI: 10.1002/marc.201700413.
222 A. Murthy, P. R. Ravi, H. Kathuria and R. Vats, *Int. J. Pharm.*, 2020, **588**, 119731, DOI: 10.1016/j.ijpharm.2020.119731.
223 J. Wang, D. Chin, C. Poon, V. Mancino, J. Pham, H. Li, P.-Y. Ho, K. R. Hallows and E. J. Chung, *J. Controlled Release*, 2021, **329**, 1198–1209, DOI: 10.1016/j.jconrel.2020.10.047.
224 H. Anter, I. Abu Hashim, W. Awadin and M. Meshali, *Int. J. Nanomed.*, 2019, **14**, 4911–4929, DOI: 10.2147/IJN.S209987.
225 A. Seth, D. Lafargue, C. Poirier, J.-M. Péan and C. Ménager, *Eur. J. Pharm. Biopharm.*, 2014, **88**, 374–381, DOI: 10.1016/j.ejpb.2014.05.017.
226 A. Parodi, P. Buzaeva, D. Nigovora, A. Baldin, D. Kostyushev, V. Chulanov, L. V. Savvateeva and A. A. Zamyatnin, *J. Nanobiotechnol.*, 2021, **19**(354), 2, DOI: 10.1186/s12951-021-01100-.
227 T. Ren, Q. Wang, Y. Xu, L. Cong, J. Gou, X. Tao, Y. Zhang, H. He, T. Yin, H. Zhang, Y. Zhang and X. Tang, *J. Controlled Release*, 2018, **269**, 423–438, DOI: 10.1016/j.jconrel.2017.11.015.
228 Y. Zhang, M. Xiong, X. Ni, J. Wang, H. Rong, Y. Su, S. Yu, I. S. Mohammad, S. S. Y. Leung and H. Hu, *ACS Appl. Mater. Interfaces*, 2021, **13**, 18077–18088, DOI: 10.1021/acsami.1c00580.
229 R. Rao, X. Liu, Y. Li, X. Tan, H. Zhou, X. Bai, X. Yang and W. Liu, *Biomater. Sci.*, 2021, **9**, 685–699, DOI: 10.1039/D0BM01772H.
230 H. Lian, T. Zhang, J. Sun, X. Liu, G. Ren, L. Kou, Y. Zhang, X. Han, W. Ding, X. Ai, C. Wu, L. Li, Y. Wang, Y. Sun, S. Wang and Z. He, *Mol. Pharmaceutics*, 2013, **10**, 3447–3458, DOI: 10.1021/mp400282r.

231 M. Ghezzi, S. Pescina, C. Padula, P. Santi, E. Del Favero, L. Cantù and S. Nicoli, *J. Controlled Release*, 2021, **332**, 312–336, DOI: 10.1016/j.jconrel.2021.02.031.
232 H. Cheng, Z. Cui, S. Guo, X. Zhang, Y. Huo and S. Mao, *Acta Biomater.*, 2021, **135**, 506–519, DOI: 10.1016/j.actbio.2021.08.046.
233 S. K. Lai, Y.-Y. Wang and J. Hanes, *Adv. Drug Delivery Rev.*, 2009, **61**, 158–171, DOI: 10.1016/j.addr.2008.11.002.
234 M. Vitulo, E. Gnodi, R. Meneveri and D. Barisani, *Int. J. Mol. Sci.*, 2022, **23**, 4339, DOI: 10.3390/ijms23084339.
235 M. Boegh and H. M. Nielsen, *Basic Clin. Pharmacol. Toxicol.*, 2015, **116**, 179–186, DOI: 10.1111/bcpt.12342.
236 A.-C. Groo and F. Lagarce, *Drug Discovery Today*, 2014, **19**, 1097–1108, DOI: 10.1016/j.drudis.2014.01.011.
237 J. A. Jiminez, T. C. Uwiera, G. Douglas Inglis and R. R. E. Uwiera, *Gut Pathogens*, 2015, **7**, 29, DOI: 10.1186/s13099-015-0076-y.
238 M. Bailey, Z. Christoforidou and M. C. Lewis, *Vet. Immunol. Immunopathol.*, 2013, **152**, 13–19, DOI: 10.1016/j.vetimm.2012.09.022.
239 A. Melero, C. Draheim, S. Hansen, E. Giner, J. J. Carreras, R. Talens-Visconti, T. M. Garrigues, J. E. Peris, M. C. Recio, R. Giner and C.-M. Lehr, *Eur. J. Pharm. Biopharm.*, 2017, **119**, 361–371, DOI: 10.1016/j.ejpb.2017.07.004.
240 I. Hubatsch, E. G. E. Ragnarsson and P. Artursson, *Nat. Protoc.*, 2007, **2**, 2111–2119, DOI: 10.1038/nprot.2007.303.
241 H. Takedatsu, K. Mitsuyama and T. Torimura, *World J. Gastroenterol.*, 2015, **21**, 11343–11352, DOI: 10.3748/wjg.v21.i40.11343.
242 S. Hua, E. Marks, J. J. Schneider and S. Keely, *Nanomedicine*, 2015, **11**, 1117–1132, DOI: 10.1016/j.nano.2015.02.018.
243 A. Vieira, L. Chaves, M. Pinheiro, D. Ferreira, B. Sarmento and S. Reis, Design and statistical modeling of mannose-decorated dapsone-containing nanoparticles as a strategy of targeting intestinal M-cells, 2016.
244 S. S. Bachhav, V. D. Dighe, D. Kotak and P. V. Devarajan, *Int. J. Pharm.*, 2017, **532**, 612–622, DOI: 10.1016/j.ijpharm.2017.09.040.
245 J. Zhang, C. Tang and C. Yin, *Biomaterials*, 2013, **34**, 3667–3677, DOI: 10.1016/j.biomaterials.2013.01.079.
246 N. Dammes, M. Goldsmith, S. Ramishetti, J. L. J. Dearling, N. Veiga, A. B. Packard and D. Peer, *Nat. Nanotechnol.*, 2021, **16**, 1030–1038, DOI: 10.1038/s41565-021-00928-x.
247 H. S. Kim and C. H. Jung, *Int. J. Mol. Sci.*, 2021, **22**, 9936, DOI: 10.3390/ijms22189936.
248 M. M. Smits and D. H. Van Raalte, *Front. Endocrinol.*, 2021, **12**, 645563, DOI: 10.3389/fendo.2021.645563.
249 R. Ismail, A. Bocsik, G. Katona, I. Gróf, M. A. Deli and I. Csóka, *Pharmaceutics*, 2019, **11**, 599, DOI: 10.3390/pharmaceutics11110599.
250 J. W. Shreffler, J. E. Pullan, K. M. Dailey, S. Mallik and A. E. Brooks, *Int. J. Mol. Sci.*, 2019, **20**, 6056, DOI: 10.3390/ijms20236056.
251 R. A. Yokel, *Nanomedicine*, 2020, **15**, 409–432.
252 E. M. Rhea and W. A. Banks, *Front. Neurosci.*, 2019, **13**, 521, DOI: 10.3389/fnins.2019.00521.
253 Y. Shi, R. van der Meel, X. Chen and T. Lammers, *Theranostics*, 2020, **10**, 7921–7924, DOI: 10.7150/thno.49577.
254 C. D. Nwagwu, A. V. Immidisetti, M. Y. Jiang, O. Adeagbo, D. C. Adamson and A. M. Carbonell, *Pharmaceutics*, 2021, 13, DOI: 10.3390/pharmaceutics13040561.
255 S. A. Chowdhary, T. Ryken and H. B. Newton, *J. Neurooncol.*, 2015, **122**, 367–382, DOI: 10.1007/s11060-015-1724-2.
256 S. M. Lombardo, M. Schneider, A. E. Tureli and N. Gunday Tureli, *Beilstein J. Nanotechnol.*, 2020, **11**, 866–883, DOI: 10.3762/bjnano.11.72.
257 W. Tang, W. Fan, J. Lau, L. Deng, Z. Shen and X. Chen, *Chem. Soc. Rev.*, 2019, **48**, 2967–3014, DOI: 10.1039/c8cs00805a.
258 N. J. Abbott, L. Ronnback and E. Hansson, *Nat. Rev. Neurosci.*, 2006, **7**, 41–53, DOI: 10.1038/nrn1824.
259 G. Li, W. Yuan and B. M. Fu, *J. Biomech.*, 2010, **43**, 2133–2140, DOI: 10.1016/j.jbiomech.2010.03.047.
260 S. Ruan, Y. Zhou, X. Jiang and H. Gao, *Adv. Sci.*, 2021, **8**, 2004025, DOI: 10.1002/advs.202004025.
261 J. Keaney and M. Campbell, *FEBS J.*, 2015, **282**, 4067–4079, DOI: 10.1111/febs.13412.
262 A. E. Caprifico, P. J. S. Foot, E. Polycarpou and G. Calabrese, *Pharmaceutics*, 2020, 12, DOI: 10.3390/pharmaceutics12111013.
263 L. Ribovski, N. M. Hamelmann and J. M. J. Paulusse, *Pharmaceutics*, 2021, 13, DOI: 10.3390/pharmaceutics13122045.
264 N. Voigt, P. Henrich-Noack, S. Kockentiedt, W. Hintz, J. Tomas and B. A. Sabel, *Eur. J. Pharm. Biopharm.*, 2014, **87**, 19–29, DOI: 10.1016/j.ejpb.2014.02.013.
265 Q. Bao, P. Hu, Y. Xu, T. Cheng, C. Wei, L. Pan and J. Shi, *ACS Nano*, 2018, **12**, 6794–6805, DOI: 10.1021/acsnano.8b01994.
266 L. L. Israel, O. Braubach, A. Galstyan, A. Chiechi, E. S. Shatalova, Z. Grodzinski, H. Ding, K. L. Black, J. Y. Ljubimova and E. Holler, *ACS Nano*, 2019, **13**, 1253–1271, DOI: 10.1021/acsnano.8b06437.
267 R. Patil, A. Galstyan, Z. B. Grodzinski, E. S. Shatalova, S. Wagner, L. L. Israel, H. Ding, K. L. Black, J. Y. Ljubimova and E. Holler, *Int. J. Nanomed.*, 2020, **15**, 3057–3070, DOI: 10.2147/IJN.S238265.
268 A. Kadari, D. Pooja, R. H. Gora, S. Gudem, V. R. M. Kolapalli, H. Kulhari and R. Sistla, *Eur. J. Pharm. Biopharm.*, 2018, **132**, 168–179, DOI: 10.1016/j.ejpb.2018.09.012.
269 M. Meenu, K. H. Reeta, A. K. Dinda, S. K. Kottarath and Y. K. Gupta, *Epilepsy Res.*, 2019, 158, DOI: 10.1016/j.eplepsyres.2019.106219.
270 X. Lu, Y. Zhang, L. Wang, G. Li, J. Gao and Y. Wang, *Drug Deliv.*, 2021, **28**, 380–389, DOI: 10.1080/10717544.2021.1883158.
271 H. Azhari, M. Younus, S. M. Hook, B. J. Boyd and S. B. Rizwan, *Int. J. Pharm.*, 2021, 600, DOI: 10.1016/j.ijpharm.2021.120411.
272 C. Zhao, J. Zhang, H. Hu, M. Qiao, D. Chen, X. Zhao and C. Yang, *Mater. Sci. Eng., C*, 2018, **92**, 1031–1040, DOI: 10.1016/j.msec.2018.02.004.
273 T. I. Janjua, A. Ahmed-Cox, A. K. Meka, F. M. Mansfeld, H. Forgham, R. M. C. Ignacio, Y. Cao, J. A. McCarroll, R. Mazzieri, M. Kavallaris and A. F. Popat, *Nanoscale*, 2021, **13**, 16909–16922, DOI: 10.1039/d1nr03553c.

274 H. S. Kim, S. J. Lee and D. Y. Lee, *Bioact. Mater.*, 2022, **8**, 35–48, DOI: 10.1016/j.bioactmat.2021.06.026.
275 H. S. Kim, M. Seo, T. E. Park and D. Y. Lee, *J. Nanobiotechnol.*, 2022, **20**, 14, DOI: 10.1186/s12951-021-01220-9.
276 J. Wei, D. Wu, Y. Shao, B. Guo, J. Jiang, J. Chen, J. Zhang, F. Meng and Z. Zhong, *J. Controlled Release*, 2022, **347**, 68–77, DOI: 10.1016/j.jconrel.2022.04.048.
277 Y. Jiang, J. Zhang, F. Meng and Z. Zhong, *ACS Nano*, 2018, **12**, 11070–11079, DOI: 10.1021/acsnano.8b05265279.
278 P. Thammasit, C. S. Tharinjaroen, Y. Tragoolpua, V. Rickerts, R. Georgieva, H. Bäumler and K. Tragoolpua, *Front. Pharmacol.*, 2021, **12**, 723727, DOI: 10.3389/fphar.2021.723727.
279 J. Wei, D. Wu, S. Zhao, Y. Shao, Y. Xia, D. Ni, X. Qiu, J. Zhang, J. Chen, F. Meng and Z. Zhong, *Adv. Sci.*, 2022, **9**, e2103689, DOI: 10.1002/advs.202103689.
280 M. Meenu, K. H. Reeta, A. K. Dinda, S. K. Kottarath and Y. K. Gupta, *Epilepsy Res.*, 2019, 158, DOI: 10.1016/j.eplepsyres.2019.106219.
281 H. Zhang, W. Jiang, Y. Zhao, T. Song, Y. Xi, G. Han, Y. Jin, M. Song, K. Bai, J. Zhou and Y. Ding, *Nano Lett.*, 2022, **22**, 2450–2460, DOI: 10.1021/acs.nanolett.2c00191.
282 A. Galstyan, J. L. Markman, E. S. Shatalova, A. Chiechi, A. J. Korman, R. Patil, D. Klymyshyn, W. G. Tourtellotte, L. L. Israel, O. Braubach, V. A. Ljubimov, L. A. Mashouf, A. Ramesh, Z. B. Grodzinski, M. L. Penichet, K. L. Black, E. Holler, T. Sun, H. Ding, A. V. Ljubimov and J. Y. Ljubimova, *Nat. Commun.*, 2019, **10**, 3850, DOI: 10.1038/s41467-019-11719-3.
283 K. Fan, X. Jia, M. Zhou, K. Wang, J. Conde, J. He, J. Tian and X. Yan, *ACS Nano*, 2018, **12**, 4105–4115, DOI: 10.1021/acsnano.7b06969.
284 J. Shen, Z. Zhao, W. Shang, C. Liu, B. Zhang, Z. Xu and H. Cai, *Artif. Cells, Nanomed., Biotechnol.*, 2019, **47**, 192–200, DOI: 10.1080/21691401.2018.1548471.
285 X. He, X. Wang, L. Yang, Z. Yang, W. Yu, Y. Wang, R. Liu, M. Chen and H. Gao, *Acta Pharm. Sin. B*, 2022, **12**, 1987–1999, DOI: 10.1016/j.apsb.2022.02.001.
286 S. Singh, N. Drude, L. Blank, P. B. Desai, H. Königs, S. Rütten, K. J. Langen, M. Möller, F. M. Mottaghy and A. Morgenroth, *Adv. Healthcare Mater.*, 2021, **10**, 2100812, DOI: 10.1002/adhm.202100812.
287 T. Dube, N. Kumar, M. Bishnoi and J. J. Panda, *Bioconjug. Chem.*, 2021, **32**, 2014–2031, DOI: 10.1021/acs.bioconjchem.1c00321.
288 B. A. Bony, A. W. Tarudji, H. A. Miller, S. Gowrikumar, S. Roy, E. T. Curtis, C. C. Gee, A. Vecchio, P. Dhawan and F. M. Kievit, *ACS Nano*, 2021, **15**, 18520–18531, DOI: 10.1021/acsnano.1c0843.
289 Y. Miura, T. Takenaka, K. Toh, S. Wu, H. Nishihara, M. R. Kano, Y. Ino, T. Nomoto, Y. Matsumoto, H. Koyama, H. Cabral, N. Nishiyama and K. Kataoka, *ACS Nano*, 2013, **7**, 8583–8592, DOI: 10.1021/nn402662d.
290 Z. Wang, J. Yao, Z. Guan, H. Wu, H. Cheng, G. Yan and R. Tang, *Colloids Surf., B*, 2021, 207, DOI: 10.1016/j.colsurfb.2021.112052.
291 X. Guo, G. Deng, J. Liu, P. Zou, F. Du, F. Liu, A. T. Chen, R. Hu, M. Li, S. Zhang, Z. Tang, L. Han, J. Liu, K. N. Sheth, Q. Chen, X. Gou and J. Zhou, *ACS Nano*, 2018, **12**, 8723–8732, DOI: 10.1021/acsnano.8b04787.
292 M. Zhang, Z. Wang, C. Wang, Y. Wu, Z. Li and Z. Liu, *ACS Nano*, 2021, **15**, 11940–11952, DOI: 10.1021/acsnano.1c03117.
293 Y. J. Kang, C. K. Holley, M. R. Abidian, A. B. Madhankumar, J. Connor and S. Majd, *Adv. Healthcare Mater.*, 2021, 10, DOI: 10.1002/adhm.202001261.
294 M. S. Alghamri, K. Banerjee, A. A. Mujeeb, A. Mauser, A. Taher, R. Thalla, B. L. McClellan, M. L. Varela, S. M. Stamatovic, G. Martinez-Revollar, A. V. Andjelkovic, J. V. Gregory, P. Kadiyala, A. Calinescu, J. A. Jiménez, A. A. Apfelbaum, E. R. Lawlor, S. Carney, A. Comba, S. M. Faisal, M. Barissi, M. B. Edwards, H. Appelman, Y. Sun, J. Gan, R. Ackermann, A. Schwendeman, M. Candolfi, M. R. Olin, J. Lahann, P. R. Lowenstein and M. G. Castro, *ACS Nano*, 2022, **16**, 8729–8750, DOI: 10.1021/acsnano.1c07492.
295 H. Zhang, C. Shi, F. Han, M. Li, H. Ma, R. Sui, S. Long, W. Sun, J. Du, J. Fan, H. Piao and X. Peng, *Biomaterials*, 2022, 289, DOI: 10.1016/j.biomaterials.2022.121770.
296 J. Lu, R. Li, B. Mu, Y. Peng, Y. Zhao, Y. Shi, L. Guo, L. Hai and Y. Wu, *Eur J. Med. Chem.*, 2022, 230, DOI: 10.1016/j.ejmech.2021.114093.
297 Y. Tian, Z. Zheng, X. Wang, S. Liu, L. Gu, J. Mu, X. Zheng, Y. Li and S. Shen, *J. Nanobiotechnol.*, 2022, **20**, 318, DOI: 10.1186/s12951-022-01493-8.
298 J. Xie, D. Gonzalez-Carter, T. A. Tockary, N. Nakamura, Y. Xue, M. Nakakido, H. Akiba, A. Dirisala, X. Liu, K. Toh, T. Yang, Z. Wang, S. Fukushima, J. Li, S. Quader, K. Tsumoto, T. Yokota, Y. Anraku and K. Kataoka, *ACS Nano*, 2020, **14**, 6729–6742, DOI: 10.1021/acsnano.9b09991.
299 D. A. Gonzalez-Carter, Z. Y. Ong, C. M. McGilvery, I. E. Dunlop, D. T. Dexter and A. E. Porter, *Nanomedicine*, 2019, **15**, 1–11, DOI: 10.1016/j.nano.2018.08.011.
300 J. Ban, S. Li, Q. Zhan, X. Li, H. Xing, N. Chen, L. Long, X. Hou, J. Zhao and X. Yuan, *Macromol. Biosci.*, 2021, 21, DOI: 10.1002/mabi.202000392.
301 H. Wang, Y. Chao, H. Zhao, X. Zhou, F. Zhang, Z. Zhang, Z. Li, J. Pan, J. Wang, Q. Chen and Z. Liu, *ACS Nano*, 2022, **16**, 664–674, DOI: 10.1021/acsnano.1c08120.
302 S. I. Aguiar, J. N. R. Dias, A. S. André, M. L. Silva, D. Martins, B. Carrapiço, M. Castanho, J. Carriço, M. Cavaco, M. M. Gaspar, R. J. Nobre, L. P. de Almeida, S. Oliveira, L. Gano, J. D. G. Correia, C. Barbas, J. Gonçalves, V. Neves and F. Aires-Da-silva, *Pharmaceutics*, 2021, 13, DOI: 10.3390/pharmaceutics13101598.
303 X. Li, V. Vemireddy, Q. Cai, H. Xiong, P. Kang, X. Li, M. Giannotta, H. N. Hayenga, E. Pan, S. R. Sirsi, C. Mateo, D. Kleinfeld, C. Greene, M. Campbell, E. Dejana, R. Bachoo and Z. Qin, *Nano Lett.*, 2021, **21**, 9805–9815, DOI: 10.1021/acs.nanolett.1c02996.
304 C. K. Elechalawar, D. Bhattacharya, M. T. Ahmed, H. Gora, K. Sridharan, P. Chaturbedy, S. H. Sinha, M. M. Chandra Sekhar Jaggarapu, K. P. Narayan, S. Chakravarty,

M. Eswaramoorthy, T. K. Kundu and R. Banerjee, *Nanoscale Adv.*, 2019, **1**, 3555–3567, DOI: 10.1039/c9na00056a.

305 M. Li, K. Hu, D. Lin, Z. Wang, M. Xu, J. Huang, Z. Chen, Y. Zhang, L. Yin, R. You, C. H. Li and Y. Q. Guan, *ACS Biomater. Sci. Eng.*, 2021, **7**, 1216–1229, DOI: 10.1021/acsbiomaterials.0c01474.

306 S. Meenu Vasudevan, N. Ashwanikumar and G. S. Vinod Kumar, *Biomater. Sci.*, 2019, **7**, 4017–4021, DOI: 10.1039/c9bm00955h.

307 Y. Yin, J. Wang, M. Yang, R. Du, G. Pontrelli, S. McGinty, G. Wang, T. Yin and Y. Wang, *Nanoscale*, 2020, **12**, 2946–2960, DOI: 10.1039/c9nr08741a.

308 O. Betzer, N. Perets, A. Angel, M. Motiei, T. Sadan, G. Yadid, D. Offen and R. Popovtzer, *ACS Nano*, 2017, **11**, 10883–10893, DOI: 10.1021/acsnano.7b04495.

309 W. Niu, Q. Xiao, X. Wang, J. Zhu, J. Li, X. Liang, Y. Peng, C. Wu, R. Lu, Y. Pan, J. Luo, X. Zhong, H. He, Z. Rong, J. B. Fan and Y. A. Wang, *Nano Lett.*, 2021, **21**, 1484–1492, DOI: 10.1021/acs.nanolett.0c04753.

310 B. Tang, W. Zeng, L. L. Song, H. M. Wang, L. Q. Qu, H. H. Lo, L. Yu, A. G. Wu, V. K. W. Wong and B. Y. K. Law, *Pharmaceuticals*, 2022, 15, DOI: 10.3390/ph15010083.

311 N. Perets, O. Betzer, R. Shapira, S. Brenstein, A. Angel, T. Sadan, U. Ashery, R. Popovtzer and D. Offen, *Nano Lett.*, 2019, **19**, 3422–3431, DOI: 10.1021/acs.nanolett.8b04148.

312 R. Upadhya, L. N. Madhu, S. Attaluri, D. L. G. Gitaí, M. R. Pinson, M. Kodali, G. Shetty, G. Zanirati, S. Kumar, B. Shuai, S. T. Weintraub and A. K. Shetty, *J. Extracell Vesicles*, 2020, 9, DOI: 10.1080/20013078.2020.1809064.

313 T. Tian, R. Liang, G. Erel-Akbaba, L. Saad, P. J. Obeid, J. Gao, E. A. Chiocca, R. Weissleder and B. A. Tannous, *ACS Nano*, 2022, **16**, 1940–1953, DOI: 10.1021/acsnano.1c05505.

314 S. Shan, J. Chen, Y. Sun, Y. Wang, B. Xia, H. Tan, C. Pan, G. Gu, J. Zhong, G. Qing, Y. Zhang, J. Wang, Y. Wang, Y. Wang, P. Zuo, C. Xu, F. Li, W. Guo, L. Xu, M. Chen, Y. Fan, L. Zhang and X. J. Liang, *Adv. Sci.*, 2022, 9, DOI: 10.1002/advs.202200353.

315 K. Wang, U. S. Kumar, N. Sadeghipour, T. F. Massoud and R. A. Paulmurugan, *ACS Nano*, 2021, **15**, 18327–18346, DOI: 10.1021/acsnano.1c07587.

316 P. Wang, X. Zheng, Q. Guo, P. Yang, X. Pang, K. Qian, W. Lu, Q. Zhang and X. Jiang, *J. Controlled Release*, 2018, **279**, 220–233, DOI: 10.1016/j.jconrel.2018.04.034.

317 A. Parmar, A. Jain, S. Uppal, S. K. Mehta, K. Kaur, B. Singh, R. Sandhir and S. Sharma, *Artif. Cells, Nanomed., Biotechnol.*, 2018, **46**, 704–719, DOI: 10.1080/21691401.2018.1468768.

318 Z. Shen, T. Liu, Y. Li, J. Lau, Z. Yang, W. Fan, Z. Zhou, C. Shi, C. Ke, V. I. Bregadze, S. K. Mandal, Y. Liu, Z. Li, T. Xue, G. Zhu, J. Munasinghe, G. Niu, A. Wu and X. Chen, *ACS Nano*, 2018, **12**, 11355–11365, DOI: 10.1021/acsnano.8b06201.

319 S. Wang, H. Shen, Q. Mao, Q. Tao, G. Yuan, L. Zeng, Z. Chen, Y. Zhang, L. Cheng, J. Zhang, H. Dai, C. Hu, Y. Pan and Y. Li, *ACS Appl. Mater. Interfaces*, 2021, **13**, 56825–56837, DOI: 10.1021/acsami.1c12406.

320 R. Sun, M. Liu, J. Lu, B. Chu, Y. Yang, B. Song, H. Wang and Y. He, *Nat. Commun.*, 2022, 13, DOI: 10.1038/s41467-022-32837-5.

321 M. M. D'Elios, A. Aldinucci, R. Amoriello, M. Benagiano, E. Bonechi, P. Maggi, A. Flori, C. Ravagli, D. Saer, L. Cappiello, L. Conti, B. Valtancoli, A. Bencini, L. Menichetti, G. Baldi and C. Ballerini, *RSC Adv.*, 2018, **8**, 904–913, DOI: 10.1039/c7ra11290d.

322 W. He, X. Li, M. Morsch, M. Ismail, Y. Liu, F. U. Rehman, D. Zhang, Y. Wang, M. Zheng, R. Chung, Y. Zou and B. Shi, *ACS Nano*, 2022, **16**(4), 6293–6308, DOI: 10.1021/acsnano.2c00320.

323 Y. Liu, Y. Zou, C. Feng, A. Lee, J. Yin, R. Chung, J. B. Park, H. Rizos, W. Tao, M. Zheng, O. C. Farokhzad and B. Shi, *Nano Lett.*, 2020, **20**, 1637–1646, DOI: 10.1021/acs.nanolett.9b04683.

324 T. Yin, Q. Fan, F. Hu, X. Ma, Y. Yin, B. Wang, L. Kuang, X. Hu, B. Xu and Y. Wang, *Nano Lett.*, 2022, **22**, 6606–6614, DOI: 10.1021/acs.nanolett.2c01863.

325 W. Hao, Y. Cui, Y. Fan, M. Chen, G. Yang, Y. Wang, M. Yang, Z. Li, W. Gong, Y. Yang and C. Gao, *J. Nanobiotechnol.*, 2021, **19**, 378, DOI: 10.1186/s12951-021-01110-0.

326 G. Deng, X. Peng, Z. Sun, W. Zheng, J. Yu, L. Du, H. Chen, P. Gong, P. Zhang, L. Cai and B. Z. Tang, *ACS Nano*, 2020, **14**, 11452–11462, DOI: 10.1021/acsnano.0c03824.

327 T. Xiao, M. He, F. Xu, Y. Fan, B. Jia, M. Shen, H. Wang and X. Shi, *ACS Nano*, 2021, **15**, 20377–20390, DOI: 10.1021/acsnano.1c08689.

328 A. Kaushik, A. Yndart, V. Atluri, S. Tiwari, A. Tomitaka, P. Gupta, R. D. Jayant, D. Alvarez-Carbonell, K. Khalili and M. Nair, *Sci. Rep.*, 2019, 9, DOI: 10.1038/s41598-019-40222-4.

329 S. Shirvalilou, S. Khoei, S. Khoee, S. R. Mahdavi, N. J. Raoufi, M. Motevalian and M. Y. Karimi, *J. Photochem. Photobiol., B*, 2020, 205, DOI: 10.1016/j.jphotobiol.2020.111827.

330 A. Marino, A. Camponovo, A. Degl'Innocenti, M. Bartolucci, C. Tapeinos, C. Martinelli, D. de Pasquale, F. Santoro, V. Mollo, S. Arai, M. Suzuki, Y. Harada, A. Petretto and G. Ciofani, *Nanoscale*, 2019, **11**, 21227–21248, DOI: 10.1039/c9nr07976a.

331 C. Berard, S. Desgranges, N. Dumas, A. Novell, B. Larrat, M. Hamimed, N. Taulier, M. A. Esteve, F. Correard and C. Contino-Pepin, *Pharmaceutics*, 2022, **14**, 1498, DOI: 10.3390/pharmaceutics14071498.

332 H. Moon, K. Hwang, K. M. Nam, Y. S. Kim, M. J. Ko, H. R. Kim, H. J. Lee, M. J. Kim, T. H. Kim, K. S. Kang, N. G. Kim, S. W. Choi and C. Y. Kim, *Biomater. Adv.*, 2022, **141**, 213102, DOI: 10.1016/j.bioadv.2022.213102.

333 Y. Endo-Takahashi, R. Kurokawa, K. Sato, N. Takizawa, F. Katagiri, N. Hamano, R. Suzuki, K. Maruyama, M. Nomizu, N. Takagi and Y. Negishi, *Pharmaceutics*, 2021, **13**, 1003, DOI: 10.3390/pharmaceutics13071003.

334 H. J. Chen, Y. Qin, Z. G. Wang, L. Wang, D. W. Pang, D. Zhao and S. L. Liu, *Angew. Chem., Int. Ed.*, 2022, 61, DOI: 10.1002/anie.202210285.

335 A. K. Singh, S. K. Mishra, G. Mishra, A. Maurya, R. Awasthi, M. K. Yadav, N. Atri, P. K. Pandey and S. K. Singh, *Drug Dev. Ind. Pharm.*, 2020, **46**, 8–19, DOI: 10.1080/03639045.2019.1698594.

336 Z. Yang, Y. Du, Q. Sun, Y. Peng, R. Wang, Y. Zhou, Y. Wang, C. Zhang and X. Qi, *ACS Nano*, 2020, **14**, 6191–6212, DOI: 10.1021/acsnano.0c02249.

337 V. Monge-Fuentes, A. Biolchi Mayer, M. R. Lima, L. R. Geraldes, L. N. Zanotto, K. G. Moreira, O. P. Martins, H. L. Piva, M. S. S. Felipe, A. C. Amaral, A. L. Bocca, A. C. Tedesco and M. R. Mortari, *Sci. Rep.*, 2021, **11**, 15185, DOI: **10.1038/s41598-021-94175-8**.

338 M. Shilo, A. Sharon, K. Baranes, M. Motiei, J. P. Lellouche and R. Popovtzer, *J. Nanobiotechnol.*, 2015, **13**, 19, DOI: **10.1186/s12951-015-0075-7**.

339 C. H. Li, M. K. Shyu, C. Jhan, Y. W. Cheng, C. H. Tsai, C. W. Liu, C. C. Lee, R. M. Chen and J. J. Kang, *Toxicol. Sci*, 2015, **148**, 192–203, DOI: **10.1093/toxsci/kfv176**.

340 S. Ohta, E. Kikuchi, A. Ishijima, T. Azuma, I. Sakuma and T. Ito, *Sci. Rep.*, 2020, **10**, 18220, DOI: **10.1038/s41598-020-75253-9**.

341 F. R. Walter, A. R. Santa-Maria, M. Meszaros, S. Veszelka, A. Der and M. A. Deli, *Tissue Barriers*, 2021, **9**, 1904773, DOI: **10.1080/21688370.2021.1904773**.

342 L. Zhang, J. Fan, G. Li, Z. Yin and B. M. Fu, *Cardiovasc. Eng. Technol.*, 2020, **11**, 607–620, DOI: **10.1007/s13239-020-00496-6**.

343 C. Saraiva, C. Praca, R. Ferreira, T. Santos, L. Ferreira and L. Bernardino, *J. Controlled Release*, 2016, **235**, 34–47, DOI: **10.1016/j.jconrel.2016.05.044**.

344 Y. H. Tsou, X. Q. Zhang, H. Zhu, S. Syed and X. Xu, *Small*, 2017, **13**, 1701921, DOI: **10.1002/smll.201701921**.

345 P. R. Lockman, J. M. Koziara, R. J. Mumper and D. D. Allen, *J. Drug Target*, 2004, **12**, 635–641, DOI: **10.1080/10611860400015936**.

346 S. Ding, A. I. Khan, X. Cai, Y. Song, Z. Lyu, D. Du, P. Dutta and Y. Lin, *Mater. Today*, 2020, **37**, 112–125, DOI: **10.1016/j.mattod.2020.02.001**.

347 M. Cooley, A. Sarode, M. Hoore, D. A. Fedosov, S. Mitragotri and A. Sen Gupta, *Nanoscale*, 2018, **10**, 15350–15364, DOI: **10.1039/c8nr04042g**.

348 P. Kolhar, A. C. Anselmo, V. Gupta, K. Pant, B. Prabhakarpandian, E. Ruoslahti and S. Mitragotri, *Proc. Natl. Acad. Sci. U. S. A.*, 2013, **110**, 10753–10758, DOI: **10.1073/pnas.1308345110**.

349 M. Nowak, T. D. Brown, A. Graham, M. E. Helgeson and S. Mitragotri, *Bioeng. Transl. Med.*, 2020, **5**, e10153, DOI: **10.1002/btm2.10153**.

350 X. Liu, B. Sui and J. Sun, *J. Mater. Chem. B*, 2017, **5**, 9558–9570, DOI: **10.1039/c7tb01314k**.

351 M. Enea, M. Peixoto de Almeida, P. Eaton, D. Dias da Silva, E. Pereira, M. E. Soares, M. L. Bastos and H. Carmo, *Nanotoxicology*, 2019, **13**, 990–1004, DOI: **10.1080/17435390.2019.1621398**.

352 G. Sharma, D. T. Valenta, Y. Altman, S. Harvey, H. Xie, S. Mitragotri and J. W. Smith, *J. Controlled Release*, 2010, **147**, 408–412, DOI: **10.1016/j.jconrel.2010.07.116**.

353 J. A. Champion and S. Mitragotri, *Pharm. Res.*, 2009, **26**, 244–249, DOI: **10.1007/s11095-008-9626-z**.

354 X. Lu, Y. Zhang, L. Wang, G. Li, J. Gao and Y. Wang, *Drug Deliv.*, 2021, **28**, 380–389, DOI: **10.1080/10717544.2021.1883158**.

355 Q. Bao, P. Hu, Y. Xu, T. Cheng, C. Wei, L. Pan and J. Shi, *ACS Nano*, 2018, **12**, 6794–6805, DOI: **10.1021/acsnano.8b01994**.

356 D. Ni, J. Zhang, W. Bu, H. Xing, F. Han, Q. Xiao, Z. Yao, F. Chen, Q. He, J. Liu, S. Zhang, W. Fan, L. Zhou, W. Peng and J. Shi, *ACS Nano*, 2014, **8**, 1231–1242, DOI: **10.1021/nn406197c**.

357 Q. Song, M. Huang, L. Yao, X. Wang, X. Gu, J. Chen, J. Chen, J. Huang, Q. Hu, T. Kang, Z. Rong, H. Qi, G. Zheng, H. Chen and X. Gao, *ACS Nano*, 2014, **8**, 2345–2359, DOI: **10.1021/nn4058215**.

358 J. Wei, D. Wu, S. Zhao, Y. Shao, Y. Xia, D. Ni, X. Qiu, J. Zhang, J. Chen, F. Meng and Z. Zhong, *Adv. Sci.*, 2022, **9**, e2103689, DOI: **10.1002/advs.202103689**.

359 Y. Jiang, J. Zhang, F. Meng and Z. Zhong, *ACS Nano*, 2018, **12**, 11070–11079, DOI: **10.1021/acsnano.8b05265**.

360 A. Joseph, C. Contini, D. Cecchin, S. Nyberg, L. Ruiz-Perez, J. Gaitzsch, G. Fullstone, X. Tian, J. Azizi, J. Preston, G. Volpe and G. Battaglia, *Sci. Adv.*, 2017, **3**, e1700362, DOI: **10.1126/sciadv.1700362**.

361 L. L. Israel, O. Braubach, A. Galstyan, A. Chiechi, E. S. Shatalova, Z. Grodzinski, H. Ding, K. L. Black, J. Y. Ljubimova and E. Holler, *ACS Nano*, 2019, **13**, 1253–1271, DOI: **10.1021/acsnano.8b06437**.

362 V. Piazzini, E. Landucci, G. Graverini, D. E. Pellegrini-Giampietro, A. R. Bilia and M. C. Bergonzi, *Pharmaceutics*, 2018, **10**, 128, DOI: **10.3390/pharmaceutics10030128**.

363 R. Dal Magro, B. Albertini, S. Beretta, R. Rigolio, E. Donzelli, A. Chiorazzi, M. Ricci, P. Blasi and G. Sancini, *Nanomedicine*, 2018, **14**, 429–438, DOI: **10.1016/j.nano.2017.11.008**.

364 J. Wei, D. Wu, Y. Shao, B. Guo, J. Jiang, J. Chen, J. Zhang, F. Meng and Z. Zhong, *J. Controlled Release*, 2022, **347**, 68–77, DOI: **10.1016/j.jconrel.2022.04.048**.

365 A. R. Neves, J. F. Queiroz, S. A. C. Lima and S. Reis, *Bioconjug. Chem.*, 2017, **28**, 995–1004, DOI: **10.1021/acs.bioconjchem.6b00705**.

366 K. Gkouvatsos, G. Papanikolaou and K. Pantopoulos, *Biochim. Biophys. Acta*, 2012, **1820**, 188–202, DOI: **10.1016/j.bbagen.2011.10.013**.

367 K. Fan, X. Jia, M. Zhou, K. Wang, J. Conde, J. He, J. Tian and X. Yan, *ACS Nano*, 2018, **12**, 4105–4115, DOI: **10.1021/acsnano.7b06969**.

368 C. Cao, X. Wang, Y. Cai, L. Sun, L. Tian, H. Wu, X. He, H. Lei, W. Liu, G. Chen, R. Zhu and Y. Pan, *Adv. Mater.*, 2014, **26**, 2566–2571, DOI: **10.1002/adma.201304544**.

369 J. Yang, L. Fan, F. Wang, Y. Luo, X. Sui, W. Li, X. Zhang and Y. Wang, *Nanoscale*, 2016, **8**, 9537–9547, DOI: **10.1039/c5nr06658a**.

370 A. Galstyan, J. L. Markman, E. S. Shatalova, A. Chiechi, A. J. Korman, R. Patil, D. Klymyshyn, W. G. Tourtellotte, L. L. Israel, O. Braubach, V. A. Ljubimov, L. A. Mashouf, A. Ramesh, Z. B. Grodzinski, M. L. Penichet, K. L. Black, E. Holler, T. Sun, H. Ding, A. V. Ljubimov and J. Y. Ljubimova, *Nat. Commun.*, 2019, **10**, 3850, DOI: **10.1038/s41467-019-11719-3**.

371 J. Shen, Z. Zhao, W. Shang, C. Liu, B. Zhang, Z. Xu and H. Cai, *Artif. Cells, Nanomed., Biotechnol.*, 2019, **47**, 192–200, DOI: **10.1080/21691401.2018.1548471**.

372 S. S. Kim, A. Rait, E. Kim, K. F. Pirollo, M. Nishida, N. Farkas, J. A. Dagata and E. H. Chang, *ACS Nano*, 2014, **8**, 5494–5514, DOI: 10.1021/nn5014484.

373 F. C. Lam, S. W. Morton, J. Wyckoff, T. L. Vu Han, M. K. Hwang, A. Maffa, E. Balkanska-Sinclair, M. B. Yaffe, S. R. Floyd and P. T. Hammond, *Nat. Commun.*, 2018, **9**, 1991, DOI: 10.1038/s41467-018-04315-4.

374 P. Sun, Y. Xiao, Q. Di, W. Ma, X. Ma, Q. Wang and W. Chen, *Int. J. Nanomed.*, 2020, **15**, 6673–6688, DOI: 10.2147/IJN.S257459.

375 D. T. Wiley, P. Webster, A. Gale and M. E. Davis, *Proc. Natl. Acad. Sci. U. S. A.*, 2013, **110**, 8662–8667, DOI: 10.1073/pnas.1307152110.

376 A. J. Clark and M. E. Davis, *Proc. Natl. Acad. Sci. U. S. A.*, 2015, **112**, 12486–12491, DOI: 10.1073/pnas.1517048112.

377 K. B. Johnsen, M. Bak, F. Melander, M. S. Thomsen, A. Burkhart, P. J. Kempen, T. L. Andresen and T. Moos, *J. Controlled Release*, 2019, **295**, 237–249, DOI: 10.1016/j.jconrel.2019.01.005.

378 K. H. Wong, M. K. Riaz, Y. Xie, X. Zhang, Q. Liu, H. Chen, Z. Bian, X. Chen, A. Lu and Z. Yang, *Int. J. Mol. Sci.*, 2019, **20**, 381, DOI: 10.3390/ijms20020381.

379 K. Ulbrich, T. Knobloch and J. Kreuter, *J. Drug Target*, 2011, **19**, 125–132, DOI: 10.3109/10611861003734001.

380 Y. C. Kuo and C. Y. Shih-Huang, *J. Drug Target*, 2013, **21**, 730–738, DOI: 10.3109/1061186X.2013.812094.

381 M. Shilo, M. Motiei, P. Hana and R. Popovtzer, *Nanoscale*, 2014, **6**, 2146–2152, DOI: 10.1039/c3nr04878k.

382 B. T. Hawkins, R. D. Egleton and T. P. Davis, *Am. J. Physiol. Heart Circ. Physiol.*, 2005, **289**, H212–219, DOI: 10.1152/ajpheart.01210.2004.

383 R. Huey, B. O'Hagan, P. McCarron and S. Hawthorne, *Int. J. Pharm.*, 2017, **525**, 12–20, DOI: 10.1016/j.ijpharm.2017.04.023.

384 H. Hua, X. Zhang, H. Mu, Q. Meng, Y. Jiang, Y. Wang, X. Lu, A. Wang, S. Liu, Y. Zhang, Z. Wan and K. Sun, *Int. J. Pharm.*, 2018, **543**, 179–189, DOI: 10.1016/j.ijpharm.2018.03.028.

385 T. E. Park, B. Singh, H. Li, J. Y. Lee, S. K. Kang, Y. J. Choi and C. S. Cho, *Biomaterials*, 2015, **38**, 61–71, DOI: 10.1016/j.biomaterials.2014.10.068.

386 T. Sepasi, F. Bani, R. Rahbarghazi, A. Ebrahimi-Kalan, M.-R. Sadeghi, S. Z. Alamolhoda, A. Zarebkohan, T. Ghadiri and H. Gao, *BioImpacts*, 2022, **13**, 133–144, DOI: 10.34172/bi.2022.23876.

387 N. U. Khan, T. Miao, X. Ju, Q. Guo and L. Han, *Brain Targeted Drug Delivery System*, 2019, pp. 129–158, DOI: 10.1016/b978-0-12-814001-7.00006-8.

388 Y. Tian, Z. Zheng, X. Wang, S. Liu, L. Gu, J. Mu, X. Zheng, Y. Li and S. Shen, *J. Nanobiotechnol.*, 2022, **20**, 318, DOI: 10.1186/s12951-022-01493-8.

389 J. Xie, D. Gonzalez-Carter, T. A. Tockary, N. Nakamura, Y. Xue, M. Nakakido, H. Akiba, A. Dirisala, X. Liu, K. Toh, T. Yang, Z. Wang, S. Fukushima, J. Li, S. Quader, K. Tsumoto, T. Yokota, Y. Anraku and K. Kataoka, *ACS Nano*, 2020, **14**, 6729–6742, DOI: 10.1021/acsnano.9b09991.

390 X. Jiang, H. Xin, Q. Ren, J. Gu, L. Zhu, F. Du, C. Feng, Y. Xie, X. Sha and X. Fang, *Biomaterials*, 2014, **35**, 518–529, DOI: 10.1016/j.biomaterials.2013.09.094.

391 Y. Anraku, H. Kuwahara, Y. Fukusato, A. Mizoguchi, T. Ishii, K. Nitta, Y. Matsumoto, K. Toh, K. Miyata, S. Uchida, K. Nishina, K. Osada, K. Itaka, N. Nishiyama, H. Mizusawa, T. Yamasoba, T. Yokota and K. Kataoka, *Nat. Commun.*, 2017, **8**, 1001, DOI: 10.1038/s41467-017-00952-3.

392 Y. Zhou, F. Zhu, Y. Liu, M. Zheng, Y. Wang, D. Zhang, Y. Anraku, Y. Zou, J. Li, H. Wu, X. Pang, W. Tao, O. Shimoni, A. I. Bush, X. Xue and B. Shi, *Sci. Adv.*, 2020, **6**, eabc7031.

393 H. Wang, Y. Chao, H. Zhao, X. Zhou, F. Zhang, Z. Zhang, Z. Li, J. Pan, J. Wang, Q. Chen and Z. Liu, *ACS Nano*, 2022, **16**, 664–674, DOI: 10.1021/acsnano.1c08120.

394 D. Wu, M. Qin, D. Xu, L. Wang, C. Liu, J. Ren, G. Zhou, C. Chen, F. Yang, Y. Li, Y. Zhao, R. Huang, S. Pourtaheri, C. Kang, M. Kamata, I. S. Y. Chen, Z. He, J. Wen, W. Chen and Y. Lu, *Adv. Mater.*, 2019, **31**, e1807557, DOI: 10.1002/adma.201807557.

395 S. Stalmans, N. Bracke, E. Wynendaele, B. Gevaert, K. Peremans, C. Burvenich, I. Polis and B. De Spiegeleer, *PLoS One*, 2015, **10**, e0139652, DOI: 10.1371/journal.pone.0139652.

396 G. Sharma, S. Lakkadwala, A. Modgil and J. Singh, *Int. J. Mol. Sci.*, 2016, **17**, 806, DOI: 10.3390/ijms17060806.

397 T. Kanazawa, F. Akiyama, S. Kakizaki, Y. Takashima and Y. Seta, *Biomaterials*, 2013, **34**, 9220–9226, DOI: 10.1016/j.biomaterials.2013.08.036.

398 J. Saint-Pol, F. Gosselet, S. Duban-Deweer, G. Pottiez and Y. Karamanos, *Cells*, 2020, **9**, 851, DOI: 10.3390/cells9040851.

399 M. Tkach and C. Thery, *Cell*, 2016, **164**, 1226–1232, DOI: 10.1016/j.cell.2016.01.043.

400 H. Tsivion-Visbord, N. Perets, T. Sofer, L. Bikovski, Y. Goldshmit, A. Ruban and D. Offen, *Transl. Psychiatry*, 2020, **10**, 305, DOI: 10.1038/s41398-020-00988-y.

401 B. Tang, W. Zeng, L. L. Song, H. M. Wang, L. Q. Qu, H. H. Lo, L. Yu, A. G. Wu, V. K. W. Wong and B. Y. K. Law, *Pharmaceuticals*, 2022, 15, DOI: 10.3390/ph15010083.

402 Y. Duan, M. Wu, D. Hu, Y. Pan, F. Hu, X. Liu, N. Thakor, W. H. Ng, X. Liu, Z. Sheng, H. Zheng and B. Liu, *Adv. Funct. Mater.*, 2020, 30, DOI: 10.1002/adfm.202004346.

403 Y. Liu, Y. Zou, C. Feng, A. Lee, J. Yin, R. Chung, J. B. Park, H. Rizos, W. Tao, M. Zheng, O. C. Farokhzad and B. Shi, *Nano Lett.*, 2020, **20**, 1637–1646, DOI: 10.1021/acs.nanolett.9b04683.

404 W. Hao, Y. Cui, Y. Fan, M. Chen, G. Yang, Y. Wang, M. Yang, Z. Li, W. Gong, Y. Yang and C. Gao, *J. Nanobiotechnol.*, 2021, **19**, 378, DOI: 10.1186/s12951-021-01110-0.

405 G. C. Terstappen, A. H. Meyer, R. D. Bell and W. Zhang, *Nat. Rev. Drug Discov.*, 2021, **20**, 362–383, DOI: 10.1038/s41573-021-00139-y.

406 A. C. Anselmo and S. Mitragotri, *J. Controlled Release*, 2014, **190**, 531–541, DOI: 10.1016/j.jconrel.2014.03.050.

407 M. Ayer, M. Schuster, I. Gruber, C. Blatti, E. Kaba, G. Enzmann, O. Burri, R. Guiet, A. Seitz, B. Engelhardt and H. A. Klok, *Adv. Healthcare Mater.*, 2021, **10**, e2001375, DOI: 10.1002/adhm.202001375.

408 H. I. Tong, W. Kang, P. M. Davy, Y. Shi, S. Sun, R. C. Allsopp and Y. Lu, *PLoS One*, 2016, **11**, e0154022, DOI: 10.1371/journal.pone.0154022.

409 M. Wu, H. Zhang, C. Tie, C. Yan, Z. Deng, Q. Wan, X. Liu, F. Yan and H. Zheng, *Nat. Commun.*, 2018, **9**, 4777, DOI: 10.1038/s41467-018-07250-6.

410 J. Lu, X. Gao, S. Wang, Y. He, X. Ma, T. Zhang and X. Liu, *Exploration*, 2023, **3**, 20220045, DOI: 10.1002/EXP.20220045.

411 M. Li, S. Li, H. Zhou, X. Tang, Y. Wu, W. Jiang, Z. Tian, X. Zhou, X. Yang and Y. Wang, *Nat. Commun.*, 2020, **11**, 1126, DOI: 10.1038/s41467-020-14963-0.

412 C. Gao, Q. Wang, J. Li, C. Kwong, J. Wei, B. Xie, S. Lu, S. Lee and R. Wang, *Sci Adv.*, 2022, **8**, eabn1805, DOI: 10.1126/sciadv.abn1805.

413 C. Bing, M. Ladouceur-Wodzak, C. R. Wanner, J. M. Shelton, J. A. Richardson and R. Chopra, *J. Ther. Ultrasound*, 2014, **2**, 1–11.

414 C. Berard, S. Desgranges, N. Dumas, A. Novell, B. Larrat, M. Hamimed, N. Taulier, M. A. Esteve, F. Correard and C. Contino-Pepin, *Pharmaceutics*, 2022, **14**, 1498, DOI: 10.3390/pharmaceutics14071498.

415 H. Moon, K. Hwang, K. M. Nam, Y. S. Kim, M. J. Ko, H. R. Kim, H. J. Lee, M. J. Kim, T. H. Kim, K. S. Kang, N. G. Kim, S. W. Choi and C. Y. Kim, *Biomater. Adv.*, 2022, **141**, 213102, DOI: 10.1016/j.bioadv.2022.213102.

416 C. W. Burke, E. t Alexander, K. Timbie, A. L. Kilbanov and R. J. Price, *Mol. Ther.*, 2014, **22**, 321–328, DOI: 10.1038/mt.2013.259.

417 A. K. O. Aslund, S. Berg, S. Hak, Y. Morch, S. H. Torp, A. Sandvig, M. Wideroe, R. Hansen and C. de Lange Davies, *J. Controlled Release*, 2015, **220**, 287–294, DOI: 10.1016/j.jconrel.2015.10.047.

418 L. L. Israel, A. Galstyan, E. Holler and J. Y. Ljubimova, *J. Controlled Release*, 2020, **320**, 45–62, DOI: 10.1016/j.jconrel.2020.01.009.

419 Y. Huang, B. Zhang, S. Xie, B. Yang, Q. Xu and J. Tan, *ACS Appl. Mater. Interfaces*, 2016, **8**, 11336–11341, DOI: 10.1021/acsami.6b02838.

420 S. D. Kong, J. Lee, S. Ramachandran, B. P. Eliceiri, V. I. Shubayev, R. Lal and S. Jin, *J. Controlled Release*, 2012, **164**, 49–57, DOI: 10.1016/j.jconrel.2012.09.021.

421 K. Mayilsamy, E. Markoutsa, M. Das, P. Chopade, D. Puro, A. Kumar, D. Gulick, A. E. Willing, S. S. Mohapatra and S. Mohapatra, *Nanomedicine*, 2020, **29**, 102247, DOI: 10.1016/j.nano.2020.102247.

422 D. Lee and T. Minko, *Pharmaceutics*, 2021, **13**, 2049, DOI: 10.3390/pharmaceutics13122049.

423 M. W. Kemp, J. P. Newnham, J. G. Challis, A. H. Jobe and S. J. Stock, *Hum. Reprod. Update*, 2016, **22**, 240–259, DOI: 10.1093/humupd/dmv047.

424 S. Sridharan, I. Sullivan, V. Tomek, J. Wolfenden, J. Skovranek, R. Yates, J. Janousek, T. E. Dominguez and J. Marek, *Heart Rhythm*, 2016, **13**, 1913–1919, DOI: 10.1016/j.hrthm.2016.03.023.

425 B. F. Cuneo and J. F. Strasburger, *Obstetrics Gynecology*, 2000, **96**, 575–581.

426 D. Vejrazkova, J. Vcelak, M. Vankova, P. Lukasova, O. Bradnova, T. Halkova, R. Kancheva and B. Bendlova, *J. Steroid Biochem. Mol. Biol.*, 2014, **139**, 122–129, DOI: 10.1016/j.jsbmb.2012.11.007.

427 N. M. Gude, C. T. Roberts, B. Kalionis and R. G. King, *Thromb. Res.*, 2004, **114**, 397–407, DOI: 10.1016/j.thromres.2004.06.038.

428 E. Kurtoglu, B. Z. Altunkaynak, I. Aydin, A. Z. Ozdemir, G. Altun, A. Kokcu and S. Kaplan, *J. Obstet. Gynaecol. Res.*, 2015, **41**, 1533–1540, DOI: 10.1111/jog.12751.

429 D. Ho, J. W. Leong, R. C. Crew, M. Norret, M. J. House, P. J. Mark, B. J. Waddell, K. S. Iyer and J. A. Keelan, *Sci. Rep.*, 2017, **7**, 2866, DOI: 10.1038/s41598-017-03128-7.

430 T. Clements, T. F. Rice, G. Vamvakas, S. Barnett, M. Barnes, B. Donaldson, C. E. Jones, B. Kampmann and B. Holder, *Front. Immunol.*, 2020, **11**, 1920, DOI: 10.3389/fimmu.2020.01920.

431 E. Bongaerts, L. L. Lecante, H. Bove, M. B. J. Roeffaers, M. Ameloot, P. A. Fowler and T. S. Nawrot, *Lancet Planet Health*, 2022, **6**, e804–e811, DOI: 10.1016/S2542-5196(22)00200-5.

432 X. Huang, F. Zhang, X. Sun, K. Y. Choi, G. Niu, G. Zhang, J. Guo, S. Lee and X. Chen, *Biomaterials*, 2014, **35**, 856–865, DOI: 10.1016/j.biomaterials.2013.10.027.

433 F. R. De Bie, D. Sharma, D. Lannoy, K. Allegaert, L. Storme, J. Deprest and F. M. Russo, *Fetal Diagn. Ther.*, 2021, **48**, 411–420, DOI: 10.1159/000515435.

434 M. M. Barzago, A. Bortolotti, F. F. Stellari, L. Diomede, M. Algeri, S. Efrati, M. Salmona and M. Bonati, *J. Pharmacol. Exp. Ther.*, 1996, **277**, 79–86.

435 P. Pourali, M. Nouri, F. Ameri, T. Heidari, N. Kheirkhahan, S. Arabzadeh and B. Yahyaei, *Naunyn Schmiedebergs Arch Pharmacol*, 2020, **393**, 867–878, DOI: 10.1007/s00210-019-01796-y.

436 E. Paul, M. L. Franco-Montoya, E. Paineau, B. Angeletti, S. Vibhushan, A. Ridoux, A. Tiendrebeogo, M. Salome, B. Hesse, D. Vantelon, J. Rose, F. Canoui-Poitrine, J. Boczkowski, S. Lanone, C. Delacourt and J. C. Pairon, *Nanotoxicology*, 2017, **11**, 484–495, DOI: 10.1080/17435390.2017.1311381.

437 S. Grafmuller, P. Manser, H. F. Krug, P. Wick and U. von Mandach, *J. Vis. Exp.*, 2013, 50401, DOI: 10.3791/50401.

438 J. P. Huang, P. C. Hsieh, C. Y. Chen, T. Y. Wang, P. C. Chen, C. C. Liu, C. C. Chen and C. P. Chen, *Placenta*, 2015, **36**, 1433–1441, DOI: 10.1016/j.placenta.2015.10.007.

439 A. Adamcakova-Dodd, M. M. Monick, L. S. Powers, K. N. Gibson-Corley and P. S. Thorne, *Part. Fibre Toxicol.*, 2015, **12**, 30, DOI: 10.1186/s12989-015-0105-5.

440 S. Grafmueller, P. Manser, L. Diener, P. A. Diener, X. Maeder-Althaus, L. Maurizi, W. Jochum, H. F. Krug, T. Buerki-Thurnherr, U. von Mandach and P. Wick, *Environ. Health Perspect.*, 2015, **123**, 1280–1286, DOI: 10.1289/ehp.1409271.

441 H. Tang, Z. Jiang, H. He, X. Li, H. Hu, N. Zhang, Y. Dai and Z. Zhou, *Int. J. Nanomed.*, 2018, **13**, 4073–4082, DOI: 10.2147/IJN.S161319.

442 Z. Jiang, H. Tang, Q. Xiong, M. Li, Y. Dai and Z. Zhou, *Colloids Surf., B*, 2022, **216**, 112553, DOI: 10.1016/j.colsurfb.2022.112553.

443 Z. Sezgin-Bayindir, A. E. Elcin, M. Parmaksiz, Y. M. Elcin and N. Yuksel, *J. Microencapsul*, 2018, **35**, 149–164, DOI: 10.1080/02652048.2018.1447615.

444 J. Vidmar, K. Loeschner, M. Correia, E. H. Larsen, P. Manser, A. Wichser, K. Boodhia, Z. S. Al-Ahmady, J. Ruiz, D. Astruc and T. Buerki-Thurnherr, *Nanoscale*, 2018, **10**, 11980–11991, DOI: 10.1039/c8nr02096e.

445 P. K. Myllynen, M. J. Loughran, C. V. Howard, R. Sormunen, A. A. Walsh and K. H. Vahakangas, *Reprod. Toxicol.*, 2008, **26**, 130–137, DOI: 10.1016/j.reprotox.2008.06.008.

446 W. H. Tse, S. Higgins, D. Patel, M. Xing, A. R. West, H. I. Labouta and R. Keijzer, *Biomater. Sci.*, 2022, **10**, 5243–5253, DOI: 10.1039/d2bm00293k.

447 S. Borghi, S. Bournazos, N. K. Thulin, C. Li, A. Gajewski, R. W. Sherwood, S. Zhang, E. Harris, P. Jagannathan, L. X. Wang, J. V. Ravetch and T. T. Wang, *Proc. Natl. Acad. Sci. U. S. A.*, 2020, **117**, 12943–12951, DOI: 10.1073/pnas.2004325117.

448 M. Resende, M. A. Nielsen, M. Dahlback, S. B. Ditlev, P. Andersen, A. F. Sander, N. T. Ndam, T. G. Theander and A. Salanti, *Malar. J.*, 2008, **7**, 104, DOI: 10.1186/1475-2875-7-104.

449 B. Zhang, L. Tan, Y. Yu, B. Wang, Z. Chen, J. Han, M. Li, J. Chen, T. Xiao, B. K. Ambati, L. Cai, Q. Yang, N. R. Nayak, J. Zhang and X. Fan, *Theranostics*, 2018, **8**, 2765–2781, DOI: 10.7150/thno.22904.

450 K. Zhao, D. Li, G. Cheng, B. Zhang, J. Han, J. Chen, B. Wang, M. Li, T. Xiao, J. Zhang, D. Zhou, Z. Jin and X. Fan, *Int. J. Mol. Sci.*, 2019, **20**, 5458, DOI: 10.3390/ijms20215458.

451 L. Li, H. Yang, P. Chen, T. Xin, Q. Zhou, D. Wei, Y. Zhang and S. Wang, *Front. Bioeng. Biotechnol.*, 2020, **8**, 64, DOI: 10.3389/fbioe.2020.00064.

452 A. King, C. Ndifon, S. Lui, K. Widdows, V. R. Kotamraju, L. Agemy, T. Teesalu, J. D. Glazier, F. Cellesi, N. Tirelli, J. D. Aplin, E. Ruoslahti and L. K. Harris, *Sci. Adv.*, 2016, **2**, e1600349.

453 Q. Yu, Y. Qiu, X. Wang, J. Tang, Y. Liu, L. Mei, M. Li, M. Yang, L. Tang, H. Gao, Z. Zhang, W. Xu and Q. He, *Int. J. Pharm.*, 2018, **546**, 115–124, DOI: 10.1016/j.ijpharm.2018.05.001.

454 T. J. Kaitu'u-Lino, S. Pattison, L. Ye, L. Tuohey, P. Sluka, J. MacDiarmid, H. Brahmbhatt, T. Johns, A. W. Horne, J. Brown and S. Tong, *Endocrinology*, 2013, **154**, 911–919, DOI: 10.1210/en.2012-1832.

455 K. L. Swingle, H. C. Safford, H. C. Geisler, A. G. Hamilton, A. S. Thatte, M. M. Billingsley, R. A. Joseph, K. Mrksich, M. S. Padilla, A. A. Ghalsasi, M.-G. Alameh, D. Weissman and M. J. Mitchell, *J. Am. Chem. Soc.*, 2023, **145**, 4691–4706, DOI: 10.1021/jacs.2c12893.

456 R. E. Young, K. M. Nelson, S. I. Hofbauer, T. Vijayakumar, M.-G. Alameh, D. Weissman, C. Papachristou, J. P. Gleghorn and R. S. Riley, *bioRxiv*, 2022, DOI: 10.1101/2022.12.22.521490.

457 A. Azagury, E. Amar-Lewis, E. Mann, R. Goldbart, T. Traitel, R. Jelinek, M. Hallak and J. Kost, *J. Controlled Release*, 2014, **183**, 105–113, DOI: 10.1016/j.jconrel.2014.03.040.

458 N. Abd Ellah, L. Taylor, W. Troja, K. Owens, N. Ayres, G. Pauletti and H. Jones, *PLoS One*, 2015, **10**, e0140879, DOI: 10.1371/journal.pone.0140879.

459 I. Burd, F. Zhang, T. Dada, M. K. Mishra, T. Borbiev, W. G. Lesniak, H. Baghlaf, S. Kannan and R. M. Kannan, *Nanomedicine*, 2014, **10**, 1343–1351, DOI: 10.1016/j.nano.2014.03.008.

460 J. L. Cohen, P. Chakraborty, K. Fung-Kee-Fung, M. E. Schwab, D. Bali, S. P. Young, M. H. Gelb, H. Khaledi, A. DiBattista, S. Smallshaw, F. Moretti, D. Wong, C. Lacroix, D. El Demellawy, K. C. Strickland, J. Lougheed, A. Moon-Grady, B. R. Lianoglou, P. Harmatz, P. S. Kishnani and T. C. MacKenzie, *N. Engl. J. Med.*, 2022, **387**, 2150–2158, DOI: 10.1056/NEJMoa2200587.

461 T. Elger, R. Akolekar, A. Syngelaki, C. De Paco Matallana, F. S. Molina, M. Gallardo Arozena, P. Chaveeva, N. Persico, V. Accurti, K. O. Kagan, N. Prodan, J. Cruz and K. H. Nicolaides, *Ultrasound Obstet. Gynecol.*, 2021, **58**, 48–55, DOI: 10.1002/uog.23694.

462 R. Akolekar, J. Beta, G. Picciarelli, C. Ogilvie and F. D'Antonio, *Ultrasound Obstet. Gynecol.*, 2015, **45**, 16–26, DOI: 10.1002/uog.14636.

463 A. Abostait, J. Tyrrell, M. Abdelkarim, S. Shojaei, W. H. Tse, I. M. El-Sherbiny, R. Keijzer and H. I. Labouta, *Mol. Pharm.*, 2022, **19**, 3757–3769, DOI: 10.1021/acs.molpharmaceut.2c00216.

464 N. S. Irvin-Choy, K. M. Nelson, M. N. Dang, J. P. Gleghorn and E. S. Day, *Nanomedicine*, 2021, **36**, 102412, DOI: 10.1016/j.nano.2021.102412.

465 A. Schmidt, D. M. Morales-Prieto, J. Pastuschek, K. Frohlich and U. R. Markert, *J. Reprod. Immunol.*, 2015, **108**, 65–71, DOI: 10.1016/j.jri.2015.03.001.

466 F. R. De Bie, S. D. Kim, S. K. Bose, P. Nathanson, E. A. Partridge, A. W. Flake and C. Feudtner, *Am. J. Bioeth.*, 2022, **23**, 67–78, DOI: 10.1080/15265161.2022.2048738.

467 K. Allegaert, *Int. J. Environ. Res. Public Health*, 2022, 19, DOI: 10.3390/ijerph191811336.

468 F. M. Russo, P. Mian, E. H. Krekels, K. Van Calsteren, D. Tibboel, J. Deprest and K. Allegaert, *Xenobiotica*, 2019, **49**, 98–105, DOI: 10.1080/00498254.2017.1422217.

469 X. Tian, Y. Chong and C. Ge, *Front. Chem.*, 2020, **8**, 446, DOI: 10.3389/fchem.2020.00446.

470 R. Bartucci, C. Åberg, B. N. Melgert, Y. L. Boersma, P. Olinga and A. Salvati, *Small*, 2020, **16**, 1906523, DOI: 10.1002/smll.201906523.

471 L. T. Curtis, M. Wu, J. Lowengrub, P. Decuzzi and H. B. Frieboes, *PLoS One*, 2015, **10**, e0144888, DOI: 10.1371/journal.pone.0144888.

472 T. A. Brocato, E. N. Coker, P. N. Durfee, Y. S. Lin, J. Townson, E. F. Wyckoff, V. Cristini, C. J. Brinker and

Z. Wang, *Sci. Rep.*, 2018, **8**(7538), 8, DOI: **10.1038/s41598-018-25878-**.

473 W. M. Pardridge and T. Chou, *Pharmaceuticals*, 2021, **14**, 535.

474 Y. Wang, Y. Wang, S. Li, Y. Cui, X. Liang, J. Shan, W. Gu, J. Qiu, Y. Li and G. Wang, *J. Nanobiotechnol.*, 2021, **19**(331), 0, DOI: **10.1186/s12951-021-01067-**.

475 J. S. Brenner, D. C. Pan, J. W. Myerson, O. A. Marcos-Contreras, C. H. Villa, P. Patel, H. Hekierski, S. Chatterjee, J. Q. Tao, H. Parhiz, K. Bhamidipati, T. G. Uhler, E. D. Hood, R. Y. Kiseleva, V. S. Shuvaev, T. Shuvaeva, M. Khoshnejad, I. Johnston, J. V. Gregory, J. Lahann, T. Wang, E. Cantu, W. M. Armstead, S. Mitragotri and V. Muzykantov, *Nat. Commun.*, 2018, **9**(2684), 7, DOI: **10.1038/s41467-018-05079-**.

476 X. Zhang, X. Zhao, Z. Hua, S. Xing, J. Li, S. Fei and M. Tan, *Biomaterials*, 2023, **292**, 121937, DOI: **10.1016/j.biomaterials.2022.121937**.

477 X. Li, E. C. Montague, A. Pollinzi, A. Lofts and T. Hoare, *Small*, 2022, **18**, 2104632, DOI: **10.1002/smll.202104632**.

478 O. B. Garbuzenko, J. Winkler, M. S. Tomassone and T. Minko, *Langmuir*, 2014, **30**, 12941–12949, DOI: **10.1021/la502144z**.

479 B. Shaghaghi, S. Khoee and S. Bonakdar, *Int. J. Pharm.*, 2019, **559**, 1–12, DOI: **10.1016/j.ijpharm.2019.01.020**.

